VIETNAM
JOURNAL OF HYDRO - METEOROLOGY

ISSN 2525 - 2208

VIETNAM METEOROLOGICAL AND HYDROLOGICAL ADMINISTRATION

No 01
12-2018

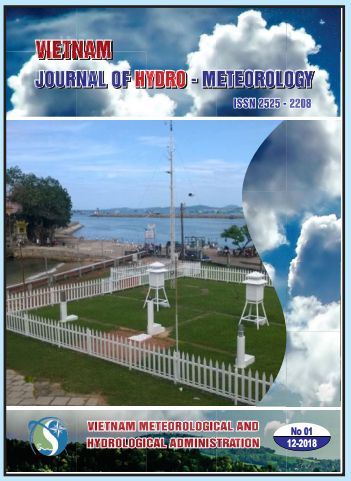

Publishing licence
No: 166/GP-BTTTT - Ministry of Information and Communication dated 17/04/2018

Editorial office
No 8 Phao Dai Lang, Dong Da, Ha Noi
TEL: 04.39364963; Fax: 04.39362711
Email: tapchikttv@yahoo.com or tapchikttv@gmail.com

Engraving and printing
Thien Ha Joint Stock Company
Tel: 04.3990.3769 - 0912.565.222

VIETNAM JOURNAL OF HYDROMETEOROLOGY
Volume 01 - 12/2018

TABLE OF CONTENT

Research Paper

INDICATORS OF CLIMATE CHANGE ACROSS THE SOUTH-CENTRAL REGION

Tran Hong Thai[1], Hoang Anh Huy[2], Nguyen Dang Mau[3], Hoang Van Dai[3]

ARTICLE HISTORY

Received: April 05, 2018 Accepted: May 25, 2018
Publish on: December 25, 2018

ABSTRACT

In this study, we focus on the findings of the indicators of climate change across the South-Central region based on assessing the trends of temperature (mean, maximum and minimum) and rainfall as well as drought conditions. The change trends of climatic variables are tested by the simple linear method at significance level of 0.05 (corresponding to the 95% confidence level). The observation data is updated up to 2017. The results show that the annual mean temperature tends to increase at 15 stations, where, the increase in temperature in the dry season is greater than that in rainy season. The increases in annual temperature are mostly from 0.01 to 0.03 per year and accepted by the 90% confidence level. The increase trends of annual rainfall are mostly from 0.1 to 1.35% per year. The A index is mostly found by increase trend that the wet condition is found at most station. In addition, the increase trend of the drought condition defined by the decrease trend of the A index at some southern stations in the South-Central region. However, the trends of both rainfall and A index are not mostly at significance level of 0.05.

Keywords: *Indicators of climate change, Rainfall, temperature, South-Central region.*

1. Introduction

Defining the indicators of climate change plays an important role in providing information and scientific basis for the response to climate change. Thus, the climate change assessment is one of the important topics of climate change studies. In reports of IPCC, the global climate change indicators are clearly defined by the increase in temperature, sea level rise and changes in rainfall as well as the decrease in global ice mass (IPCC, 2007, 2013). In Vietnam, climate change assessment has been considered in many studies since 1990s (Ngu and Hieu, 1991, 1999; Hieu, and Tuan, 1991, Lien, 2000). Over the past 10 years, studies on climate change assessment have been strongly developed. Indicators of climate change defined by assessing the changing trends of climatic variables has been clearly indicated (Ha and Tan, 2009; Thanh and Tan 2012; Ngu, 2008; Thang et al., 2010; Thang et al., 2016; Thang et al., 2017; Thang et al., 2013; Tan et al., 2010; Lien, 2000; Lien et al., 2007; Hang et al., 2009; Tuyen, 2007). Compiled from research results, adequate assessments on climate change indicators across Vietnam have been presented in reports of MONRE (MONRE, 2009, 2012, 2016).

However, the previous studies were mainly based on the data that updated up to 2010 or 2014. These studies mostly focused on the gen-

TRAN HONG THAI
tranthai.vkttv@gmail.com
[1]Vietnam Meteorological and Hydrological Administration
[2]HaNoi University of Natural Resources and Environment
[3]Vietnam Institute of Meteorology, Hydrology and Climate change

eral climate variables and some of its extreme events. But, the drought/wet conditions are not considered, particularly for areas strongly impacted by droughts such as the South - Central region. In reality, the South-Central region has the lower annual rainfall than other climatic regions and has a long dry season, up to nine months of dry season (Ngu and Hieu, 2004). Thus, the issues of water shortage and drought seriously effect on socio-economic development and human's activities. In recent years, there have been many serious drought events in the South-Central region, such as the drought events in 1983, 1993 and 1998 (Thang et al., 2015) and in the 2015 - 2016 (DWR, 2016). In addition, the significance level of the trend was not tested.

From these above issues mentioned, we focus on defining the climate change indicators in the South-Central region through analyzing the trends of general variables (temperature and rainfall) and drought/wet conditions based on the observation data updated up to 2017.

2. Data and method

2.1. Data used

In this study, we use observation data of temperature (T2m), maximum temperature (Tx), minimum temperature (Tn), rainfall (R) and evaporation (E). These data are updated up to 2017 from 15 stations in the South-Central region (Table 1).

Table 1. The information of 15 stations used in the study

No	Name of stations	longitude	latitude	Variables
1	Da Nang	108.18	16.03	T2m, Tx, Tn, E, R
2	Tam Ky	108.50	15.55	T2m, Tx, Tn, E, R
3	Tra My	108.22	15.35	T2m, Tx, Tn, E, R
4	Ba Tơ	108.72	14.77	T2m, Tx, Tn, E, R
5	Quang Ngai	108.78	15.13	T2m, Tx, Tn, E, R
6	Hoai Nhon	109.02	14.53	T2m, Tx, Tn, E, R
7	Quy Nhon	109.22	13.77	T2m, Tx, Tn, E, R
8	Son Hoa	108.98	13.05	T2m, Tx, Tn, E, R
9	Tuy Hoa	109.28	13.08	T2m, Tx, Tn, E, R
10	Nha Trang	109.20	12.25	T2m, Tx, Tn, E, R
11	Cam Ranh	109.17	11.95	T2m, Tx, Tn, E, R
12	Trường Sa	111.92	8.65	T2m, Tx, Tn, E, R
13	Phan Thiet	108.10	10.93	T2m, Tx, Tn, E, R
14	Ham Tan	107.75	10.68	T2m, Tx, Tn, E, R
15	Phu Quy	108.93	10.52	T2m, Tx, Tn, E, R

2.2 Methods used

2.2.1 Wet/drought conditions defined

Wet/drought conditions cannot be observed by measuring instruments at meteorological and hydrological stations. Thus, the question is how can drought be identified? Many authors show that it is possible to identify wet/drought conditions through indices such as Standardized Precipitation Index (SPI) and accumulated rainfall, etc.

As mentioned in many studies (Ngu and Hieu, 2004; Tri, 2015; Mau, 2015; Thang, 2015; Thang et al., 2015) the A (or K) index is the suitable index for identifying the wet/drought con-

ditions in Vietnam because this index is a type of water balance equation between the water in (via rainfall) and water out (via evaporation). Basically, a water balance equation can be used to describe the flow of water in and out of a system. A system can be one of several hydrological domains, such as a column of soil or a drainage basin.

In this study, the A index is defined as follows:

$$A = \frac{R}{E} \quad (1)$$

Where R is the rainfall; E is the evaporation.

According to this method, the drought condition occurs when the A index<1.That is, the amount of evaporation is greater than the amount of rainfall. The stronger drought condition is found when the A index is smaller. The wet condition occurs when the A index>1.

2.2.2 Assessment of climate change

Climate trend defined:

For identifying climate change trend in the South-Central, we use the simple linear regression equation as used in many studies (IPCC, 2007, 2013; MONRE, 2009, 2012, 2016; Thang et al., 2015). In statistics, simple linear regression is a linear regression model with a single explanatory variable. That is, it concerns two - dimensional sample points with one independent variable and one dependent variable (conventionally, the x and y coordinates in a Cartesian coordinate system) and finds a linear function (a non-vertical straight line) that, as accurate as possible, predicts the dependent variable values as a function of the independent variables. The adjective simple refers to the fact that the outcome variable is related to a single predictor.

Given a data set X: x_1, x_2, x_3,…, x_n of n statistical units. The remainder of the article assumes an ordinary least squares regression. In this case, the slope of the fitted line is equal to the correlation between y and x corrected by the ratio of standard deviations of these variables. The intercept of the fitted line is such that the line passes through the center of mass of the data points.

Considering the simple linear equation:

$$x_t = b_0 + b_1 t \quad (2)$$

where

$$b_1 = \frac{\sum_{t=1}^{n}(x_t - \bar{x})(t - \bar{t})}{\sum_{t=1}^{n}(t - \bar{t})^2}$$

$$b_0 = \bar{x} - b_1 \bar{t}$$

We can find:

- b_1: the slope of the fitted line (linear changing rate)

- b_o: mean value mass of the data points

From that, we can find the increase/decrease rates during the study period (D) as:

$$D = b_1 n \quad (3)$$

Where: n is sample sizes

We can define the correlation coefficient (r_{xt}):

$$r_{xt} = \frac{\sum_{t=1}^{n}(x_t - \bar{x})(t - \bar{t})}{\left[\sum_{t=1}^{n}(x_t - \bar{x})^2 \sum_{t=1}^{n}(t - \bar{t})^2\right]^{\frac{1}{2}}} \quad (4)$$

Testing the trend:

The rxt and sample sizes (n) are the criteria for deciding the confidence of the trend. In this study, we test the significance level at 0.05 (corresponding to the confidence of 95%) for the trends.

Assume that: H0 is corresponding to r=0 (*)

The first criteria tested (*) is:

r - 0≥ dα : r is significance level

r – 0< dα : r is not significance lvel

dα has been sure to:

H_0 is true : $P\{|r - 0| \geq d\alpha\} = \varepsilon$

The t is defined by the below equation:

$$t = \frac{r}{\sqrt{1 - r^2}/\sqrt{n - 2}} \quad (5)$$

In statistics, the t has the Student probability, then we have:

$|t| \geq t\alpha$: r is significance level

$|t| < t\alpha$: r is not significance level

If H_0 is true, we have $P\{|t| \geq t\alpha\} = \alpha$

Following the above theory, based on the rxt and sample sizes (n), we can identify the trend of climate variable that is accepted at the 0.5 significance level (or at the 95% confidence level) as listed in the Table 2.

Table 2. The correlation coefficients corresponding to sample sizes (n) at the 95% confidence level for defining the significance level of 0.05

n-2	10	20	30	40	50	60	70	80	90	100
α = 0.05	0.576	0.423	0.349	0.304	0.273	0.250	0.232	0.217	0.205	0.195

Climate variability defined:

For defining the annual variability, we use the coefficient of variation (Cv). The Cv (%) is defined by the below equation:

$$C_v = \frac{S_x}{\bar{x}}.100 \quad (6)$$

Where S_X is the standard deviation; $\bar{x}$ is the mean value.

3. Results

3.1 Changes in temperature

Table 3 presents the rates of temperature change (T2m, Tx, Tn) (°C per year) at 15 stations. In Table 3, the values are bold and shaded in follow that reflect the trend of change that satisfies the 0.05 significance level under the r test. These results show that the trends of temperature are increasing at stations in the South-Central region. These increase trends are at the significance level of 0.05 at most stations. However, some trends are not at the significance level of 0.05; for example at the Da Nang, Son Hoa, Hoai Nhon and Phu Quy stations (Table 3).

Changes in average temperature (T2m):

During 1961 - 2017, the annual T2m has the increase trend at 15 stations. Across the South - Central region, the annual T2m rose from 0.01 to 0.03°C/year, corresponding to the rate of 0.57 to 1.7°C between 1961-2017. However, the maximum increase rate is only found at Cam Ranh station. In fact, the increase in temperature is around from 0.01 to 0.02°C/year, corresponding to the rate of 0.57 to 1.14°C between 1961-2017. Excluding Cam Ranh station, the most significant increases of annual T2m are found at the stations: Tra My, Ba To and Truong Sa. In contrast, the lower increases of annual T2m are found most stations in the South-Central region. The increase trend of annual T2m is found as the significance level of 0.05; Particularly, the trend of Son Hoa station does not reach the significance level of 0.05 (Table 3).

Interestingly, the T2m in the dry season has more increase rate than that in the rainy season. During dry months, the annual T2m has a typical increase from 0.01 to 0.03°C/year. In contrast, the T2m trend in the rainy season is slight from 0.0°C/year to 0.01°C/year at most stations. In addition, the trend in the dry season has the significance level of 0.05 at most stations, particularly in Da Nang and Son Hoa stations, which does not reach the significance level of 0.05. In the rainy season, the T2m trend does not reach the significance level of 0.05 at more stations, for example at Tam Ky, Hoai Nhon, Son Hoa, Ham Tan and Phu Quy stations (Table 3).

Changes in maximum temperature (Tx):

The increase trend of annual Tx during 1961-2017 is found at most stations. Where, the increase rates are mostly from 0.01 to 0.04°C/year, corresponding to the increase rate of 0.57 to over 2.0°C between 1961 and 2017. In particular, the greatest increase rate is found at the Cam Ranh and Truong Sa stations. However, the trend of annual Tx is not found at the Nha Trang station. Remarkably, the increase trends of annual Tx do not reach the significance level of 0.05 at

most stations. The increase trends at Ba To, Son Hoa and Nha Trang stations do not reach the significance level of 0.05 (Table 3).

The increasing trend of Tx is relatively different between the rainy season and the dry season. The Tx in the dry season experiences the increase trend at 15 stations, with increases in 0.01 to 0.05°C/year. In particular, the greatest increase rates are also found at the Cam Ranh and Truong Sa stations. Additionally, the increase trend at Nha Trang station is not found at Nha Trang station. For the dry season, the increase trend of Tx satisfies the significance level of 0.05 at most stations. In contrast, the trend does not reach the significance level of 0.05 at Quy Nhon, Son Hoa and Nha Trang stations (Table 3). For the rainy season, the change of Tx is found from -0.01 to 0.04°C/year. The greatest increase rates are from 0.03 to 0.04°C/year found at Cam Ranh and Truong Sa stations, respectively. However, the decrease rate of Tx is found at Son Hoa station, with the rate of -0.01°C/year. In addition, the change trend is not clearly found at Da Nang, Tra My, Ba To, Quang Ngai, Nha Trang and Phu Quy stations. The trend of Tx in the rainy season reaches the significance level of 0.05 found at 7/15 stations (Tam Ky, Hoai Nhon, Quy Nhon, Tuy Hoa, Cam Ranh, Truong Sa and Phan Thiet stations) (Table 3).

From these above analyses, the annual and dry season Tx are likely to increase at most stations in the South-Central region. In addition, the increase trend of the annual and dry season Tx reaches the significance level of 0.05 at most stations. However, the increase trend in the rainy season Tx is not clearly found at 6 stations. Remarkably, the decrease trend is found at the Son Hoa station, with the decrease rate of 0.01°C/year.

Changes in minimum temperature (Tn):

The results show that the increase trends of the annual and both two seasons are found at most stations. Moreover, the trend of Tn is not much variable among 15 stations. Additionally, the significance level of 0.05 is found at most trends of Tn. During 1961-2017, Tn tends to increase, with a typical increase from 0.01 to 0.03°C/year. In particular, the increase trend of dry Tn is greater than the increase trend of the rainy Tn. In terms of the significance level of 0.05, the increase trend of Tn satisfies this significance level at most stations. In contrast, the trend did not meet the significance level of 0.05 at Son Hoa station (dry season), Hoai Nhon and Truong Sa (rainy season) and Hoai Nhon (annual) (Table 3).

The Table 3 shows the greatest increase trend of annual Tn (0.03°C/year) at Da Nang, Ba To, Nha Trang and Phan Thiet stations. In the dry season, the greatest increase trend (0.03°C/year) is found at Da Nang, Tra My, Ba To, Quang Ngai, Cam Ranh and Ham Tan stations. In the rainy season, the greatest increase trend is found at Da Nang, Ba To, Nha Trang and Phan Thiet stations. In contrast, the increase trend of Tn is not clearly determined at some stations such as Hoai Nhon (rainy season and annual) and Truong Sa (rainy season) stations.

In general, the trend of Tn is more clearly found than the of T2m and Tx. The trend of Tx is much variable among stations than those of T2m and Tn. Averaging values from 15 stations in the South-Central region, the increase rate is from 0.01 to 0.02 found by T2m, Tx and Tm. However, the increase rate of rainy season Tn is greater than that of T2m and Tx. Referring the contributing to the increase rate in T2m at each station, the contribution of Tn is more than that of Tx.

Table 3. Changing rate of T2m, Tx and Tn (°C/year) (the trend is at significance level of 0.05 is bold and shaded by yellow color)

Station	T2m			Tx			Tn		
	Dry season	Rainy season	Annual	Dry season	Rainy season	Annual	Dry season	Rainy season	Annual
Da Nang	0.01	0.01	0.01	0.02	0.00	0.01	0.03	0.03	0.03
Tam Ky	0.02	0.01	0.01	0.03	0.02	0.03	0.02	0.01	0.02
Tra My	0.03	0.01	0.02	0.02	0.00	0.01	0.03	0.01	0.02
Ba To	0.02	0.01	0.02	0.02	0.00	0.01	0.03	0.03	0.03
Quang Ngai	0.01	0.01	0.01	0.02	0.00	0.02	0.03	0.02	0.03
Hoai Nhon	0.01	0.00	0.01	0.02	0.02	0.02	0.01	0.00	0.00
Quy Nhon	0.01	0.01	0.01	0.01	0.02	0.01	0.02	0.02	0.02
Son Hoa	0.01	0.00	0.01	0.01	-0.01	0.01	0.01	0.01	0.01
Tuy Hoa	0.01	0.01	0.01	0.02	0.02	0.02	0.02	0.02	0.02
Nha Trang	0.01	0.01	0.01	0.00	0.00	0.00	0.02	0.03	0.03
Cam Ranh	0.03	0.02	0.03	0.05	0.03	0.04	0.03	0.02	0.02
Truong Sa	0.03	0.01	0.02	0.04	0.04	0.04	0.02	0.00	0.01
Phan Thiet	0.01	0.02	0.01	0.02	0.02	0.02	0.02	0.03	0.03
Ham Tan	0.03	0.00	0.01	0.03	0.01	0.02	0.03	0.01	0.02
Phu Quy	0.02	0.00	0.01	0.02	0.00	0.01	0.02	0.01	0.02
South-Central region	0.02	0.01	0.01	0.02	0.01	0.02	0.02	0.02	0.02

3.2. Changes in rainfall and wet/drought conditions

The results of calculating the changes in precipitation and A index as well as determining the trend at the significance level of 0.05 are presented in Table 4. In general, the rainfall trend tends to increase across most stations in the South-Central region, with the greatest increase rate of up to 2.89%/year of dry season at Tuy Hoa station, corresponding to the increase rate of 164.7% between 1961 and 2017. However, the trend of rainfall does not have the significance level of 0.05 at most stations. According to the increase in rainfall, index A also tends to increase at most stations, with the greatest increase rate of 0.3%/year of dry season at Tra My station, corresponding to the increase rate of 17% between 1961 and 2017. The increase in A index also does not have the significance level of 0.05 at around half the number of stations. On averaging values of 15 stations in the South-Central region, the annual rainfall has an increase rate of 0.71%/year, corresponding to the increase rate of 40.47% between 1961 and 2017. In particular, the increase rate of rainfall is found by greater values in the dry season than in the rainy season. Where, the increase rates are found by 1.46%/year and 0.25%/year for dry and rainy seasons, respectively. The A index has an increase rate from 0.01%/year (rainy season) to

0.07%/year (dry season) and 0.04% of increase rate of annual A index.

Changes in rainfall:

During 1961-2017, the increase trend of dry and rainy seasons as well as annual is found at most stations. In contrast, the slight decrease in the rainfall trend is found at Ham Tam (dry season, rainy season and annual) and Phu Quy (dry season and annual). The significance level of 0.05 testing shows that trend of rainfall is not significance level found at most stations.

During 1961-2017, the rainfall of dry season has an increase trend at most stations in South-Central region, with the increase rate of value ranges from 0.4%/year (Phan Thiet) to 2.89%/year (Tuy Hoa). In contrast, the decrease trend with slightly rate is found at Ham Tan (-0.97%/year) and Phan Thiet (-0.13%/year) stations. The trend of rainfall has the significance level of 0.05 that is found at the Da Nang, Tuy Hoa, Nha Trang, Truong Sa, Phan Thiet and Ham Tan stations, in which, the decrease trend at Ham Tan has the significance level of 0.05 (Table 4). It is noteworthy that the total amount of rainfall in the dry season in the South-Central is very small. In fact, the contribution to total amount of rainfall in the dry season is not much. For that, just an unseasonal heavy rain event in the dry season also significantly changes the total amount of rainfall in the dry season and leads to a change in trend of time-series data.

The Table 4 also shows the increase trend of rainfall in the rainy season with a slightly increase rate from 0.17%/year (Nha Trang) to 1.02%/year (Truong Sa). In addition, we also find the decrease trend of rainfall in the rainy season at Da Nang, Tra My, Quang Ngai and Ham Tan stations. However, the decrease rate in rainfall at these stations is very low. The significance level of 0.05 is only found at 4 stations (Son Hoa, Tuy Hoa, Nha Trang and Phan Thiet). These stations have the 95% of confidence that are located in the southern areas of the South-Central (Table 4). It is very important that the amount of rainfall in the South-Central is very huge. Thus, the contribution in the total value in the rainy season is relatively large.

The annual rainfall has the increase trend at most stations in the South-Central region. The increase rate is found as from 0.1 %/year (Phu Quy) to 1.41%/year (Ba To), corresponding to the increase rate from 5.7% to 80.37% between 1981-2017, respectively. The decrease trend of annual rainfall is found at Ham Tan station, with the decrease rate of 0.72%/year, corresponding to the rate of 41.04%. The significance level of 0.05 in the annual rainfall trend is found at Tuy Hoa, Ha Trang, Phan Thiet and Ham Tan stations (Table 4).

From these above analyses, we find that the increase trend of rainfall at most stations found in annual and both two seasons. However, we also find the decrease trend of rainfall in dry season at Ham Tan and Phu Quy stations which are located in the southern areas of the South-Central region. These decrease trends show the increase in intensity of drought in the southern areas of South-Central region.

Changes in A index:

According to the increase trend of rainfall, the A index also has the increase trend at most stations. The increase trend of the A index is found in both dry and rainy seasons. The number of stations has the trend of A index at the significance level of 0.05 that is more than the trend of rainfall. In Averaging from 15 stations in the South-Central region, the annual A index has an increase trend with the trend rate of 0.04%/year. In which, the increase rate of rainy season is smaller than the annual trend. However, the increase rate of dry season is bigger than the annual trend. The trend of the A index is not clearly found at Phan Thiet station for annual and both two seasons. Especially, the decrease trend of the A index is found at the Ham Tan and Phu Quy stations (Table 4).

For the dry season, the increase rate of the A index is mostly from 0.01%/year to 0.3%/year. In which, the greatest increase rates are found at the northern stations of the South-Central region.

The very small increase rates mostly found from Hoai Nhon station to Nha Trang station. The trend of dry season A index is not clearly found at Phan Thiet station. The increase in the intensity of drought condition is found by the decrease rate of the A index at Ham Tan and Phu Quy stations. In dry season, the trend of A index has the significance level of 0.05 at most stations (Table 4).

For the rainy season, the results in the Table 4 show that the A index has the increase trend at many stations (Tam Ky, Tra My, Ba To, Son Hoa, Hoai Nhon, Cam Ranh and Truong Sa). The increase rate of A index is found from 0.01%/year to 0.03%/year. However, the change trend is not clearly found at 7 stations (Da Nang, Quang Ngai, Quy Nhon, Nha Trang, Phan Thiet, Ham Tan and Phu Quy). The trend of A index in the rainy season has the significance level of 0.05 that is found at some stations (Tam Ky, Tra My, Ba To, Son Hoa, Cam Ranh and Truong Sa) (Table 4). As can be seen, in the period 1961-2017, wet conditions in the rainy season in the South -Central region has an increase trend at many stations that having the increase trend of A index. However, the changing trend of wet condition in the rainy season is not clearly found at many stations that the trend of A index is not found (Table 4).

Table 4. Rate of changes in rainfall and drought index (A index) (% per year) (the trend is at significance level of 0.05 is bold and shaded by yellow color)

Station	R			A		
	Dry season	Rainy season	Annual	Dry season	Rainy season	Annual
Da Nang	1.89	-0.04	0.72	0.05	0.00	0.02
Tam Ky	2.46	0.44	1.28	0.22	0.03	0.11
Tra My	2.64	-0.04	1.08	0.30	0.03	0.15
Ba Tơ	2.26	0.94	1.41	0.21	0.03	0.11
Quang Ngai	1.09	-0.32	0.19	0.07	0.00	0.03
Hoai Nhon	1.86	0.24	0.86	0.05	0.01	0.02
Quy Nhon	1.03	0.25	0.57	0.01	0.00	0.01
Son Hoa	1.34	0.39	0.33	0.05	0.01	0.02
Tuy Hoa	2.89	0.39	1.35	0.03	0.01	0.01
Nha Trang	1.30	0.17	0.70	0.01	0.00	0.00
Cam Ranh	1.77	0.37	0.94	0.04	0.01	0.02
Trương Sa	2.05	1.02	1.42	0.12	0.04	0.07
Phan Thiet	0.40	0.36	0.37	0.00	0.00	0.00
Ham Tan	-0.97	-0.59	-0.72	-0.02	0.00	-0.01
Phu Quy	-0.13	0.17	0.10	-0.02	0.00	-0.01
South-Central region	**1.46**	**0.25**	**0.71**	**0.07**	**0.01**	**0.04**

4. Conclusion and discussion

From the above results of the calculation and analysis, some indicators of climate change in the South-Central region can be found as:

Changes in temperature:

It can be seen that the clearest indicator of temperature (T2m, Tx and Tn) is the increase trends during 1961-2017 in the South-Central region, having the significance level of 0.05 at most stations

- Average temperature (T2m): The increase

rate of T2m is mostly found from 0.01°C/year to 0.03°C/year. In which, the increase rate of T2m in the dry season is greater than in the rainy season. Averaging from 15 stations across the South-Central region, the T2m has the increase rates that are 0.02, 0.01 and 0.01°C/year corresponding to the dry season, rainy season and annual, respectively.

- Maximum temperature (Tx): The Tx has an increase trend at most stations in the South-Central region. However, the increase rate is much variable among stations, with the rate defined from 0.0°C/year (mostly in the rainy season) to 0.05°C/year (mostly in the dry season). Thus, the annual Tx also has the huge range of increase rate, from 0.01°C/year to 0.04°C/year. On average from 15 stations, the increase rate in the dry season, rainy season and annual is 0.02, 0.01 and 0.02°C/year, respectively.

- Minimum temperature (Tn): The increase rate of the Tn is found from 0.0 to 0.03°C/year at stations in the South-Central region. However, the increase rate is mostly ranged from 0.02 to 0.03°C. Averaging in South-Central region, the increase rate of the Tn is similar in the dry season, the rainy season and annual, with the increase rate that is 0.02°C/year. In general, the increase rate of Tn is slightly higher than increase rate of the Tx.

Changes in rainfall and wet/drought conditions:

- Rainfall (R): Rainfall has the increase trend in both dry and rainy seasons at most stations in the South-Central region. The decrease trend is only found at southern stations of region (Ham Tan, Phu Quy). The significance level of 0.05 is not found at most stations. On average from 15 stations, the increase rate in the dry season, rainy season and annual is 1.46, 0.25 and 0.71%/year, respectively.

- Wet/drought conditions: During 1961-2017, drought condition in the dry season in the South-Central region does not clearly change or slightly decrease at many stations. In particular, the increase in intensity of drought is found at stations in the south of the South-Central region. In the rainy season, the increase in the wet condition is found at most stations. However, the changing trend of the wet condition is not found at many stations in the center and south of the South-Central region.

Discussion:

In this study, the A index is only calculated for data at the 6-month scale (for dry and rainy seasons). Thus, the A index at the season scale does not reflect the extremes of the wet/drought conditions in the South-Central region.

Acknowledgements: This study is grant of funding code: BDKH.04/16/20.

References

1. MONRE, 2009. Climate change, sea level rise scenarios for Vietnam. NARENCA.

2. MONRE, 2012. Climate change, sea level rise scenarios for Vietnam NARENCA..

3. MONRE, 2016. Climate change, sea level rise scenarios for Vietnam. NARENCA.

4. IPCC, 2007. Climate Change 2007: The Scientific Basis. Contribution of Working Group I to the Fourth Assessment Report of the Intergovernmental Panel on Climate Change. *Cambridge University Press.* United Kingdom and New York, NY, USA;

5. IPCC, 2013. Climate Change 2013: The Physical Science Basis. Contribution of Working Group I to the Fifth Assessment Report of the Intergovernmental Panel on Climate Change [Stocker, T.F., D. Qin, G.-K. Plattner, M. Tignor, S.K. Allen, J. Boschung, A. Nauels, Y. Xia, V. Bex and P.M. Midgley (eds.)]. *Cambridge University Press*, Cambridge, United Kingdom and New York, NY, USA, 1535 doi:10.1017/CBO9781107415324.

6. Thanh, N.D. and Tan, P.V., 2012. Non-parametric test for trend detection of some meteorological elements for the period 1961-2007. *VNU Journal of Science*. 3S: 129-135.

7. Mau, N.D., Thang, N.V. and Khiem, M.V., 2016. Changes in rainfall during the summer

monsoon over Vietnam projected by PRECIS model, *VNU Journal of Science*. 3S: 153-166.

8. Ngu, N.D., 2008. Climate change. *Science and Technics Publishing House*.

9. Ngu, N.D. and Hieu, N.T., 1991. Climate change and its impacts in Vietnam during last 100 years - Nature and people. Su That House.

10. Ngu, N.D. and Hieu, N.T., 1999. Climate change in Vietnam in the next decades. *The Vietnam Institute of Meteorology and Hydrology*.

11. Ngu, N.D. and Hieu, N.T., 2004. Climate and Climate resources in Vietnam. *Agriculture House.*

12. Hieu, N.T. and Tuan, D.D., 1999. Scenarios for climate change in the Southeast Asia and Vietnam. *The Vietnam Institute of Meteorology and Hydrology*.

13. Thang, N.V. et al., 2010. Study on the influence of climate change on natural conditions, natural resources and proposing strategic solutions for prevention, mitigation and adaptation to serve the socio-economic sustainable development in Viet Nam. *Technical report of the national project*, Code: KC.08.13/06-10;

14. Thang, N.V. et al., 2013. Chapter 3 of the Viet Nam Special Report on Managing the Risks of Extreme Events and Disasters to Advance Climate change Adaptation. NARENCA.

15. Thang, N.V. et al., 2016. Impacts of Tropical Cyclone Over Vietnam During 1961 - 2014. *VNU Journal of Science*. 3S: 210-216.

16. Thang, N.V. et al, 2017. Changes in climate extreme in Vietnam. *Vietnam Science and Technology (VISTECH)*, 1 (1): 79-87.

17. Tuyen, N.V., 2007. Trend of the tropical cyclone's activity across the Northwest Pacific, East Vietnam sea according the different classifications. *Scientific and Technical Hydro-Meteorological Journal*.

18. Tan, P.V. et al., 2010. Study the impacts of global climate change on climate extreme factors and events in Vietnam, predictability and strategic response. *Final report KC08.29/06-10*.

19. DWR, Ministry of Agriculture and Rural Development (MARD): http://www.vncold.vn/Web/Content.aspx?distid=4061

20. Lien, T.V, 2000. Impacts of climate change and sea level rise on the coastal areas in Vietnam. *Agriculture House*.

21. Lien, T.V., Cuong, H.D. and Son, T.A., 2007. Developing climate change scenarios for in Vietnam for 2010 - 2100, *Scientific and Technical Hydro-Meteorological Journal*.

22. Tri, T.D., Mau, N.D. and Thang, N.V., 2015. Assessment of the 1961-2010 meteorological drought condition based on the A index for Phu Yen- Binh Thuan region. *Scientific and Technical Hydro-Meteorological Journa*l.

23. Hang, V.T., Huong, C.T. and Tan, P.V., 2009. Trend of maximum daily rainfall in Vietnam during 1961-2007. *VNU Journal of Science*. 3S: 423-430.

Research Paper

STUDY OF DROUGHTS IN CA MAU PROVINCE: CHARACTERISTICS AND PREDICTION CAPABILITIES

Nguyen Van Thang[1], Mai Van Khiem[1], Tran Dinh Trong[1]

ARTICLE HISTORY

Received: April 14, 2018; Accepted: May 15, 2018
Publish on: December 25, 2018

ABSTRACT

This paper studies the characteristics of droughts in Ca Mau and its prediction capabilities. It shows that drought cycle in Ca Mau annually occurs with dry season. The most severe droughts occur in January, February and March with the frequency of 90 – 95%. Average duration of drought season is about 4 months which can be longer in few years. Longer duration drought and more severe intensity drought mostly occur in the El-Nino year. In addition, by applying the Regional Spectral Model (RSM) for drought prediction, the results show that the RSM model captures well the inter-annual variation of the SPI index at timescale of 12 months, especially during severe water scarcity periods. Underestimated errors in the predicted SPI value can be bias-corrected for more proper determination of droughts from the RSM output. An important issue of drought prediction is warning of drought intensity during either dry or rainy season. The assessment of long-term water scarcity using the SPI index can provide warning of drought intensity in future.

Keywords: *Drought, Duration, Intensity, The RSM model, The SPI index.*

1. Introduction

Located in the West of the South Vietnam, the climate in Ca Mau province is characterized by distinct rainy and dry seasons. Droughts occur almost every year in Ca Mau, in dry season (i.e. winter and early spring) with varying intensity. Moreover, drought season in the El-Nino year usually has longer duration and more severe intensity (Nguyen et al., 1995; Nguyen and Nguyen, 2003).

In order to study characteristics of drought in Ca Mau, we proposed a number of drought indices in which monthly and annual indices are recognized as the most suitable indicators. These indices not only represent the water balance at monthly and yearly timescale but also provide the basis for determining the dry and wet season in the study area. However, the drought index is not able to represent the level of water scarcity in rainy season when precipitation, although higher than evaporation, is still lower than the climatic average value (McKee et al., 1993). Therefore, the Standardized Precipitation Index (SPI) is also used with different timescales (6 and 12 months) for assessing the level of temporary precipitation deficit as well as precipitation deficit over a long preceding period (Nguyen, 1995; Nguyen, 2014; McKee et al., 1993).

2. Data and method

2.1 Statistical method

NGUYEN VAN THANG
nvthang.62@gmail.com
[1]Viet Nam Institute of Meteorology, Hydrology and Climate change

Drought frequency calculation:

$$P_t(H) = \frac{M(H)_t}{N(H)_t} \quad (1)$$

Determining drought trend

One of trend analysis methods which are usually applied in the study of climate variability is regression analysis. The regression method described in this study is the regression between the climatic variable (x) and the time (t), i.e. the variation of x in t: x = f (t).If f(t) is a linear function, then the trend will be linear. In other cases, a non-linear trend is considered (Nguyen V. Th., 2007; Hoang D. C. and Nguyen T. H., 2012; Juang and Kanamitsu, 1997].

To study the linear trend, we construct the regression equation:

$$x(t) = at + b \quad (2)$$

where a, b is the regression coefficient determined by:

$$a = \frac{\sum_{t=1}^{n}(x_t - \bar{x})(t - \bar{t})}{\sqrt{\sum_{t=1}^{n}(x_t - \bar{x})^2 \sum_{t=1}^{n}(t - \bar{t})^2}} \quad (3)$$

$$b = \bar{x} - a\bar{t} \quad (4)$$

$$\bar{x} = \frac{1}{n}\sum_{t=1}^{n} x_t \quad (5) \qquad \bar{t} = \frac{1}{n}\sum_{t=1}^{n} t \quad (6)$$

From this equation, the linear trend of time series is recognized by the slope a. The sign of the slopea determines the increase(a> 0) or decrease (a <0) trend while the absolute value of a indicates magnitude of this trend.

For practical purpose, the total time series can be splited into different sub-series to analyze the trend. Then the trends of different periods can be determined based on different slopes (a).

Determining drought season, drought onset and withdraw date

Determining the date of drought onset and demise from the monthly time series applying the Conrat method:

$$n(BĐH) = 15 \text{ month i} + \frac{K_i - 2}{K_i - K_{(i+1)}} xD_i \quad (7)$$

where,

n(BDH): drought onset date

i, i+1: two adjacent months with $K_i < 2 < K_{(i+1)}$

D_i: number of days in month i

$$n(KTH) = 15 \text{ months i} + \frac{K_i - 2}{K_i - K_{(i+1)}} xD_i$$

n(KTH): date of drought demise

$K_i > 2 > K_{(i+1)}$

2.2 Dynamical approach

In this study, the regional spectral model (RSM) is used for drought prediction in Ca Mau by applying and analyzing the Standardized Precipitation Index (SPI). The SPI index is proposed by Mckee T. B., Doesken N. J. and Kleist J., from the Colorado State University in1993. The SPI index is calculated as the difference between the precipitation amount R(total amount for week, month, season or year) and the long-term average of precipitation then is divided by the standard deviation :

$$SPI = \frac{R - \bar{R}}{\sigma} \quad (8)$$

In this study, the long-term average and the standard deviation are computed for the period of 1986-2005. The SPI index is based on the amount of precipitation in a specific period and is highly recommended by decision makers and researchers due to its versatility. This index can be calculated at different timescales (e.g. 3, 6, 12, 24, 48 months) thus can provide early warning of drought with level of drought intensity although applying simple calculation. Drought occurs as SPI is lower than -1.0 and drought demises as SPI returns to positive value.

The RSM applied in this study is a hydrostatic model with simulation domain from 0oN to 30^{o}N and from 95 - 125^{o}E (Figure 1). The horizontal resolution is 26x26km with 28 vertical levels implementing the time step of 60s. The applied parameterization schemes in the RSM model are shown in Table 1.

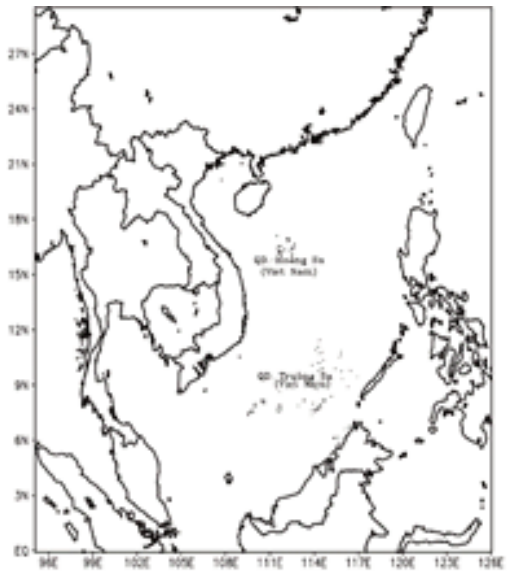

Fig.1. Simulation domain of the RSM model

Table 1. Parameterization scheme using in the RSM model (Juang et al., 1994; Saha, 2006)

Physics options	Reference
Microphysics	Hong et al. 1998
Longwave radiation (RRTM)	Mlawer et al. 1997
Shortwave radiation	Chou and Suarez, 1999; Hou et al, 2002.
Surface layer (JMonin-Obukhov)	Skamarock et al. 2005
Land surface	Pan and Mahrt, 1987
Planetary Boundary Layer	Troen and Mahrt, 1986
Cumulus Parameterization (SAS)	Pan and Wu 1994, Grell, 1993.
Vertical diffusion	Hong et al, 1996

3. Results and discussions

3.1. Drought characteristics in Ca Mau

- Drought frequency

Table 2 presents the frequency of drought appearance in each month with three intensity levels of slight, moderate and severe. Slight droughts (or abnormally dry events) start early in November and end in May which is later than moderate and severe droughts. The appearance frequency of slight droughts is highest in December (30,8%) and April (25,6%). Slight droughts do not occur from June to October. The strong El Niño event of 1997-1998 lasted about 12 months from May/1997 to April/1998. During that time, the amount of rainfall decreased about 9 months over some Viet Nam's climatic regions by this El Nino; the most serious lack of the amount of rainfall took place in October and November/97 over the Central region, especially the coastal zone (Vu V. Th., 2016; Tran Th., 2008).

Moderate droughts start in December and end in April with highest frequency of appearance in December and January (20,5%). There is not moderate drought from May to November.

Severe droughts start in December and end in April with highest appearance frequency in February (79,5%), followed by March (64,1%) and January (61,5%).

In general, droughts occur in February with highest frequency (97,4%), then January and March (both these two months have frequency of 89,7%).

Table 2. Frequency of drought appearance in months (period 1979 - 2017)

		I	II	III	IV	V	VI	VII	VIII	IX	X	XI	XII
Slight drought	STH	3	5	5	10	2	0	0	0	0	0	3	12
	%	7.7	12.8	12.8	25.6	5.1	0.0	0.0	0.0	0.0	0.0	7.7	30.8
Moderate drought	STH	8	2	5	2	0	0	0	0	0	0	0	8
	%	20.5	5.1	12.8	5.1	0.0	0.0	0.0	0.0	0.0	0.0	0.0	20.5
Severe drought	STH	24	31	25	10	0	0	0	0	0	0	0	10
	%	61.5	79.5	64.1	25.6	0.0	0.0	0.0	0.0	0.0	0.0	0.0	25.6
Total	STH	**35**	**38**	**35**	**22**	**2**	**0**	**0**	**0**	**0**	**0**	**3**	**30**
	%	**89.7**	**97.4**	**89.7**	**56.4**	**5.1**	**0.0**	**0.0**	**0.0**	**0.0**	**0.0**	**7.7**	**76.9**

Table 3. Drought season and duration in Ca Mau during period of 1979 - 2017

Drought onset	Drought demise	Duration (month)
29/XI/1978	13/IV/1979	4.5
15/I/1980	18/III/1980	2.1
25/XI/1980	4/IV/1981	4.3
15/XII/1981	18/III/1982	3.1
26/XI/1982	13/V/1983	5.6
25/XII/1983	14/IV/1984	3.7
21/XII/1984	25/III/1985	3.1
2/I/1986	25/IV/1986	3.8
16/XII/1986	18/III/1987	3.1
16/XII/1987	15/IV/1988	4.0
9/XII/1988	13/III/1989	3.1
25/XI/1989	15/IV/1990	4.7
15/XII/1990	20/III/1991	3.2
29/XI/1991	15/IV/1992	4.6
4/XII/1992	4/V/1993	5.0
19/XII/1993	10/V/1994	4.7
26/XII/1994	5/V/1995	4.3
19/I/1996	13/IV/1996	2.8
15/XII/1996	4/IV/1997	3.7
18/XI/1997	15/V/1998	5.9
NO	NO	
21/XII/1999	17/III/2000	2.9
4/XII/2000	9/II/2001	2.2
14/XII/2001	16/V/2002	5.1
14/XII/2002	1/V/2003	4.6
26/XI/2003	15/IV/2004	4.7
24/XI/2004	14/V/2005	5.7
15/I/2006	15/IV/2006	3.0
27/XI/2006	1/IV/2007	4.2
15/XI/2007	15/IV/2008	5.0
30/XII/2008	14/IV/2009	3.5
21/XII/2009	15/V/2010	5.8
29/XI/2010	18/III/2011	3.6
17/XII/2011	5/III/2012	2.6
20/XI/2012	15/IV/2013	4.9
5/XII/2013	15/IV/2014	4.4
11/I/2014	14/V/2015	4.1
15/XII/2015	15/V/2016	5.0
15/II/2017	13/IV/2017	1.9

- Drought season, duration and classification

Table 3 presents the calculated date for drought onset and drought demise using drought index Ht during period of 1979 - 2017. During 39 years, drought occurred almost every dry season with average duration of about 4 months. Short drought season (less than 3 months) occurred in 1979 - 1980 (although the onset date of drought season is in January 1980 and demise date in March 1980, this event is still consiodered as drought season 1979 - 1980) with duration of 2,1 months; 1995 - 1996: 2,8 months,

1999 - 2000:2,9 months, 2000 - 2001: 2,2 months; 2011 - 2012: 2,6 months and 2016 - 2017: 1,9 months. However, drought season can prolong more than 5 months such as 1982 - 1983, 1992 - 1993, 1997 - 1998, 2001 - 2002, 2004 - 2005, 2007 - 2008, 2009 - 2010, 2015 - 2016. There is not drought in the dry season of 1998 - 1999.

Of the more than 5-month-drought years above, the El Nino phenomenon occurred in 1982 - 1983, 1997 - 1998, 2004 - 2005, 2009 - 2010, 2015 – 2016, whereas the ENSO of neutral state was in 1992 - 1993, 2001 - 2002 and the La Nina phase occurred in 2007 - 2008.

Short drought duration or no drought occurred in the La Nina year, excepted the drought seaon of 1979-1980 occurred in a weak phase of El Nino.

On average, there are more than 4 months of drought per year with the highest record of 6 months in 1994 and 2010. However, severe drought occurred in 2010 was stronger than that in 1994 with 5 and 3 months relatively. There are twelve years with 5 months of drought, in which 4 severe droughts occurred in 1993, 1998, 2002, 2003. There are 18 years with 4 months of drought in which severe droughts occurred in 2004, 2005, 2016. In general, severe drought occurred with highest frequency during study period (100 per total 165 drought months) and there are 25 months of moderate drought and 40 months of slight drought.

Table 4. Yearly number of drought month with different intensity level

Year	Slight	Moderate	Severe	Total	Year	Slight	Moderate	Severe	Total
1979	0	0	3	3	**1999**	2	0	0	2
1980	2	0	2	4	**2000**	1	1	2	4
1981	0	0	2	2	**2001**	2	2	0	4
1982	0	0	3	3	**2002**	0	1	4	5
1983	1	1	3	5	**2003**	0	1	4	5
1984	2	2	1	5	**2004**	0	0	4	4
1985	1	2	1	4	**2005**	0	0	4	4
1986	1	2	2	5	**2006**	2	1	2	5
1987	3	0	2	5	**2007**	1	2	2	5
1988	0	1	3	4	**2008**	1	0	2	3
1989	1	0	3	4	**2009**	1	1	2	4
1990	1	0	3	4	**2010**	1	0	5	6
1991	0	2	2	4	**2011**	3	0	2	5
1992	2	1	2	5	**2012**	0	0	3	3
1993	1	0	4	5	**2013**	0	2	2	4
1994	2	1	3	6	**2014**	1	0	3	4
1995	0	1	3	4	**2015**	1	1	3	5
1996	2	0	2	4	**2016**	0	0	4	4
1997	1	0	3	4	**2017**	3	0	1	4
1998	1	0	4	5	**Total**	40	25	100	165

- Trend of drought in Ca Mau

Based on trend analysis methods from series of drought indices, we calculated the drought trend for Ca Mau. As analyzed above, the drought index Ht is considered as the most suitable index for studying the characteristic and intensity of drought in Vietnam. Therefore, in order to be consistent with the assessment, the yearly Ht series is used to construct the linear trend equation and calculate the correlation coefficient, which determines the temporal variability.

Linear trend equation of the yearly Ht index is:

$$Y = 0.0035t + 0.3511$$

As can be seen, the higher value of the index Ht, the more severe drought occurs. During the last 40 years, there is an increase trend of drought in Ca Mau at the rate of 0.0035 unit per year.

- Assessment of water scarcity in Ca Mau

At timescale of 6 months, the calculated SPI index for the period of 1979 - 2017 highlights the occurrence of the water scarcity in Ca Mau during the period of 1981 - 1982, 1983 - 1987, 1990 - 1991, 2004 - 2005, 2013 - 2016 and es-

pecially in 2010 with very severe water scarcity.

During the timescale of 12 months, Ca Mau experiencesd a long period of water scarcity includes 1983 - 1992, 2004 - 2005, 2010 - 2011, 2013 - 2017.

The water scarcity condition existents in long time, leading to the occurrence of severe droughts. For example, water scarcity during 1981 - 1982 (at timescale of 6 months) causes long severe drought in 1982/1983; or water shortage during 1983 - 1987, 1990 - 1991 (timescale of 6 months) and 1983 - 1992 (timescale of 12 months) causes severe drought in 1992/1993; or water scarcity during 2004 - 2005 causes severe drought in 2004/2005; or water scarcity during 2013 - 2016 and 2013 - 2017 causes extreme severe drought in 2015/2016.

3.2 Prediction capability using the RSM model

Firstly, the SPI index calculated from the RSM model is compared with the SPI index calculated from the observation data using the Mean Error (ME) and Mean Absolute Error (MAE) [Saha, 2014]. The results show that the RSM model predicts higher value of the SPI index (ME is positive) in comparison with observation at all 5 leadtimes from 1 to 5 months. Longer leadtimes tend to have higher overestimated bias. MAE represents the magnitude of error for SPIprediction using the RSM model in comparison with the observation at Ca Mau station.

In general, the lowest error is achieved as using the SPI index at timescale of 12 months with MAE is approximately 1.0. In contrast, the RSM model predicts the SPI index at timescale of 3 months with highest error as MAE is from 2,2 to 3,5. In terms of leadtime differences, the leadtime of 1 month leads to highest MAE in comparison with all timescale from 1 to 6 months of the SPI index.

Table 5. Mean Error (ME) and Mean Absolute Error (MAE) of SPI prediction using the RSM model

Leadtime	1-month		3-months		6-months		12-months	
	ME	MAE	ME	MAE	ME	MAE	ME	MAE
leadtime01	0.3	2.8	0.1	3.5	0.1	1.9	0	0.9
leadtime02	0.3	2.4	0.3	2.6	0.2	1.6	0.1	1.1
leadtime03	0.3	2.2	0.3	2.3	0.2	1.3	0	0.9
leadtime04	0.5	2.1	0.4	2.2	0.4	1.3	0.5	1.1
leadtime05	0.6	2.3	0.4	2.6	0.2	1.3	0.3	1.1

Table 6. Probability of correct prediction for drought using the RSM model

Leadtime	1-month prediction	3-month prediction	6-monthprediction	12-monthprediction
leadtime01	29	35	44.7	5.8
leadtime02	9.7	22.5	23.4	17.3
leadtime03	12.9	25	25.5	13.5
leadtime04	9.7	20	23.4	11.5
leadtime05	12.9	22.5	21.3	15.4

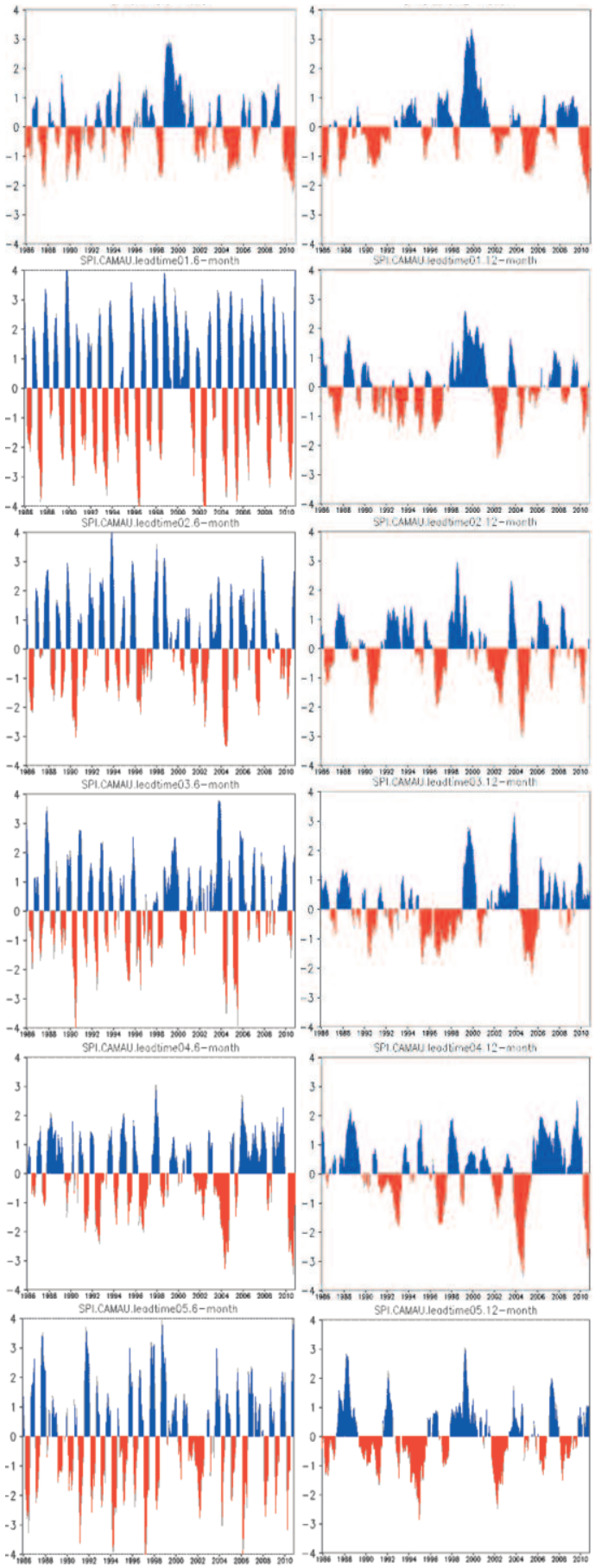

Fig. 2. Inter-annual variation of the SPI at timescale of 6 months (left) and 12 months (right) from observation and the RSM model

Table 6 presents the probability of correct prediction (PC) for monthly drought using the RSM model with the SPI index in which drought month determined by less than -1 of SPI value. The results show that the highest PC is attained as using the SPI index at timescale of 6 months (21-45%), especially the PC at leadtime of 1 month reaches 44,7%. Applying the SPI index at timescale of 3 months, the PC is higher than 20% in comparison with other leadtimes. The prediction results implementing the SPI index at timescale of 1 and 12 months are worse than at timescale of 3 and 6 months with PC is mostly from 10 to 17%.

For more detailed assessments of the prediction capability using the RSM model, the inter-annual variations of the SPI at timescale of 6 months and 12 months are calculated and presented in Figure 2.The results highlight that although the PC value at timescale of 6 months is higher than that of 12 months, the RSM model is unable to capture well the duration and intensity of droughts in compared with observation. The droughts at 6 months timescale predicted from the RSM model have shorter duration than observation but more severe in intensity. Meanwhile, within the timescale of 12 months, the RSM model generally captures better the drought characteristics in Ca Mau. According to the observation, noticeable water scarcity events occurred in Ca Mau in 1986, 1988, 1990-1992, 2004-2006 and 2010. In comparison with observation, the RSM model represents almost these water scarcity periods, especially with leadtime of 2 months. The duration of predicted water scarcity periods is approximate to the observation but the magnitude of error is still high. Generally, the RSM model can be implemented for prediction of water scarcity at long timescale in Ca Mau. However, bias correction is required for better prediction results.

4. Conclusion

Droughts in Ca Mau occur at annual cycle (i.e. every year) coinciding with dry season, however their trend becomes more and more severe. The most severe droughts occur in January, February, March with the frequency of 90 – 95%. Average duration of drought season is about 4 months which can be longer in few years. Longer duration drought and more severe intensity drought mostly occur in the El-Nino year.

In this study, the RSM model and the SPI index are applied for drought prediction in Ca Mau. The results show that the RSM model capture well the inter-annual variation of the SPI index at timescale of 12 months at the meteorological observation station Ca Mau, includes severe water scarcity condition existences in long time. There are still the underestimated errors in the prediction of the SPI value. However, these errors tend to have systematical bias which can be bias corrected or adjusted the index threshold for proper determining droughts from the model output.

Since drought occurs every year, drought prediction is not limited to the prediction of drought season and drought frequency, the more important issue is warning and prediction of drought intensity during either dry or rainy season. The calculation and assessment of long-term water scarcity using the SPI index can provide warning of drought intensity in future.

Acknowledgements

This paper is part of a ministry level project entitled: "Studies of scientific basis for determining the level of natural disaster ricks due to droughts and seawater intrusion, applying test for the South of Vietnam", code: TNMT.2017.05.06 funded by the Ministry of Natural Resources and Environment.

Authors acknowledge the support and contribution of the research team at the Center for Meteorology and Climatology, of the Vietnam Institute of Meteorology, Hydrology and Climate change for participating in research, supporting and contributing to the completion of the paper.

Also, special thank to a research contract entitled: "The analysis of the drought impact and existing forecasting system in the areas targeted by project OSRO/VIE/702/EC in Gia Lai and Ca Mau Provinces", jointly signed by the Food and Agriculture Organization of the United Nations ("FAO") under ECHO/-XA/BUD/2017/91013 and the Center for Meteorology and Climatology, for supporting.

References

1. Nguyen, D.N., Nguyen, T.H., 1995. Methodology for preparing climate information for national economic sectors. *Scientific and Technical Publisher*.

2. Nguyen, D.N., Nguyen, T.H., 2003. Drought and desertification in Vietnam. *Scientific and Technical Publisher*.

3. Nguyen, T. H., 1995. Drought distribution and its impacts. Vietnam Institute of Meteorology. *Hydrology and Climate Change.*

4. Hoang, D. C., Nguyen, T. H., 2012. Lecture on statistic in climatology. *Natural Science and Technology Publisher*.

5. Juang, H.H., Kanamitsu, M., 1994. The NMC nested regional spectral model. *Mon Weather Rev.* 122: 3-26.

6. Juang H. H., Hong, S., Kanamitsu M., 1997. The NCEP regional spectral model: an update. *Bull Am Meteor Soc.* 78: 2125-2143.

7. Nguyen, V.T., et. al., 2007. Research and develop a technology for drought prediction and early warning in Viet Nam. *Final report of the Ministerial level project.*

8. Nguyen, V. T., et. al., 2014. Study on drought forecast and warning system in Viet Nam in period of 3 months. *Final report of the National project KC.08/11-15*

9. McKee, T. B., N. J. Doesken, and J. Kleist, 1993. The relationship of drought frequency and duration to time scale. Preprints, Eighth Conf. on Applied Climatology, Anaheim, CA, Amer. *Meteor. Soc.,* 179 - 184.

10. Saha, S., Coauthors, 2006. The NCEP Climate Forecast System. *J. Climate*, 19, 3483-3517.

11. Saha, S., Moorthi, S., Wu X, Wang, J., Nadiga, S., Tripp, P., Pan H-L., Behringer, D., Hou Y-T., Chuang H-y, Iredell M., Ek M, Meng J., Yang R., Van den Dool H, Zhang Q., Wang W., Chen M., 2014. The NCEP Climate Forecast System Version 2. *Journal of Climate.* 27: 2185-2208.

12. Tran, T.H., et al, 2008. Building the maps of droughts and the water deficit level of the South of the Middle and the Highland. *Final report of the Ministerial level project.*

13. Vu, V.Th., et al, 2016. Research thermodynamic mechanism causing heavy rain and possibility of forecasting heavy rains in the South and South Highlands due to South West monsoon – tropical cyclone interaction in the EAST Sea. *Final report of the Ministerial level project*.

Vietnam Journal of Hydrometeorology, ISSN 2525-2208, Volume 01: 20 - 29

Research Paper

A STUDY ON DROUGHT IN THE SOUTH-CENTRAL REGION: DETECTION FROM THE OBSERVATION AND THE BIAS-CORRECTION RAINFALL PROJECTIONS OF NATIONAL CLIMATE CHANGE SCENARIOS

Mai Kim Lien[1], Tran Duy Hien[2]

ARTICLE HISTORY

Received: March 15, 2018; Accepted: April 20, 2018 Publish on: December 25, 2018

ABSTRACT

This article presents the results of detecting the trend of drought conditions in the South-Central region based on the past observation and bias-correction rainfall projections. The past observation of daily rainfall is updated up to 2017 and collected from Vietnam Meteorological and Hydrological Administration. The bias-correction daily rainfall projections are collected from Vietnam Institute of Meteorology, Hydrology and Climate change (IMHEN) during the periods of 1986 - 2005, 2016 - 2035, 2036 - 2065 and 2080 - 2099 according to both RCP4.5 and RCP8.5 scenarios. The Standardized Precipitation Index (SPI) and minimum value of SPI (SPI_min) are used to define the mean drought condition and the most extreme drought condition. The past trend of drought conditions is found that the decreasing trends of mean drought condition and increasing trends of the severity level. The future trend of drought conditions according to both RCP4.5 and RCP8.5 is found that it is similar to the past trend. Where, the mean drought condition is generally found by slight decreasing trends. However, the most extreme of drought condition is significantly found by increasing trends of drought at shorter timescales (1- and 3-month time scales).

Keywords*: Drought condition, extreme drought, SPI, SPI_min, South-Central region.*

1. Introduction

Comparing with other climatic regions, the South - Central region has lowest dry seasonal rainfall. The dry season in the South-Central is longer than in other regions that mostly ranged from December (in the previous year) to August (in the next year). The climatology peak of the dry season is from January to March. Especially, the dry/drought condition in the South-Central region is known as having the strongest intensity in Vietnam (Ngu and Hieu, 2004).

As above mentioned, the dry/drought condition extremely has impacted on socio-economic sectors, environment and human life. Thus, many studies were focused on the dry/drought condition in the South- Central region. Thang et al. (2007) showed the very extreme drought events that ever occurred during 1980 - 2005 in the South - Central region as listed in 1983, 1993 and 1998. Where, extreme winter - spring drought events occurred in 1983, 1993, 1998 and summer - autumn drought in 1982, 1985, 1988, 1993 and 1998. Especially, the very extreme drought event in the dry season 2015 - 2016 due to impacts of El Nino event (DWR, 2016).

Recent years, the global warming issue is considered as the major factor for increasing extreme events in terms of frequency and intensity (IPCC, 2007, 2013). In Vietnam, many climate changes scenarios have been published by Ministry of Natural resources and Environment (MONRE) since 2009 (MONRE, 2009, 2012, 2016). These scenarios showed the increasing

MAI KIM LIEN
lien_va21@yahoo.com
[1]Department of Climate Change, MONRE
[2]Science and Technology, MONRE

trend of temperature in the future according to GHG scenarios.

In 2016, MONRE published the "Climate change and sea level rise scenarios for Vietnam" based on the calculations of IMHEN (IMHEN, 2016). Where, the information of temperature and rainfall as well as some of its extreme events that can be found. However, the very important information is drought condition is not detected. Thus, the drought condition detected by these bias-corrected rainfall projections is very important information for implementing responding to climate change. Especially, the information related to the drought projection is significantly required for assessment of climate change on many important sectors. From these mentioned above, we try to detect the drought projection for the South-Central region that is calculated by the bias-correction rainfall collected from IMHEN (2016).

2. Data and method

2.1. Data collected

In this study, we collected daily rainfall for 11 stations (Table 1) from sources as listed as:

- Daily rainfall observed: The 1975-2017 daily rainfall is collected from VMHA.

- Daily rainfall projected according to RCP4.5 and RCP8.5 scenarios: In this study, the bias-correction daily rainfall for 1980 - 2005, 2046 - 2065 and 2080 - 2099 is collected from IMHEN (IMHEN, 2016). The Table 2 presents the number of the projections that are used in this study.

Table 1. List of stations used in the study

No.	Name of station	Longitude	Latitude
1	Da Nang	108.18	16.03
2	Tam Ky	108.5	15.55
3	Tra My	108.21	15.35
4	Ba To	108.71	14.76
5	Quang Ngai	108.78	15.13
6	Hoai Nhon	109.01	14.53
7	Quy Nhon	109.21	13.76
8	Son Hoa	108.98	13.05
9	Tuy Hoa	109.28	13.08
10	Nha Trang	109.2	12.25
11	Cam Ranh	109.16	11.95

Table 2. Simulations and projections used in the study (IMHEN, 2016)

No.	Regional climate models (RCMs)	Global climate models (GCMs)	Resolution of RCMs
1	CCAM	ACCESS1-0	10km
2		CCSM4	
3		CNRM-CM5	
4		GFDL-CM3	
5		MPI-ESM-LR	
6		NorESM1-M	
7	RegCM	ACCESS1-0	20km
8		NorESM1-M	
9	PRECIS	HadGEM2-ES	25km
10		GFDL-CM3	
11		CNRM-CM5	
12	CLWRF	NorESM1-M	30km
13	MRI-20km_A	NCAR-SST	20km
14	MRI-20km_B	HadGEM2- SST	
15	MRI-20km_C	GFDL - SST	
16	MRI-20km_D	Tổ hợp SST	

2.2 Methods of study

Definition of the drought condition:

The Standardized Precipitation Index (SPI) is used to define the drought condition (WMO, 2012). The SPI was designed to quantify the precipitation deficit for multiple timescales. These timescales reflect the impact of drought on the availability of the different water resources. Soil moisture conditions respond to precipitation anomalies on a relatively short scale. Groundwater, streamflow and reservoir storage reflect the longer-term precipitation anomalies. For these reasons, McKee et al. (1993) originally calculated the SPI for 3-, 6-,12-, 24- and 48-month timescales.

The SPI calculation for any location is based on the long-term precipitation record for a desired period. This long-term record is fitted to a probability distribution, which is then transformed into a normal distribution so that the mean SPI for the location and desired period is zero (Edwards and McKee, 1997). Positive SPI values indicate greater than median precipitation and negative values indicate less than median precipitation. Because the SPI is normalized, wetter and drier climates can be represented in the same way; thus, wet periods can also be monitored using the SPI.

In recent years, the SPI for 3-, 6-,12-, 24- and 48-month timescales are used to define the drought condition of many types of drought as Meteorological, Agriculture and Hydrological drought conditions, respectively (WMO, 2012; Liu et al., 2013; James et al., 2015; Marzena Osuch et al., 2016; Dongwoo Jang, 2018).

SPI is defined by the below equation (WMO, 2012):

$$SPI = \frac{R - R}{\sigma} \quad (1)$$

where σ is the standard deviation of rainfall; R and $\overline{R}$ are the rainfall and climatology rainfall, respectively.

In general, the drought condition occurs when the SPI<0 (Thang et al., 2007; Tri et al., 2015; WMO, 2012). In this study, the extreme drought event is defined by the minimum value of the SPI (called as SPI_min). Thus, the trend of SPI_min means that the trend of the most extreme drought condition is defined.

As mentioned above, the drought and extreme drought conditions are considered for many timescales of 1-, 3-, 6- and 12-month (SPI_1, SPI_3, SPI_6 and SPI_12). As mentioned by WMO (2012) and many studies (Thang et al, 2007; Tri et al., 2015), we can define many types of drought based on the timescales of SPI as:

- SPI_1: Meteorological drought
- SPI_3 and SPI_6: Agriculture drought;
- SPI_12: Hydrological drought.

Definition of the drought trend:

For identifying the drought trend in the South-Central, we use the simple linear regression equation as used in many studies (IPCC, 2007, 2013; MONRE, 2009, 2012, 2016; Thang et al., 2015).

Given a data set X: $x_1, x_2, x_3, \ldots, x_n$ of n statistical units.

Consider the simple linear equation:

$$x_t = b_0 + b_1 t \quad (2)$$

where

$$b_1 = \frac{\sum_{t=1}^{n}(x_t - \bar{x})(t - \bar{t})}{\sum_{t=1}^{n}(t - \bar{t})^2}$$

$$b_0 = \bar{x} - b_1 \bar{t}$$

We can find:

- b_1: the slope of the fitted line (linear changing rate)
- b^o: mean value mass of the data points

From that, we can find the increase/decrease rate of the duration study as: $D = b_1 n$ (3)

where n is sample sizes.

We can define the correlation coefficient (r_{xt}):

Definition of the change rate of projection:

The change of projection is defined by comparing the future SPI (or SPI_min) with baseline SPI (or SPI_min). These two future periods are the period of 2046 - 2065 and 2080 - 2099. The baseline period is 1986 - 2005. The change of

SPI (or SPI_min) is defined by the below equation as:

$$\Delta SPI_{future} = \frac{\left(SPI^{*}_{future} - \overline{SPI^{*}_{1986\text{-}2005}}\right)}{SPI^{*}_{1986\text{-}2005}} * 100$$

Where ΔSPIfuture is the future change rate (%) of SPI (or SPI_min); SPI^{*}_{future} and $SPI^{*}_{1986\text{-}2005}$ are the future SPI (or SPI_min) and past SPI (or SPI_min), respectively.

In this study, the SPI index is calculated by mean ensemble of the bias-correction rainfall projections for each scenario and each period.

3. Results of study

3.1 Assessment of the past drought condition in the South - Central region

Results of the 1975 - 2017 trend of the SPI at timescales are presented in the Fig.1. In general, the increasing trend of SPI is found at most of stations. The increasing rate of SPI is found from 0.02 to 0.06/decade. In which, the increasing rate of longer timescales is higher than shorter timescales. This trend means that the decrease trend of mean drought condition at all timescales. This decreasing trend of the mean drought condition is ordered by the increase trend of the rainfall projection (see more trend of rainfall in MONRE, 2016).

Remarkably, the important result is that the increase trend of the extreme drought condition is found (Fig. 2). As Fig. 2, we can find the significant decrease trend of SPI index at 1- and 3-month timescales. The decrease rate of SPI_min index at these two timescales is mostly from 0.02 to 0.06/decade at most stations. For 6-month timescale, the decrease trend of the SPI_min is only found at stations in the southern part of the South-Central. However, the increase trend is found at all stations (Fig. 2).

From these above analyses, the mean drought condition at all timescales is found as decreasing in intensity according to the increase of rainfall. However, the most extreme of drought at timescales from 1- to 3-month is found that increasing in intensity.

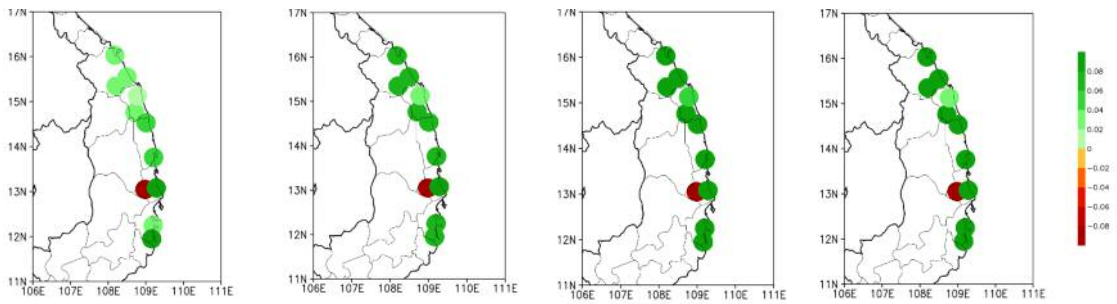

(a) (b) (c) (d)

Fig. 1. The change rate of the SPI index (unit/decade): (a) SPI_1, (b) SPI_3, (c) SPI_6 và (d) SPI_12

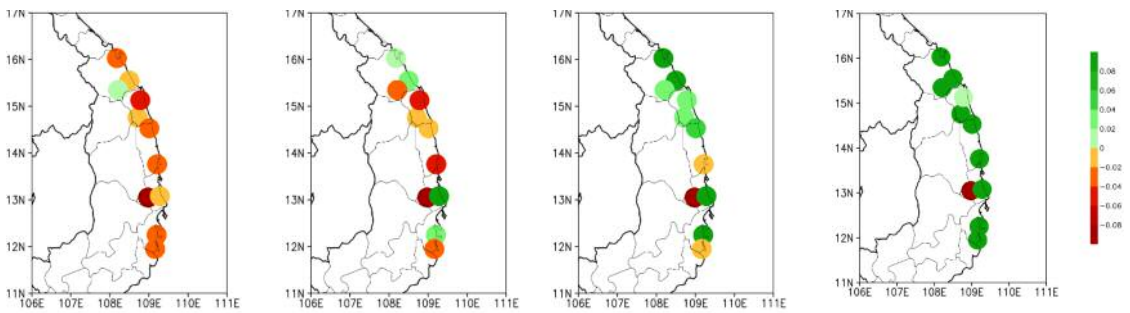

(a) (b) (c) (d)

Fig. 2. SPI_Min: (a) SPI_1, (b) SPI_3, (c) SPI_6 và (d) SPI_12

3.2 The projections of drought condition according to scenarios

3.2.1 Drought condition projections for 2016 - 2035

The Fig.3 shows the results of the changes in SPI (%) of 2016 - 2035 compared with baseline period at 1-, 3-, 6- and 12-month timescales. We clearly find increasing trends of SPI at all timescales. These results show that the mean drought condition in the South-Central region is expected to decrease compared with the baseline period. In general, the SPI of the 2016 - 2035 projected to increase by from 0 to 0.8% compared with the baseline period. The increasing rate of the shorter timescales (1- and 3-month) is smaller than longer timescale (6- and 12-month).

Comparing the Fig. 4 with the Fig. 3, according to both RCP4.5 and RCP8.5 scenarios, the significant difference between trend of SPI and SPI_min can be found. Meanwhile, SPI is defined by increasing trend of projections for all timescales at all stations as shown in the Fig.3. In contrast, SPI_min at 1- to 6-month timescales is defined by an obvious decreasing trend of projections at stations in the central and southern areas of the South - Central region as shown in the Fig.4. Comparing with the baseline period, the decreasing rate of the SPI_min from 2016 to 2035 is identified from 0 to 0.2%. Where, the higher decrease rate of SPI_min is found by projection according to the RCP8.5 (Fig. 4).

These results indicate that the mean drought condition in the South-Central during 2016 - 2035 is expected to decrease compared with the baseline period. However, the severity of drought condition is expected to increase at the central and southern stations, especially on the shorter timescales. The increasing trends of extreme drought at shorter timescales are found by both RCP4.5 and RCP8.5 projection scenarios. Although, the very long timescale (12-month), the increasing trend of extreme drought is not found by these projections.

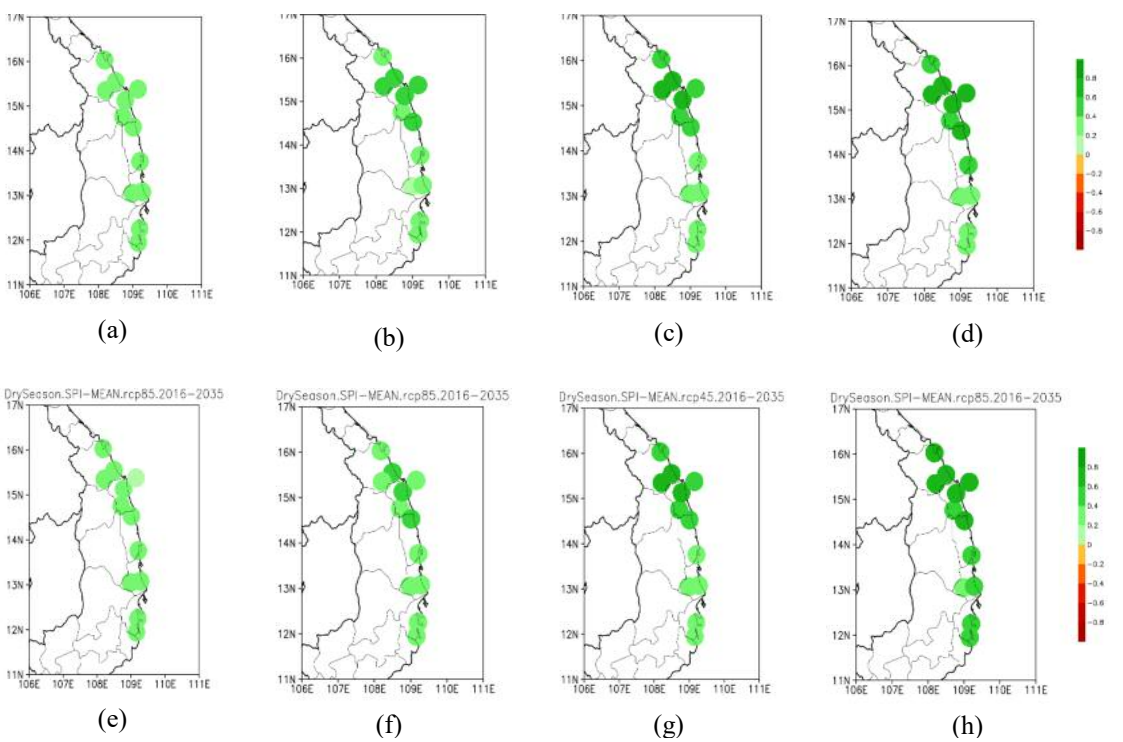

Fig. 3. Changes in SPI index (%) at timescales calculated from bias-correction rainfall for 2016-2035 compared with baseline period according to RCP4.5 (above maps) and RCP8.5 (below maps) scenarios: SPI_1 (a, e), SPI_3 (b, f), SPI_6 (c, g) and SPI_12 (d, h)

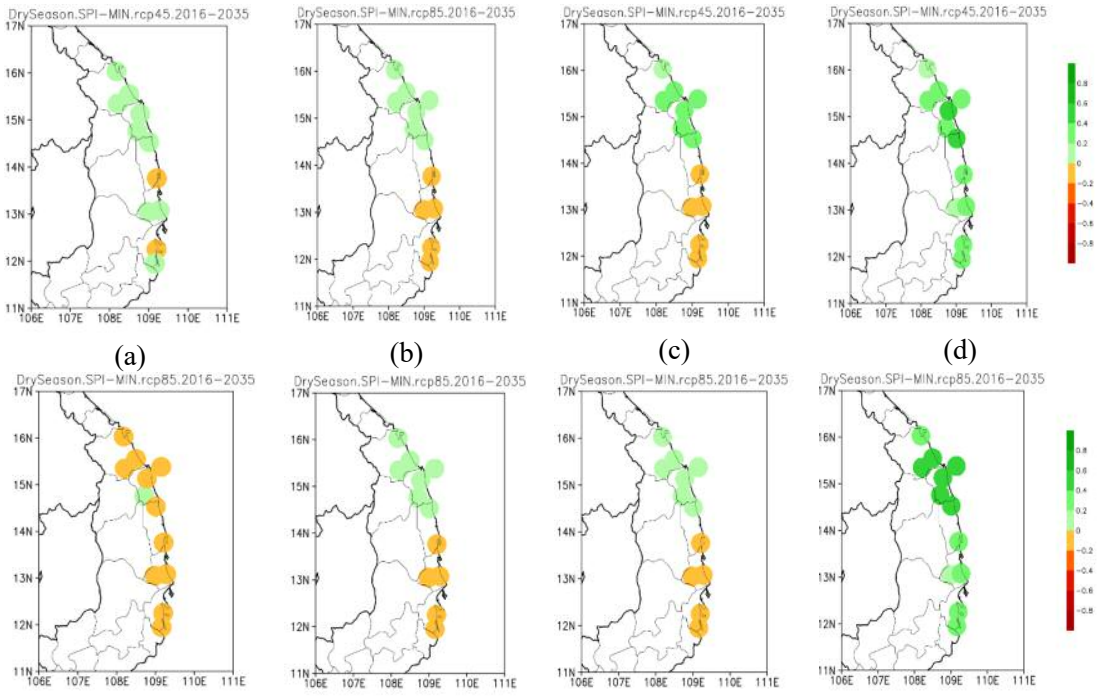

Fig. 4. SPI_Min: SPI_1 (a, e), SPI_3 (b, f), SPI_6 (c, g) and SPI_12 (d, h)

3.2.2 Drought condition projections for the period of 2046 - 2065

For the mid -21st century (2036 - 2065) (Fig. 5 and Fig. 6), the trend projections of SPI and SPI_min are similar to that of the 2016 - 2035 period examined by both RCP4.5 and RCP8.5 scenarios.

In general, the mean drought condition of the 2036 - 2065 period in the South - Central region is found less than the baseline period. The increasing rate of SPI is found from 0.2 to 0.8% compared with the baseline period. The most increasing rate is found by the SPI at the longer timescales (Fig. 5).

The interesting results that the severity extreme of the drought condition defined by SPI_min is shown in Figure 6. As expected for the beginning period of the 21st century, the trend of SPI_min is found by decreasing trends at most of stations in the central and southern part of the South-Central region, especially for drought condition at the shorter timescales. The decreasing rate of the SPI_mean ranged from 0 to 0.2% compared with the baseline period (Fig.6). Comparing the Fig.6 with Fig.4, we can find the significant differences that the extreme drought of 2036 - 2065 period according to RPC8.5 scenario is found by increasing trends for all timescales.

For the projections of the period 2036 - 2065, this means that the extreme drought according to RCP4.5 scenario at shorter timescales is expected to increase. However, the RCP8.5 scenario shows the increasing trend of extreme drought at all timescales. In addition, the number of the station that having the increasing trend according to RCP8.5 scenario is higher than RCP4.5.

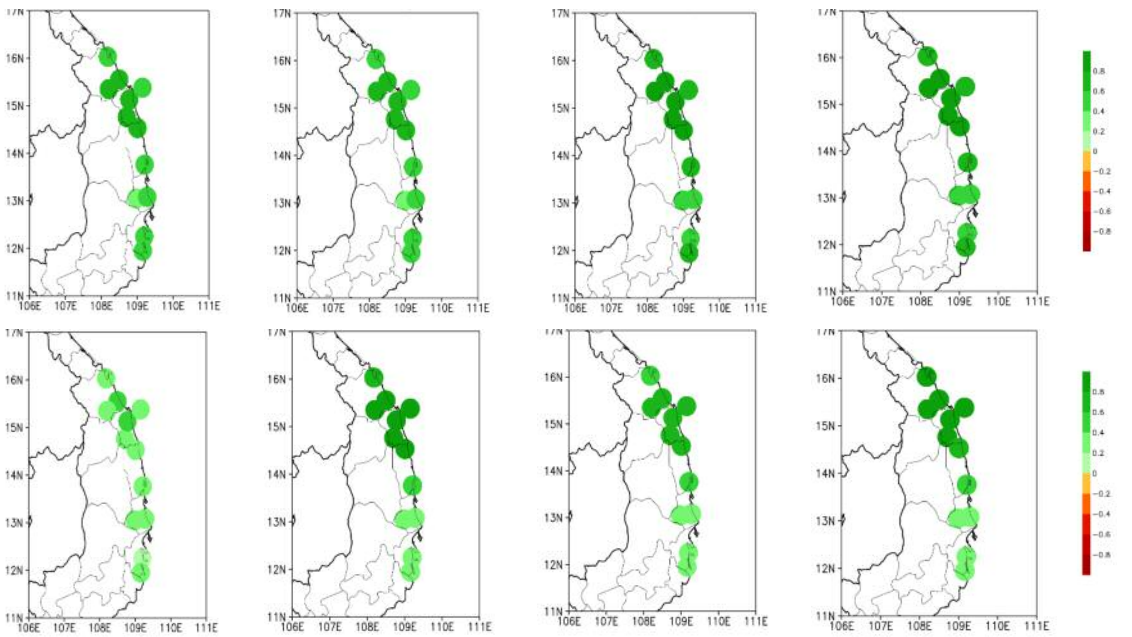

Fig.5. Same as Fig.3. but for 2046-2065: SPI_1 (a, e), SPI_3 (b, f), SPI_6 (c, g) and SPI_12 (d, h)

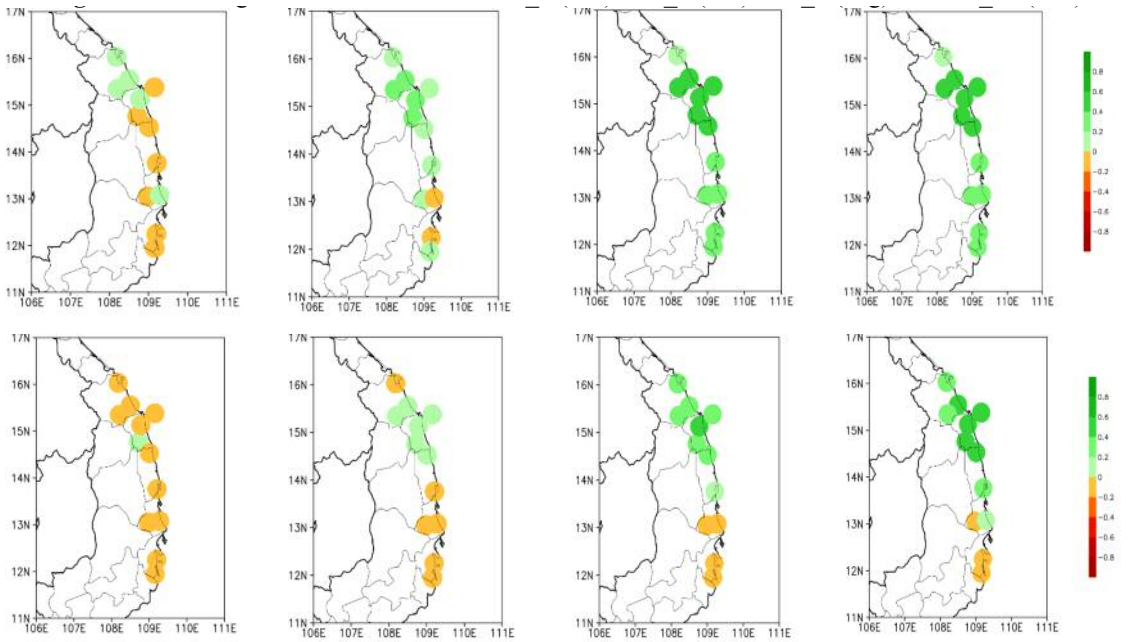

Fig.6. Same as Fig.5. but for SPI_Min: SPI_1 (a, e), SPI_3 (b, f), SPI_6 (c, g) and SPI_12 (d, h)

3.2.3 Drought condition projections for 2080-2099

For the end - 21st century (2080 - 2099), the trends of SPI and SPI_min are projected by the same trend with the beginning and mid - 21st century.

Fig. 7 shows that the SPI at all timescales of 2080 - 2099 is higher than that of the baseline period. The increasing rate of the period 2080 - 2099 compared with baseline ranged from 0 to 0.8%. Whereas, the increase of SPI index at longer timescales is higher than shorter timescales. This means that the changes in mean drought condition at shorter timescales are not clearly found, especially at southern stations of the region. The noticeable increasing trend of drought condition is found at longer timescales.

As like the 2016-2035 and 2036-2065 peri-

ods, the SPI_min of 2080 - 2099 varied from smaller values than that of the baseline period. However, these smaller values are mostly found at the SPI_min at 1- and 3-month timescales (Fig. 8). This means that the extreme drought of 2080 - 2099 at shorter timescales is expected to be more serious than that of the baseline period.

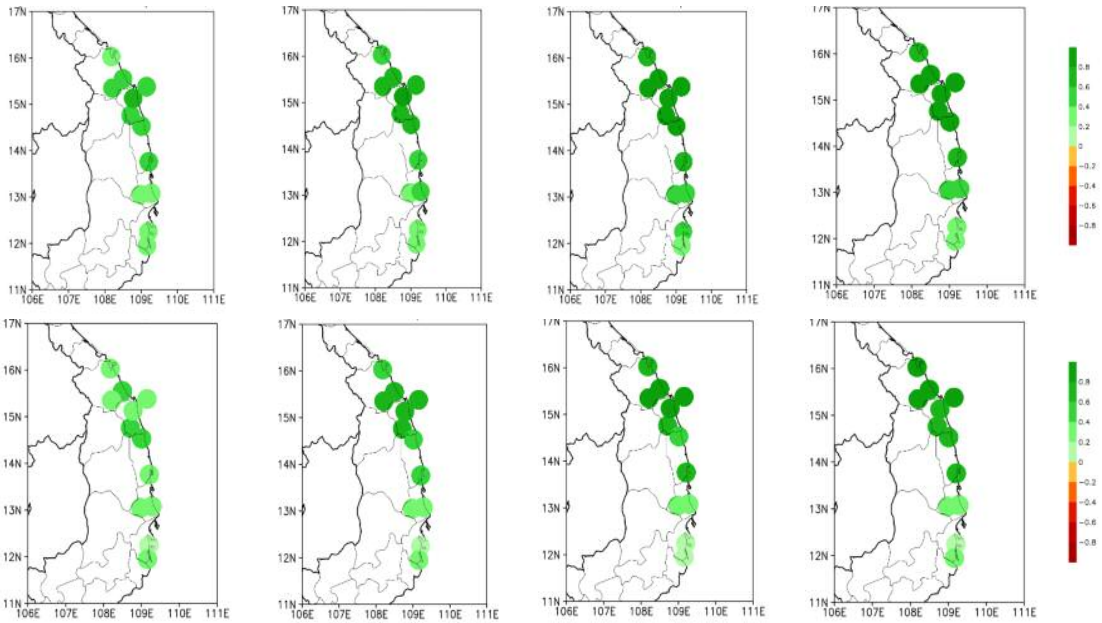

Fig. 7. Same as Fig.3. but for 2080-2099: SPI_1 (a, e), SPI_3 (b, f), SPI_6 (c, g) and SPI_12 (d, h)

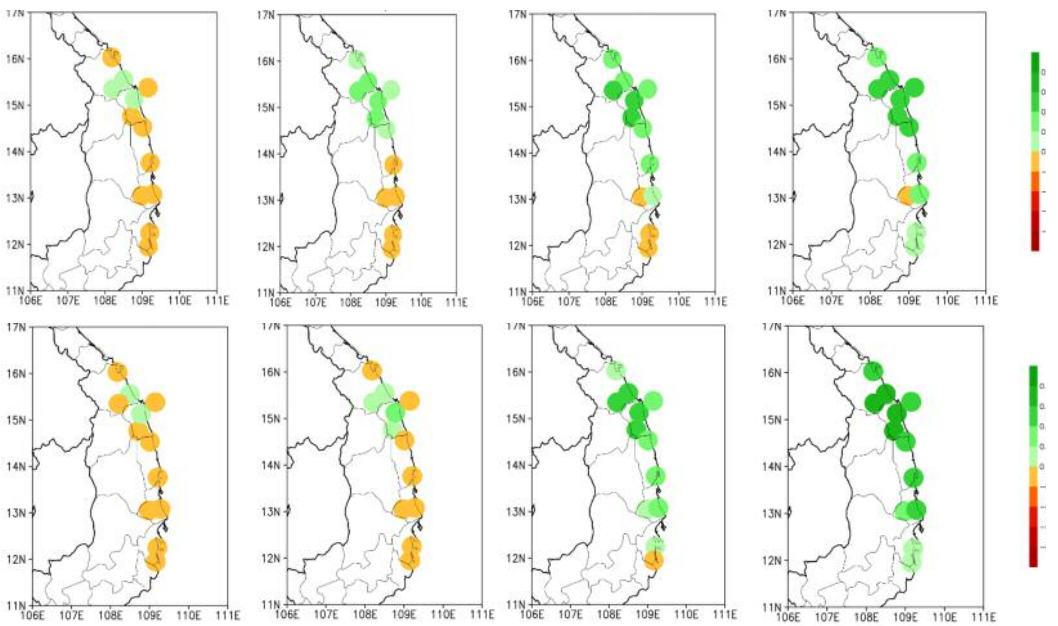

Fig.8. SPI_Min: SPI_1 (a, e), SPI_3 (b, f), SPI_6 (c, g) and SPI_12 (d, h)

4. Conclusion and discussion

4.1. Conclusion

From these calculations and analysis above which based on the past observed data and future bias-correction rainfall, some conclusions can be drawn:

(1) The SPI calculations for multiple timescales show the average wetter condition trend during 1961- 2017. However, the changes

in drought condition at the central and southern stations in the South-Central region is not significant. Especially, the most extreme of drought condition is detected by increase in severity level due to the decrease trend of the SPI_min index.

(2) The future trends (2016 - 2035, 2036 - 2065 and 2080 - 2099 periods) of SPI and SPI_min indices according to both RCP4.5 and RCP8.5 scenarios are generally found the same pattern with that of the past trend. Whereas, the future mean drought condition at four timescales is expected to decrease. The slight increase rate of future SPI index is found by the central and southern stations of the South-Central region and by the shorter timescales. Although the decreasing trend of mean drought examined, the increasing trend of the most extreme drought condition is found according to both RCP4.5 and RCP8.5 scenarios. This increasing trend of the most extreme drought condition is significantly found by the shorter timescales and by the central and southern stations in the South-Central region.

4.2. Discussion

In this study, we try to find the changes in drought condition of the future periods compared with the baseline period based on the bias-cor-rection rainfall of IMHEN. This bias-correction rainfall was used in the *"Climate change and sea level rise scenarios"* published by MONRE. Thus, our results are presented in this study that can provide useful information for implement-ing responding to climate change in the South-Central region.

Acknowledgements: This study is grant of funding code: TNMT.2016.05.22

References

1. Jang, D.W., 2018. Assessment of Meteorological Drought Indices in Korea Using RCP 8.5 Scenario, *Water 2018*. 10: 283, doi:10.3390/w10030283, MDPI.

2. DWR. Ministry of Agriculture and Rural Development (MARD): http://www.vncold.vn/Web/Content.aspx?distid=4061

3. Edwards, D.C. and McKee, T.B., 1997. Characteristics of 20th century drought in the United States at multiple time scales. *Climatology Report. 97(2)*. Department of Atmospheric Science, Colorado State University, Fort Collins, Colorado.

4. IMHEN, 2016. Climate change and sea level rise scenarios for Vietnam, MONRE project.

5. IPCC, 2007. Climate Change 2007: The Scientific Basis. Contribution of Working Group I to the Fourth Assessment Report of the Intergovernmental Panel on Climate Change. *Cambridge University Press, Cambridge.* United Kingdom and New York, NY, USA.

6. IPCC, 2013. Climate Change 2013: The Physical Science Basis, Contribution of Working Group I to the Fifth Assessment Report of the Intergovernmental Panel on Climate Change [Stocker, T.F., D. Qin, G.-K. Plattner, M. Tignor, S.K. Allen, J. Boschung, A. Nauels, Y. Xia, V. Bex and P.M. Midgley (eds.)]. *Cambridge University Press*, Cambridge**,** United Kingdom and New York, NY, USA, pp 1535, doi:10.1017/CBO97811074153

7. James, H. Stagge, L.M., Tallaksen, L.G., Anne, F.V.L., Kerstin, S., 2015. Candidate Distributions for Climatological Drought Indices (SPI and SPEI). *International Journal of Climatology*, 35 (13): 4027 - 4040, https://doi.org/10.1002/joc.4267.

8. Liu, L., Hong, Y., Looper, J., Riley, R., 2013. Climatological Drought Analyses and Projection Using SPI and PDSI: Case Study of the Arkansas Red River Basin. *Journal of Hydrologic Engineering*. 18 (7).

9. Osuch, M.M, Romanowicz, R.J., Lawrence, D. and Wong, W.K., 2016. Trends in projections of standardized precipitation indices in a future climate in Poland. *Hydrol, Earth Syst. Sci.*, 20: 1947-1969, doi:10.5194/hess-20-1947-2016

10. Mau, N.D, Thang, N.V and Khiem, M.V., 2016. Changes in rainfall during the summer monsoon over Vietnam projected by PRECIS

model. *VNU Journal of Science*. 3S (2016): 153-166.

11. McKee, T.B., Doesken N.J. and Kleist, J., 1993. The relationship of drought frequency and duration to timescale, *In: Proceedings of the Eighth Conference on Applied Climatology.* Anaheim, California, 17-22 January 1993. Boston, American Meteorological Society, 179 - 184.

12. MONRE, 2009. Climate change, sea level rise scenarios for Vietnam, NARENCA.

13. MONRE, 2012. Climate change, sea level rise scenarios for Vietnam. NARENCA, 2012.

14. MONRE, 2016. Climate change, sea level rise scenarios for Vietnam. NARENCA, 2016.

15. Ngu, N.D and Hieu, N.T., 2004. Climate and Climate resources in Vietnam. *Agriculture House*.

16. Thang, N.V et al., 2017. Changes in climate extreme in Vietnam. *Vietnam Science and Technology* (VISTECH). 1 (1): 79-87.

17. Thang, N.V et al., 2007. Research and develop a technology for drought prediction and early warning in Viet Nam, MONRE project, 2007.

18. Thang, N.V et al., 2014. Definition of the criteria of drought condition for the South-Central region. *Scientific and Technical Hydro-Meteorological Journa*l. 639: 49-55.

19. Thang, N.V et al., 2015. Study on drought forecast and warning system in Viet Nam for 3-month range, Code: KC.08.17/11-15.

20. Tri, T.D, et al., 2014. Projections of drought condition for South-Central region by using the PRECIS model. *Scientific and Technical Hydro-Meteorological Journal.* 644: 5-8.

21. Tri, T.D. et al., 2015. Trend of the drought condition in the South-Central region during 1961 - 2010. *Journal of Natural resources and Environment*. 217:18-20.

22. WMO, 2012. Standardized Precipitation Index User Guide, WMO-No. 1090, Geneva 2, Switzerland.

Vietnam Journal of Hydrometeorology, ISSN 2525-2208, Volume 01: 30 - 34

Research Paper

AN INVESTIGATION OF RAINFALL DEFICIENCY IN OCTOBER AND NOVEMBER IN THE CENTRAL VIETNAM DURING THE 1997 - 1998 EL NINO EVENT

Nguyen Van Thang[1], Vu Van Thang[1]

ARTICLE HISTORY

Received: April 14, 2018; Accepted: May 15, 2018
Publish on: December 25, 2018

ABSTRACT

In this article, the rainfall deficiency in October, November over the Central Vietnam during the 1997 - 1998 El Nino event are investigated based on large-scale moisture transport circulation, wind at 10m and 850hPa levels and sea-level pressure.The results show that there were 9 months in total of 12 months from May1997 to April1998 of this El Nino event observed the rainfall deficiency over some climatic regions of Viet Nam. In which, the most significant deficiency occurred in October, November 1997 in the Central Vietnam in a range of 100 - 150 mm, especially the deficiency reached up to 200 mm at some heavy rainfall centers such as Ky Anh, Hue, Tam Ky, Tra My, Ba To. This deficiency seems to be caused by a weakening of the North East monsoon circulation in comparison to the long-term mean, which leads to formation of an anomalous anticyclonic vortex over the East Sea. The appearance of anticyclonic vortex causes a decrease in moisture transport that suppling to rainfall in the Central Viet Nam. In addition, there is only a main source of moisture from East Sea that favors rainfall formation over Central Viet Nam is lower than climatology.

Keywords: *El Nino, Moisture transport, Rainfall deficit*

1. Introduction

For years, moisture transport on a global and regional scale has been studied in many regions of the world. The relationship between water vapor transport in the atmosphere and rainfall at the specific places, inparticularlythose affected by monsoons, is indicated by the researches (Vu Van Thang, 2016; Nguyen Van Thang, 2017; Liu 2003; Simonds, 1999; Xiaoxia, 2010; Zhou, 2005). The shortage of moisture leading to drought in some areas, especially in El Nino conditions have been studied by some authors (Vu Van Thang, 2014; Liu, 2004; Valsala, 2005; Vu Van Thang, 2016; Zhang, 2015).

Moisture transport is considered one of the elements of circulation because it is computed from humidity and wind. Therefore, moisture transport has an effect on not only rate but also rainfall distribution at any region. In El Nino condition, this effect become clearer. Due to effect of El Nino, drought could last on many regions of Viet Nam from 5 -7 months, especially in the Central and Central Highlands (Nguyen Trong Hieu, 2014). The reduction in rainfall by El Nino events in Viet Nam has been statistically analyzed and the physical mechanism causing that decrease is determined through characteristics ofatmospheric circulation and moisture transport (Nguyen Duc Ngu, 2017; Vu Van Thang, 2016;Nguyen Van Thang, 2017; Vu Van Thang, 2016). Nguyen Van Thang et

NGUYEN VAN THANG
nvthang.62@gmail.com
[1]Viet Nam Institute of Meteorology, Hydrology and Climate change

al.(2017)showed that the prominent features of atmospheric circulation related to the shortage of rain in Vietnam during El Nino 2014 - 2016 are decline of the Pacific Ocean high-pressure; the southeastward shift of the equatorial low pressure enhancing of air pressure on the Pacific Ocean Equator. According to Vu Van Thang et al.(2014), 2016 reasons of autumn rainfall reduction in Central Vietnam under El Nino condition are the weakening of North East monsoon circulation leading to formation of an anomalous anticyclonic vortex over East Sea which decreases moisture suppling to rainfall in Central Viet Nam. The shortage of rain in May El Nino in the Central Highlands is due to the weakening of the southwest monsoon circulation which reduces the moisture source from the Indian Ocean through the Bay of Bengal to provide rainfall in the area.

The goals of this paperareto indicate the role of circulation on autumn rain reduction in Vietnam during the 1997 - 1998 El Nino event.

2. Data and method

The total moisture transport vectors (Q, kgm 1s 1) of air column is computed based on (Nguyen Thi Hien Thuan, 2004; Sminov, 2000;Xiaoxia, 2010), using the following equations:

$$\vec{Q} = -\frac{1}{g}\int_{Ps}^{P0}(\vec{V}q)dp \qquad (1)$$

where g is the gravitational acceleration (ms^{-2}); V⃗is wind vectors; q is specific humidity (gkg^{-1}); p_s and p_o are respectively the lower and upper atmospheric limits of the atmosphere column. The total moisture transport vector is caculated for East Asia region (10^0S - 50^0N, 60^0E - 160^0E), then it is averaged for October, November 1997.

The gridded data include the zonal wind (u, m s^{-1}), the meridional wind(v,m s^{-1}) at 10m and 850 hPa level with a resolution of 0.5x0.5 (reanalysis data CFSR), wind u, v and specific humidity (q, kg kg^{-1}) at 1000, 925, 850, 700, 600, 500, 400 và 300hPa levels at a resolution off 2.5 x 2.5. The Asian Precipitation Highly Resolved Observational Data Integration Towards Evaluation (APHRODITE) rainfall data with resolution of 0.25x0.25 obtained from:

www.chikyu.ac.jp.

3. Results

The strong El Niño event of 1997-1998 lasted about 12 months from May1997 to April1998. During that time, about 9 months occurred the decrease in rainfall over some Viet Nam's climatic regions by this El Nino; the most serious lack of rainfall took place in October and November 1997 over the Central, especially the coastal zone (Vu Van Thang, 2016).

The rainfall anomaly distribution maps in October and November 1997 (Fig.1) show that in October1997 (Fig.1a), the El Nino caused reduction in rainfall over the Central with a range of 100-150mm; the largest decrease (about 200mm) occurred at the heavy rainfall centers including Ky Anh, Hue, Tam Ky, Tra My and Ba To. In contrast, effects of this El Niño linked to rainfallincrease from 20 - 40 mm over the North and the South, especially an increase of more than 60 mm at Bac Quang station. In November 1997 (Fig.1b), reduction in rainfall occurred over almost Viet Nam regions except the South. In the North decreased from 30 - 60 mm, the coastal region of Ha Tinh - Da Nang had faster decline in a range of 100 - 150 mm, some places decreased greater than 150mm such as Ky Anh, Hue. In the South, rainfall increased from 40 - 60 mm.

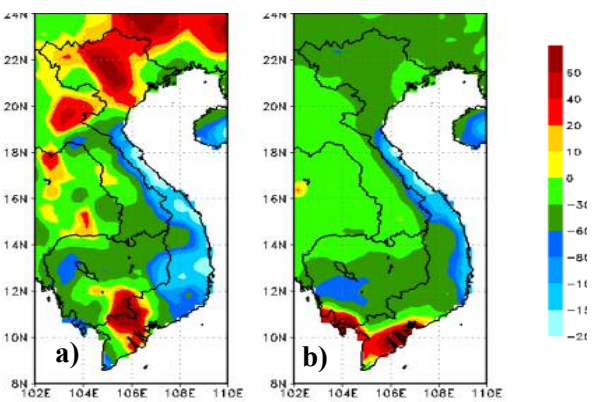

Fig. 1. Rainfall anomaly(mm) over Viet Nam: a) October, b) November 1997

The shortage of rainfall in Central Viet Nam in October/1997 by El Nino is explained based on circulation elements such as wind vector, sea level pressure and total moisture transport vector. Wind vector anomalies at 10m (Fig.2a) and 850hPa (Fig. 2a) levels in October1997 show that there is an anticyclonic circulation in the middle East Sea. The anticyclonic wind circulation in Fig.2 linked to an anomalous of high sea level pressure anomaly (Fig.4a). It is quite same as in November (Fig.3), however the anticyclonic circulation moves to the southern East Sea and extends to the west of Philippine. The anticyclonic wind circulation in Fig.3 is consistent with an anomalous of high sea level pressure anomaly in Fig.4b. The presence of the anticyclones in the end of autumn is resulted from the weakening of the North East monsoon at 10m and 850 hPa levels. Besides, the reduction of major moisture source over East Sea that supplying moist for rainfall in Vietnam leads to the weakening of the low-level wind circulation that carries moist air from the offshore Pacific Ocean to the East Sea and Central Viet Nam.

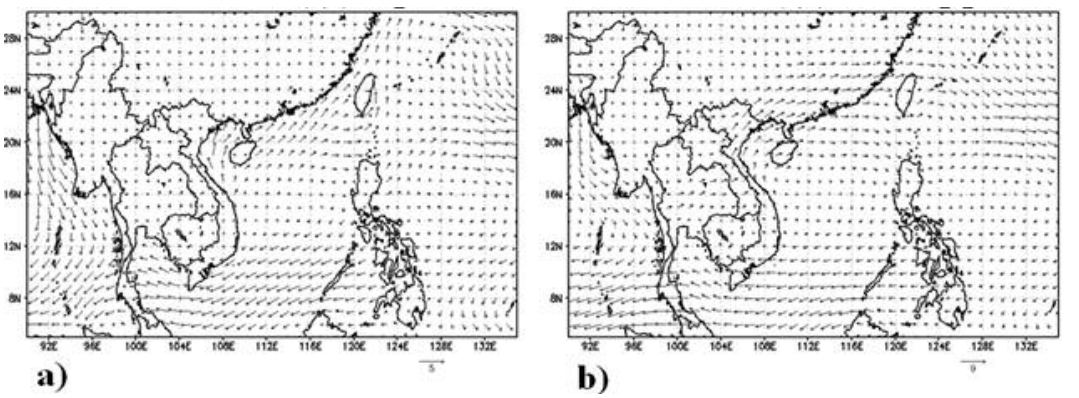

Fig. 2. Anomaly of sea level pressure(m s^{-1}) October/1997: a)- 10m; b)-850hPa.

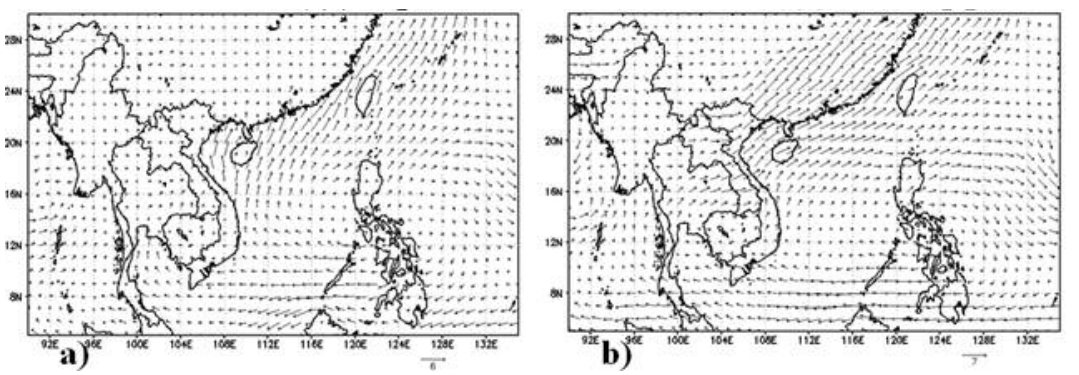

Fig. 3. Wind vector anomaly (m.s^{-1}) November1997: a) 10m; b)850hPa.

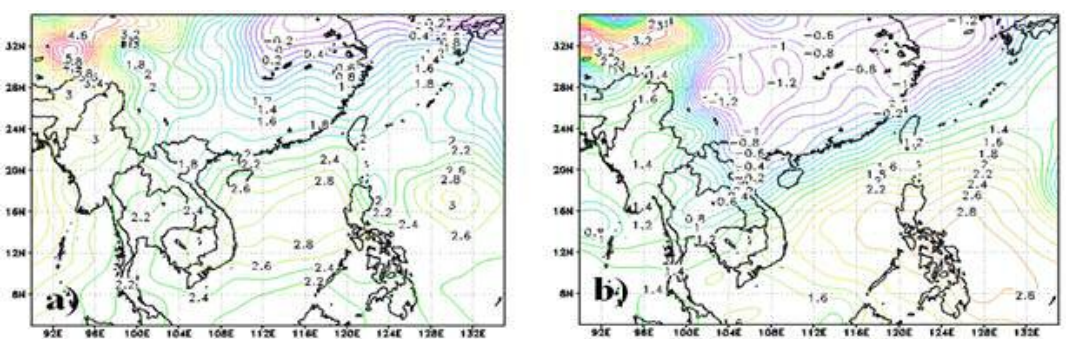

Fig. 4. Sea level pressure anomaly (hPa): a) October/1997, b) November/1997

The distribution of total moisture transport vector in October and November 1997 (Fig. 5a, Fig. 6a) shows that only one main source of moisture that supplying for rainfall over the research region in these 2 months which is from East Sea. However, there is a reduction of 10-20 kg m-1s-1 in content of this moisture sourc compared to the long-term mean. The reason is due to exitence of an anomalous anticyclonic vortex over the East Sea which is indicated in Figs. 2-4. The anomalous moisture transport in October1997 (Fig. 5b) show that the easterly and north-easterly moisture transport vectors to the Central is weaker than the normal. In addition, moisture transport from the Southern Hemisphere could not reach the Central. The total moisture transport vector in November 1997 (Fig.6a) shows range of large moisture source over the East Sea is narrower and its location moves to south of the East Sea much more than that in October 1997. The moisture in the offshore Pacific Ocean is lower in comparison to the long-term mean. The anomaly of moisture transport vector in November 1997 (Fig.6b) shows a reduction in easterly and north-easterly moisture transport vector.

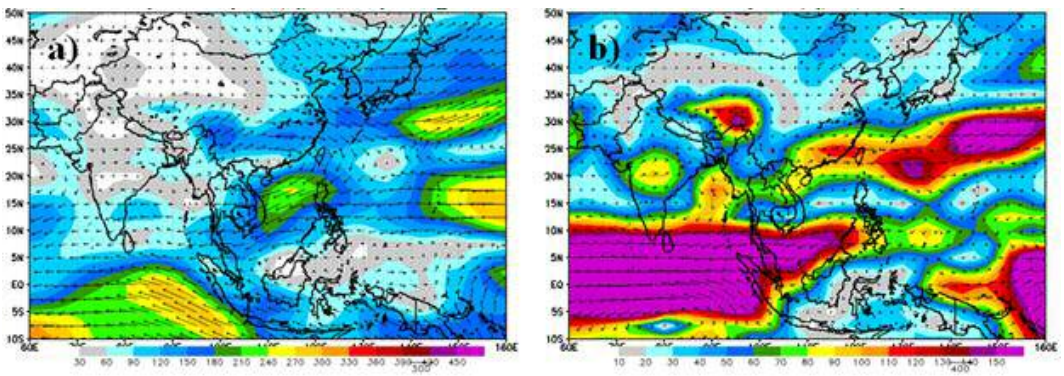

Fig. 5. Total moisture transport (kg m^{-1} s^{-1}) October/1997: a) Vectors, b) Anomaly

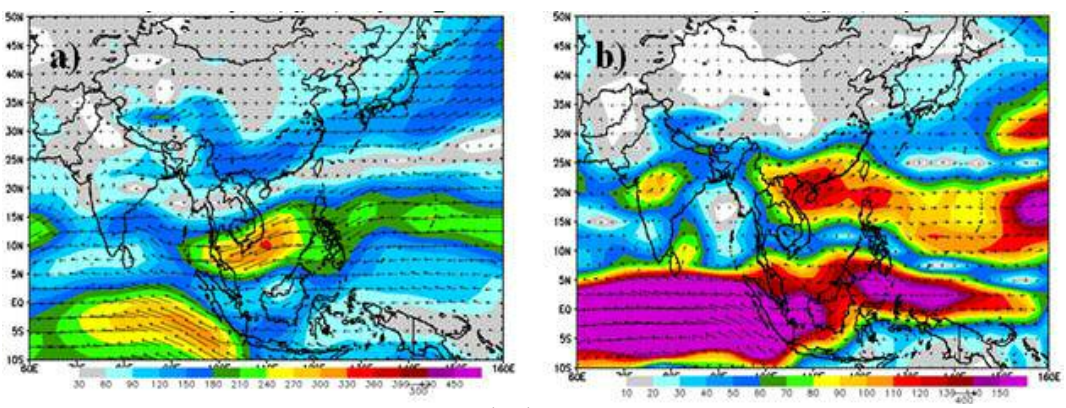

Fig. 6. Total moisture transport (kg m^{-1} s^{-1}) November 1997: a) Vectors, b) Anomaly

In summary, the deficit of rainfall over the Central Viet Nam in this El Nino event in October and November1997, especially at heavy rainfall centers relates to: (1) a weakening of the North East monsoon over the East Sea in comparison to the long-term mean; (2) The presence of anomalous anticyclone in the middle East Sea leading to the reduction of moisture source to the Central Viet Nam; (3) Existing only one source of moisture that supplying for rainfall in the research region; (4) Moisture content in the East Sea is lower than the long -term mean. It can be seen that the reasons leading the deficit of rainfall in this event is suitable to general mechanise. It can be seen that the reasons for the lack of rainfall in this event over the Central are similar tothe general mechanism indicated in the research of Vu Van Thang (2016).

4. Conclusion

During the 1997-1998 El Niño event from May1997 to April1998, there are 9 months in total of 12 months that occurring the rainfall deficiency over some Viet Nam's climatic regions. In which, the most serious deficiency took place in October and November 1997 over the Central, especially the coastal zone. The average of rainfall deficiency is in a range of 100 -150 mm; In particular, the deficiency reached up to 200 mm at some heavy rainfall centers such as Ky Anh, Hue, Tra My, Tam Ky and Ba To.

The shortage of rainfall in the Central Viet Nam in the last months of autumn (October and November 1997) under El Nino condition are related to the weaker North East monsoon circulation over the East Sea compared to the long-term mean that favors to form an an anomalous anticyclonic vortex over the East Sea that causing the reduction in moisture transport to the Central Viet Nam; the moisture transport in north and northeast direction is lower than the long-term mean. In addition, there is only a main source of moisture from East Sea that favors especially rainfall formation over Central Vietnam is lower than the climatology.

References

1. Liu, J., and R. E., Stewart, 2003. Water Vapor Fluxes over the Saskatchewan River Basin. *J. Hydrometeor*, 4: 944 - 959.

2. Liu, J., R. E, Stewart., and K. K. Szeto, 2004. Moisture Transport and Other Hydrometeorological Features Associated with the Severe 2000/01 Drought over the Western and Central Canadian Prairies. *J. Climate*.17: 305 - 319.

3. Nguyen, D. N., 2017. 2015/2016 El Niño event and Its impact on Vietnam. J*ournal of climate change science*. 1: 29-36.

4. Nguyen, V.T., Nguyen, T.H., Mai, V. K., Vu, V. T., 2017. The characteristics of atmospherical circulation and status of rainfall deficit in Viet Nam during 2014 - 2016 El Nino event. *Journal of climate change science*. 4: 2-14.

5. Nguyen, T. H. T., 2004. Calculatingmoisture transport in the atmosphere. *The report of scientific workshop 11th in Viet Nam Institute of Meteorology, Hydrology and Environment*.

6. Nguyen,T. H., 2014. Research the basic characteristics and impact of ENSO to drought, heavy rainfall at Vietnam and the prediction. *Associate Report for the basic mechanism, teletercodeNCCB-DHUD.2011-G/12*.

7. Valsala, V. K., and M. Ikeda, 2005. An Extreme drought event in the 2002 summer monsoon rainfall and its mechanism proved with a moisture flux analysis. *SOLA*. 1: 173- 176, doi:10.2151.

8. Vu, V.T., Nguyen, V.T., Pham, T.T.H., Nguyen, T.H., 2012. Characteristics of moisture transport in Vietnam under El Nino condition. The report of scientific workshop 11th in Viet Nam Institute of Meteorology, Hydrology and Enviroment. *Scientifc and Technical Publishe*r.

9. Vu, V.T., Nguyen, V.T., Nguyen, T.H., Nguyen, V. H., Do, T.N., Nguyen, T.H., Hoang, D.C., 2014. The shortage of rainfall in May during El Nino periods in the Central Highlands and role of moisture transport. *Scientific and Technical hydro – MeteorologicalJournal*. 644: 1- 4.

10. Vu, V.T., 2016. Characteristics of moisture transport in the ENSO events in Vietnam. *Earth sciences dissertation*.

11. Vu, V. T., Nguyen, H. T., Nguyen, T. V., Nguyen, H. V., Pham, H. T. T., & Nguyen, L. T., 2016. Effects of ENSO on autumn rainfall in Central Vietnam. *Advances in Meteorology*.

12. Simonds, I., D. Bi, and P. Hope, 1999. Atmospheric water vapour flux and its association with rainfall over China in summer. *J. Clim*. 12: 1353-1367.

13. Sminov, V., and G. Moor, 2000. Short-term and seasonal variability of the atmospheric water vapour transport through the Mackenzie River Basin. *J. of Hydromet*. 2: 441- 452.

14. Xiaoxia, Z., Y. Ding, and P. Wang, 2010. Moisture transport in the Asian summer monsoon region and its relationship with summer precipitation in China. *Acta Meteor. Sinica*. 24 (1): 31-42.

15. Zhang, R., and A. Sumi, 2002. Moisture Circulation over East Asia during El Nin˜o Episode in Northern Winter,Spring and Autumn. *J. Meteor. Soc*. Japan. 80 (2): 213 - 227.

16. Zhou, T. J., and R. C. Yu, 2005. Atmospheric water vapor transport associated with typical anomalous summer rainfall patterns in China. *J. Geophys. Res*. 110: D08104, doi:10.1029/2004JD005413.

Research Paper

INTEGRATION OF SWAT AND MODFLOW MODEL TO ASSESS THE SURFACE AND GROUNDWATER AVAILABILITY: A CASE STUDY OF DONG NAI BASIN IN 2015 - 2016

Do Xuan Khanh[1], Nguyen Bach Thao[2]

ARTICLE HISTORY

Received: 12 February, 2018; Accepted: 12 April, 2018

Publish on: 25 December , 2018

ABSTRACT

Water is one of the most essential natural resources . A good assessment of both surface and groundwater always leads to an effective and sustainable water resources management. In Vietnam, the management of water resources has mainly focused on surface water, however, the problems related to groundwater have not been managed properly. This study aims to assess surface and groundwater availability in Dong Nai river basin by integrating SWAT and MODFLOW models. These models run individually and integrated through the recharge rates. The simulation results were then compared and showed good agreement with observed data. The results showed Tuyen Lam, Da Huoai and Dak Song districts are the locations which have high surface water availability, in the range of 40 - 50 l/s/km^2. The groundwater simulation indicated the areas having high groundwater availability are located at the same places with the regions having high surface water. Dak Song is the region having the highest groundwater availability with around 9 l/s/km^2.

Keywords*: Surface water, groundwater, SWAT, MODFLOW, Dong Nai, recharge rates.*

1. Introduction

These days, water scarcity is a widespread problem around the world. Water availability becomes a matters of interest in everywhere, especially in arid or semiarid areas.Traditionally, management of water resources has concentrated on surface water or groundwater as if they were separate entities (Winter et al., 1998). However, surface water and groundwater are not separate components in the hydrological cycle (Dowlatabadi et al., 2015). In Vietnam, water resources management has mainly focus on thesurface water (Chau and Khanh, 2017, Au et al., 2013; Phung et al., 2014), while problems related to groundwater have not been managed in a rigorous manner. In most of the studies have been done, modellingis the most suitable method for simulating surface and groundwater availability.

The Soil and Water Assessment Tool (SWAT) and MODFLOW are 2 well-known and widely-used surface and groundwater models, respectively.These two models represent two different environments and each is limited in its simulation domain with their corresponding strong points and drawbacks. In one side, SWAT is a basin scale, semi-distributed model and is often used to simulate hydrological processes in surface and in shallow aquifer. Its calculation is based on hydrological response units (HRUs), which are conceptual units of homogeneous land

DO XUAN KHANH
khanh.thuyluc@tlu.edu.vn
[1] Thuyloi University
[2] Hanoi University of Mining and Geology

use, management, slope, and soil characteristics that extend below the surface to a soil profile depth (Arnold et al., 1998). SWAT model can only simulate shallow groundwater flow in a restricted layer, around 6 m below ground surface, in which the seepage below it is assumed to be lost and out of the system(Neitsh et al., 2011). In the other side, MODFLOW presents as a three dimensional, distributed finite - difference groundwater model and it can simulate ground water flow for variably saturated subsurface systems including shallow and deep aquifers. However the model is limited to investigating groundwater-surface interaction, as it cannot simulate surface process. On the other words, the groundwater model was not adequately linked to surface water model(Anh et al., 2009; Hiep et al., 2012; Quynh et al., 2014). In those studies, groundwater recharge, an important input for groundwater model, could not be calculated from hydrological components, which are precipitation, evapotranspiration and surface runoff, however it was determined through trial and error method during calibration process.

In recent decades, there were some conjunctive simulations of surface water and groundwater using SWAT and MODFLOW (Putthividya et al., 2017; Kim et al., 2008; Guzman et al., 2015; Dowlatabadi et al., 2015).In those studies, there were several methods to integrate SWAT and MODFLOW, however the integration through recharge rates between HRUs in SWAT and cells in MODFLOW is the most feasible method. Those studies were successful in evaluation of water availabilityin various regions of the world and became a useful data to support the water management policy.

Dong Nai river basin is one of four major river basin in Central Highland in Vietnam. This region were dominated by many ethnic populations whose have low standard of living. Their income mostly comes from agricultural products including perennial tree such as coffee, rubber and pepper or annual trees which are much dependent on water resources. The role of surface and groundwater in this area is both very important. Therefore an adequate assessment of water availability for surface and groundwater is really necessary.This study aims to integrate SWAT and MODFLOW model to assess the surface and groundwater availability in Dong Nai river basin. The model accuracy was ensured through the calibration and validation process with observed data.

2. SWAT, MODFLOW and their integrated structure

2.1 SWAT model

SWAT is a physically based and semi-distributed model developed by Agricultural Research Services of United States Department of Agriculture. It is a basin scale model using to simulate: hydrology of basin, water quality, climate change, crop growth, sediment yield and impact of land management practices (Fadil et al. 2011). In SWAT the basin is divided in to sub-basin and the sub-basin are further divided into Hydrologic Response Units (HRUs) which present as units with similar land use, slope and soil type. The model calculates the water balance for each HRU base on the following equation (Eq. 1) (SWAT user manual)

$$SW_t = SW_o + \sum_{i=1}^{t} (R_{day} - Q_{surf} - E_a - W_{seep} - Q_{qw})_i \quad (1)$$

Where SW_t is the final soil water content at time t (mm), SW_o is the initial soil water content (mm), R_{day} is precipitation in day i (mm), Q_{surf} is the amount of surface runoff in day i (mm), E_a is the amount of return flow in day i (mm), Q_{seep} is the amount of water entering the vadose zone from soil profile in day i (mm) và Q_{qw} is the amount of return flow in day i (mm).

Recharge to both shallow and deep aquifers is estimated

$$w_{rchrg,i} = \left(1 - exp\left[-1/\delta_{gw}\right]\right).w_{seep} + exp\left[-1/\delta_{gw}\right].w_{rchrg,i-1} \quad (2)$$

Where $w_{rchrg,i}$ is the amount of recharge entering the aquifer on day i (mm); δ_{gw} is the delay time or drainage time of the overlying geologic formations (days); w_{seep} is the total amount of water exiting the bottom of the soil profile on day *i* (mm); and $w_{rchrg,i-1}$ is the amount of recharge entering the aquifer on day *i-1* (mm).

The basic input required for SWAT simulation are topography, land use map, soil map and weather data. Figs. 1 - 2 show some important features in Dong Nai river basin. Out of the total study area, 56.5% is covered by forest, 36.2 % is covered by agriculture land and the rest is shared by other classes. The elevation ranges from 59 m to 2282 m. Fluvisols, Acrisols and Ferralsols are the major soil association of Dong Nai basin. The locations of 7 rain gauge stations including Dak Nong, Duc Xuyen, Dai Nga, Dai Ninh, Lien Khuong and Da Lat were presented in Fig. 1a. There were two water level stations in Dong Nai basin. They are Dak Nong and Thanh Binh station and will be used for calibration and validation processes.

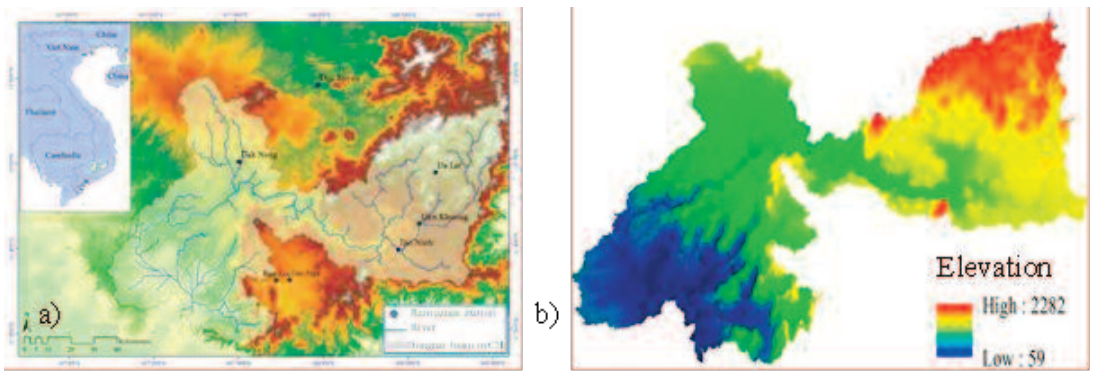

Fig. 1.a) Location and b) topography data in Dong Nai river basin

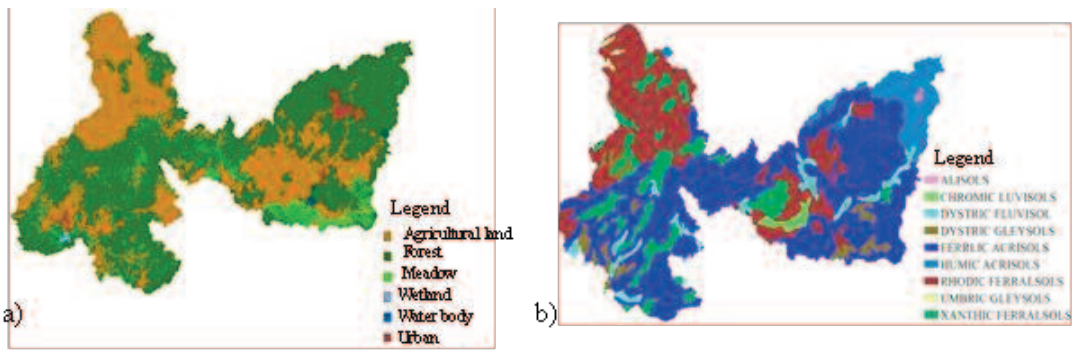

Fig. 2. a) Land-cover and b) soil data in Dong Nai river basin

2.2 MODFLOW model

MODFLOW is a three - dimensional finite-difference groundwater flow modelling program written by the United States Geological Survey (USGS). Its graphical User Interface (GUI), including Visual MODFLOW was developed by Waterloo Hydrogeologic. The model can simulate steady and non-steady flows in a saturated system, in which aquifer layers can be confined, unconfined, or a combination of confined and unconfined (Dowlatabadi et al., 2015).The model can consider all common boundary conditions including fixed pressure head, groundwater recharge, variable or constant fluxes and etc. In MODFLOW, the aquifer system is meshed by a discretized domain consisting of an array of node and associated finite difference cells (Chiang and Kinzelbach, 1998). It is governing equation is based on Darcy's law which is described by the following partial differential equation

$$\frac{\partial}{\partial x}\left(K_{xx}\frac{\partial h}{\partial x}\right)+\frac{\partial}{\partial y}\left(K_{yy}\frac{\partial h}{\partial y}\right)+\frac{\partial}{\partial z}\left(K_{zz}\frac{\partial h}{\partial z}\right)-W=S_s\frac{\partial h}{\partial t} \quad (3)$$

where K_{xx}, K_{yy} and K_{zz} are the hydraulic conductivities along the x, y and z axes parallel to the major axes of hydraulic conductivities, h is the piezometric head, W is a volumetric flux per unit volume representing sources/sink of water, S_s is the specific storage of the porous medium, and t is time.The ground surface of basin has been created by using the 30 m resolution Digi-

tal Elevation Map (DEM) (Fig. 3a). The main geometric-structure and hydrogeological characteristics of the study area were based on the geological and lithological descriptions of 400 boreholes located in Central Highland areas.Their characteristics are very complex, however they can be categorized in to four main geological layers (Table 1). The grid size of the model is 1 km x 1 km (Fig. 3b) and the boundary condition are river network, recharge rate and pumping wells.

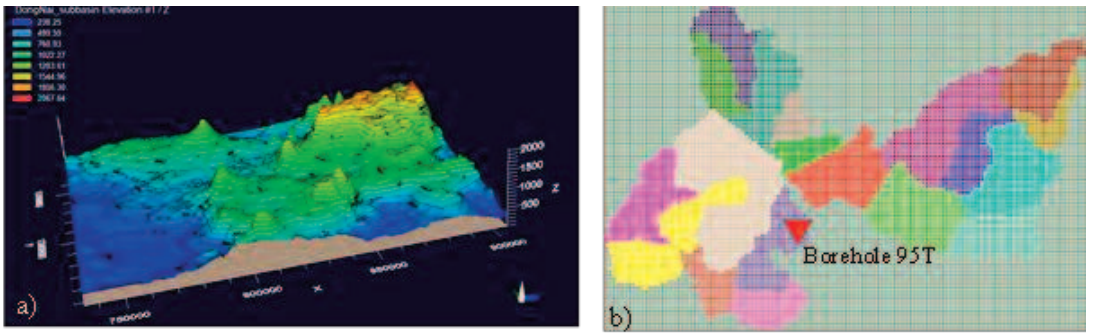

Fig. 3. Three dimensional visualization of model

Table 1. Geometric-structure and hydrogeological characteristics of basin

Layer in model/ Geological type	Lithological description	Average Thickness (m)	Hydraulic Conductivity (K, cm/s)		Storage (S)			
			Range of *K* (cm/s)	Average *K* (cm/s)	Specific Yield: S_y (-)	Specific Storage Coefficient: *Ss* (1/m)	Effective porosity (-)	Total porosity (-)
Layer1: Quaternary (Q)	Alluvium sand, silty clay, gravel	5 ÷ 10	2.3E-05 ÷ 1.8E-02	1.90E-03	9.30E-02	1.00E-05	7.50E-02	9.40E-02
Layer 2: Neogen (N)	Sandstone, gravestone, agrilitxe with peat, diatomite and tholeit basalt	50	3.0E-05 ÷ 1.5E-02	2.10E-03	8.80E-02	1.00E-05	7.10E-02	8.90E-02
Layer 3: Basalt Pleistocene (Q_{II})	Weathering basalt and porous basalt with tuff	70	1.2E-07 ÷ 6.9E-01	8.80E-03	8.80E-02	1.00E-05	7.00E-02	8.80E-02
Layer 4: Basalt Neogen-lower Pleistocene (bN_2-Q_I)	Basalt compact alternate with porous basalt	30	4.6E-05 ÷ 9.9E-03	1.70E-03	7.50E-02	1.00E-05	6.00E-02	7.60E-02

2.3 Structure of integrated SWAT and MODFLOW model

Fig. 4a shows the schematic diagram of combined surface water model (SWAT) and groundwater model (MODFLOW). The upper layers including root zone, vadose zone and shallow aquifer are belong to SWAT model, and the lower layer - deep aquifer is belong to MODFLOW model.

In this study, SWAT and MODFLOW were setup to run individually and integrated through the recharge rates. These recharge rates were firstly estimated by SWAT model and presented as groundwater recharge values in HRUs level.

In the integration process, the recharge rate of the HRU should be exchanged with cells and used as input data for MODFLOW (Fig. 4b). Due to the semi-distributed features of SWAT, spatial location of each HRU in sub-basins cannot be determined. Thus, to reflect HRU locations, one HRU is created for each sub-basin by dominant land use, soil and slope option (Dowlatabadi et al., 2015)

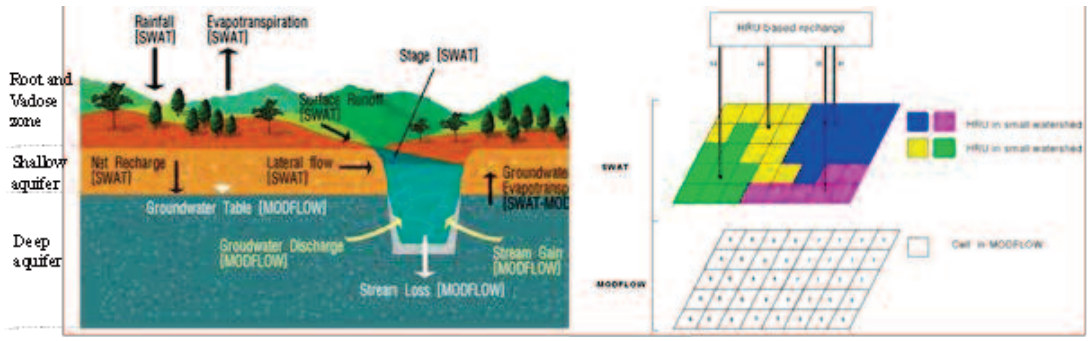

Fig. 4. Schematic diagram of a) combining SWAT and MODFLOW b) exchange recharge rate from SWAT to MODFLOW (Kim et al., 2008)

3. Results and Discussions

3.1 Surface water availability in Dong Nai river basin

Dong Nai river basin was divided into 19 sub-basins as shown in Fig.3b. Fig. 5 shows the comparison between simulated and observed monthly stream flow from 1986 to 2010 in Dak Nong and Thanh Binh stations. There were a good agreement between simulated and observed in term of graph's shape and their corresponding peaks. The NSE and R^2 coefficient in calibration process are shown in Table 2.Table 3 presents some major parameters as hydrology component of SWAT that much affect to the simulation results. The best ranges of these parameters were found through the calibration process and were used for validation step. Fig. 6 shows the validated results in 2015/2016 year in Dak Nong and Thanh Binh station, respectively. Their NSE and R2 coefficient also were presented in Table 2. According to Moriasi et al. 2007,with the value of R2 is larger 0.5 and NSE is greater than 0.75 the simulation results can be judged very well.

Table 2. Results of calibration and validation

Station	R^2		NSE	
	Calibration	Validation	Calibration	Validation
Dak Nong	0.83	0.93	0.82	0.94
Thanh Binh	0.74	0.81	0.74	0.80

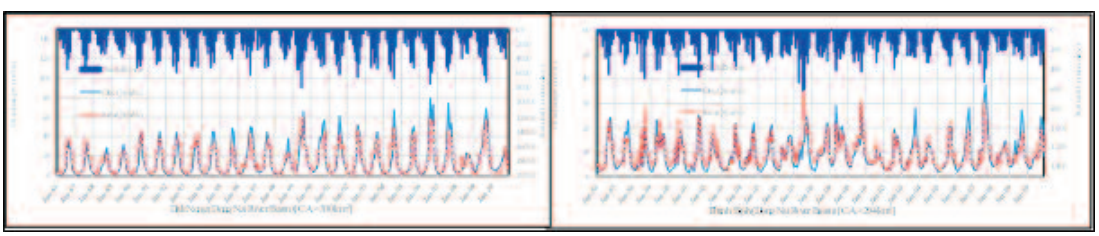

Fig. 5. Comparison between simulated and observed monthly stream flow in calibration process (1986 - 2010)

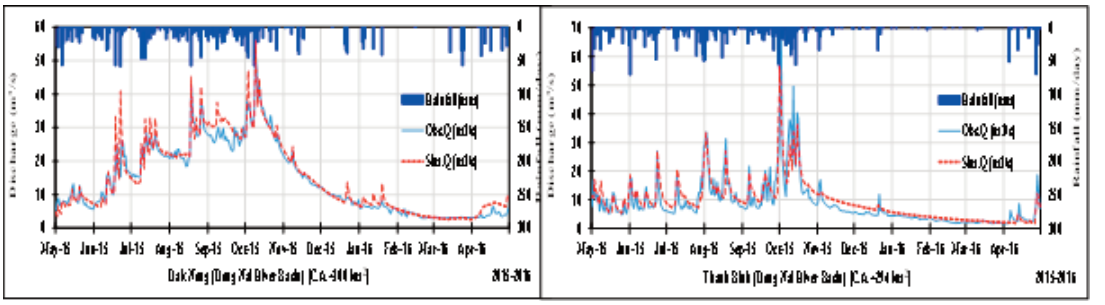

Fig. 6. Comparison between simulated and observed monthly stream flow in validation process (2015/16 year)

Table 3. Calibrated SWAT parameters, their description and best range value

No	Parameters	Definition	Range
1	ALPHA_BF	Base flow alpha factor (*days*)	0.1-0.2
2	GW_DELAY	Groundwater delay time (*days*)	31-51
3	CN2	SCS runoff curve number of moisture condition II	60-70
4	ESCO	Soil evaporation compensation factor	0.5-0.9
5	REVAPMIN (*mm*)	Threshold water depth in the shallow aquifer for revap to the deep aquifer	300-500
6	GW_REVAP	Groundwater revap coefficient	0.02-0.2
7	QWQMIN (*mm*)	Threshold water depth in shallow aquifer required for return flow to occur	600-800
8	SOL_AWC	Soil available water storage capacity(*mm H2O/mm soil*)	0.2-0.4
9	R_RCHRG	Groundwater recharge coefficient for deep aquifer	0.05-0.4
10	SOL_K	Soil conductivity (*mm/hr*)	15-50

The surface water availability in Dong Nai river basin in 2015/16 was presented in Figure 7. The areaswhich have high surface water potential are Tuyen Lam, Da Huoai and Dak Song districts in whichflow module are in the range of 40 - 50 l/s/km^2. In contrast, the Proh and Phuoc Trung communes are the locations that having lowest flow module with around 15 - 20 l/s/km^2.

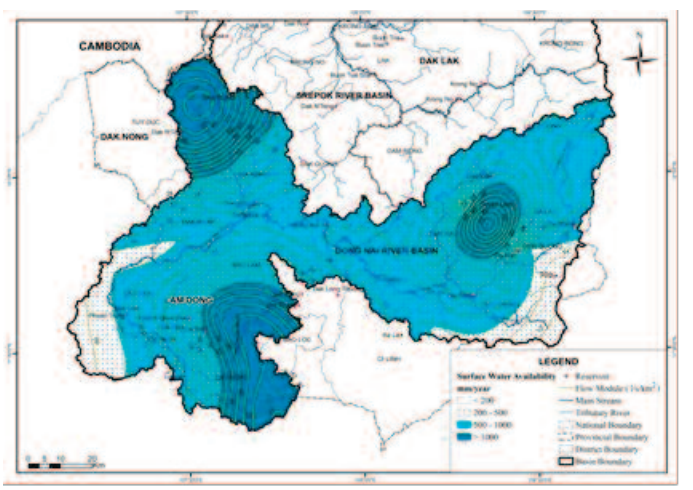

Fig. 7. Surface water availability in Dong Nai river basin in 2015/16

3.2 Groundwater availability in Dong Nai river basin

The groundwater model was setup to run in turn in 2 conditions of flow a) steady state to get the initial water head for transient state and b) transient state to get groundwater availability. The model was first calibrated to fit the observed groundwater levels until it reached to an acceptance normalized root mean square (RMS). Fig. 8 a shows the scatter diagram of calculated and observed head.The RMS was 3,062%, indicated a good simulation results.Fig. 8b shows the comparison between simulated and observed groundwater level from 2008 to 2016 in borehole 95T. The graph showed a good match between observed and simulation result in term of the-graph's shape and their corresponding peaks.

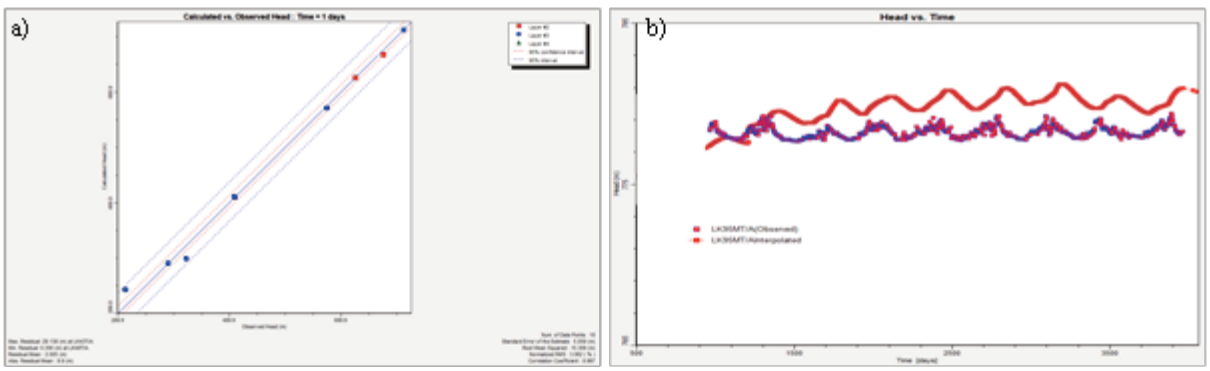

Fig. 8. Comparison between observed and simulation groundwater level in borehole 95T

Fig. 9 illustrates the groundwater level a availability in Dong Nai river basin in 2015/16. It showed that the areas having high groundwater availability locate at the same places with the areas having high surface water availability. Dak Song is the region havingthe highest groundwater availability with around 9 l/s/km^2. The other districts such as Da Huoai and Tuyen Lam also have high water potential with approximately 1.2l/s/km^2.

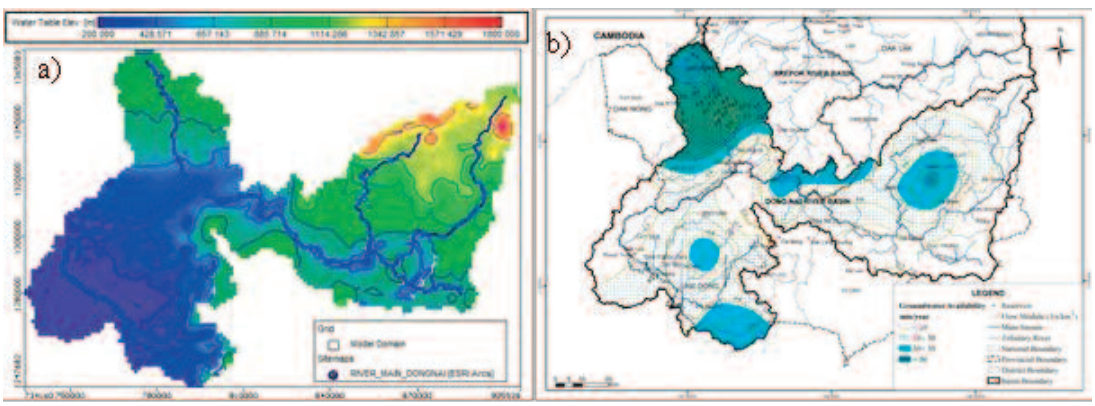

Fig. 9. Groundwater a) level and b) availability in Dong Nai river basin in 2015 - 2016

4. Conclusion

In this study, the SWAT and MODFLOW models were used for combined simulation of surface and groundwater in the DongNai basin. The SWAT and MODFLOW were run individually and linked together with recharge rates. The recharge values extracted from the HRUs of SWAT model were used in the cells of MODFLOW as the hydrological input. The simulation results including the stream flow and groundwater level of two corresponding models were then compared and showed good agreements with observed data. The results showed Tuyen Lam, Da Huoai and Dak Song districts are the locations which have high surface water potential which

is in the range of 40 - 50 l/s/km^2. In contrast, the Proh and Phuoc Trung communes are the regions that having lowest surface flow module with around 15 - 20 l/s/km^2. The groundwater simulation indicated the areas having high groundwater availability are located at the same places with the regions having high surface water availability. Dak Song is the region havingthe highest groundwater availabilitywith around 9 l/s/km^2. Da Huoai and Tuyen Lam are also the areas which have high water potential with approximately 1.2l/s/km^2.

References

1. Anh. T.N., Hoang, N.T., Son, N.T., Giang, N.T., 2009. Khả năng áp dụng mô hình MODFLOW tính toán và dự báo trữ lượng nước dưới đất miền đồng bằng tỉnh Quảng Trị. *Tạp chí khoa học DHQG*. 25(3): 372-380.

2. Au, N.T.T., Liem, N.D., Loi, N.K., 2013. Applying GIS technique and SWAT model to assessing water discharge in Dakbla watershed. *Journal of National University*, 29(3): 1-13.

3. Arnold, J.G., Srinivasan, R., Muttiah, R.S., William, J.R., 1998. Large area hydrologic modeler and assessment part I: model development. J. Am. *Water Resources*. As. 34: 73-89.

4. Chau, T.K. and Khanh, D.X., 2017. Study on water balance in Sesan river basin in drought year 2015/2016. J*ournal of Meteorological*, 678: 44-53.

5. Chiang, W.H., Kinzelbach, W., 1998. Processing mudflow: a simulation system for modeling groundwater flow and pollution. *Humburg*, Zurich, p. 325.

6. Dowlatabadi, S., Zomorodian, S.M.A., 2015. Conjunctive simulation of surface water and groundwater using SWAT and MODFLOW in Firoozabad watershed. *KSCE*, 1-12.

7. Fadil, A., Rhinane, H., Kaoukaya, A. Kharchaf, Y., Bachir, A., 2011. Hydrologic modeling of the Bouregreg watershed (Morocco) using GIS and SWAT model, 3: 279-289.

8. Hiep, H. V., Ty, T. V. (2012). Đánh giá tài nguyên nước dưới đất tỉnh Trà Vinh sử dụng mô hình MODFLOW. *Tạp chí khoa học DH Cần Thơ*, 23: 42-51.

9. Kim, N.W., Chung, I.M., Won, Y.S., Arnold, J.G., 2008. Development and application of the integrated SWAT-MODFLOW model. *Journal of Hydrology*, 356: 1-16.

10. Moriasi, D.N., Arnold, J.G., Liew, V., Bingner, R.L., Harmel, R.D., Veith, T.L., 2007. Model evaluation guidelines for systematic quantification of accuracy in watershed in simulations. Trans. *ASBE*, 50(3): 885-99.

11. Neitsch, S.L., Arnold, J.G., Kiniry, J.R., William, J.R., 2011. Soil and water assessment toll theoretical documentation version 2009. *Texas water resources institute technical repor*t No. 406. College station, Texas.

12. Putthividhya, A., Laonamsai, J., 2017. SWAT and MODFLOW modelling of spatial-temporal runoff and groundwater recharge distribution, *World environmental and water resources congress*, 51- 65.

13. Quan, N.H. and Thang, M.T., 2014. Application of swat model in assessment water resources of upper stream of Thinai lagoon serving sustainable development of Binhdinh province, *Journal of Science and Technology*, 17(14): 109-118.

14. Quynh, T.T.N., Tien, N.D., 2014. Đánh giá trữ lượng khai thác tiềm năng các tầng chứa nước dưới đất tại thành phó Tam Kỳ, tỉnh Quảng Nam bằng phần mềm Vísual Modflow. *Tạp chí khoa học và công nghệ, trường DH Huế*, 1: 110-122.

15. Winter, T.C., Harvey, J.W., Franke, O.L. and Alley, W.M., 1998. Groundwater and surface water a single resources. U. S. Geological survey circular 1139, Denver Colorado 79.

Research Paper

STUDY ON A CASE STUDY OF ABNORMAL HEAT WAVES IN THE WINTER IN THE NORTHERN AREAS OF VIET NAM IN 2010 AND 2015

Vo Van Hoa[1],Vu Anh Tuan[2], Du Duc Tien[2], Mai Khanh Hung[2], Luong Thi Thanh Huyen[2], Luu Khanh Huyen[2]

ARTICLE HISTORY

Received: April 14, 2018; Accepted: May 15, 2018

Publish on: December 25, 2018

ABSTRACT

Under the condition of climate change, the abnormal extreme weather phenomena has been increasing in both of frequency and intensity, especially the abnormal heat waves in the winter. The paper shows the results of thermodynamic analysis that caused two abnormal heat waves in the winter in northern areas of Viet Nam (one case occurred in the early winter, the other occurred at the end of winter). Based on the large-scale synoptic pattern analysis, we found that the key reason that caused abnormal heat waves in the winter in northern areas of Viet Nam is due to the unusual activities of western hot low pressure and western Pacific subtropical high pressure in combination with "foehn" effect caused by Hoang Lien Son high rock mountain . In some cases, the combination between strong cold surge that descending from the south China and western hot low pressure also caused an abnormal heat wave in the winter.

Keywords: *Abnormal heat wave, western hot low pressure, foehn effect.*

1. Introduction

In recent years, weather and climate conditions have become increasingly complex. The abnormal changes of weather and climate, such as droughts, storms and heavy rain, have caused many difficulties and even great losses for production and business in many fields of socio-seconomic development activities. On the other hand, the fluctuations of climate and weather have made difficult to forecast. The lack of long-term climate and weather forecasts is a major constraint for policy makers and managers in proposing, planning and developing national-wide and local socio-economic development plans. At the national and local levels, leaders and even local people have to deal passively with nature. That really has a great impact on the economic and social life of the country.

In Viet Nam, in the past 10 years, due to the effects of climate change, the weather regime in most parts of Viet Nam has changed considerably. Heat wave is also an abnormal increase in the highest temperature value as well as the duration of a period of heat wave. Based on observation data, the everage temperature of 2010 is considered as the hottest year in the series of ob-

VO VAN HOA
vovanhoa80@yahoo.com
[1]Red-river Delta Regional Hydro-Meteorological Center
[2]National Center for Hydro-Meteorological Forecasting

served data. However, the year 2015 broke the record. However, the most typical example of climate change is the unusually winter. Specifically, the phenomenon of snow, ice, frost, ... occurred on a large scale. Unbelievable snow is observed in recent years. Even in the middle of the winter, the maximum daily temperature in the northern mountainous provinces observed 32 - 34^{0}C, making it feel like as in the summer. Due to the influence of El Nino phenomenon 2015 - 2016, in the middle of winter, the northern provinces still have hot days as summer, the daily temperature was up to 32 - 33^{0}C. Therefore, the winter 2015 - 2016 was identified as an unusually warm winter. Specifically, during the period from February 12 - 14, 2016, due to the impact of the low pressure is compressed by the cold surge in the north combined with the field of divergence on the 5000 meters, the northern provinces appeared relatively high temperature 31 - 33^{0}C, some higher places such as Lac Son: 35.2^{0}C; Hoa Binh: 34.5^{0}C; Bac Me: 33.7^{0}C; ... in the center of Hanoi, the temperature was also 33.3^{0}C. Apart from high temperature, the humidity in the day was also very low, only 30-35%. This is a rare event in recent years because of the climate phenomenon that must occur in October and November every year.

In fact, there were a lot of national researchs that mentioned to winter moonson in Asia. Wallace and Gutzler (1981) ultilized 500hPa geopotential height anomalous in the winter of North hemisphere in order to build a forecast equation of change of Siberia high-pressure based on 3 impact centers including Scandinava center (55^{0}N, 20^{0}E), Seberia center (55^{0}N, 75^{0}E) and Japan center (40^{0}N, 145^{0}E). The result verification pointed out that the positve value of forecasting equation mean that the significant change of Siberia high-pressure in comparison with the normal. Yi Zhang and et al (1997) had paid attention to climatology and annual cycle of winter moonson in Asia from 1979 to 1995 based on NCAR's reanalysis dataset. The temporal and spatial distribution of winter moonson in Asia is belong to the cold mass's origin, path and progress. These results was pointed out in Sirapong and et al (2014). In average, there are 2 extreme cold surges in the winter. The extreme cold surge usually occurred in 7 to 9 days with the highest pressure at Seberia center around 1060 hPa. The intensity of Siberia high-pressure usually change according to season and reach to maximum in January. However, the extreme cold surges usually occurred in October and March. Hansen and et al (1999) pointed out the temperature increasing in Siberia region is faster than the increasing of global average temperature. Moreover, the temperature increasing on the land is higher than the ocean that caused the re-distributing of global pressure system. This caused the annual intensity change of Siberia high-pressure such as another large-scale pressure system. Bingiyi Wu and Jia Wang (2002) studied the impact of pole oscillation and Siberia high-pressure on the change of East Asia winter moonson and found that Siberia high-pressure is direct and key impact factor. The affect of Siberia high-pressure on surface temperature mainly impacted to the south of 50^{0}N, Pacific northwest and south of China. The similar results were found in research of Bin Wang and et al (2001).

It can be seen that under the influence of climate change, many weather and climate phenomena in Viet Nam have changed in a more extreme and unusual trend, including abnormal heat wave in winter in the northern mountainous provinces. In order to understand and predict these changes, it is necessary to have studies to evaluate the magnitude, trend and behavior of abnormal heat wave in the winter in the northern mountainous areas as well as their impact in recent decades. The paper shows out the results

of thermodynamic analysis that caused two abnormal heat waves in the winter in northern areas of Viet Nam (one case occurred in the early winter, the other occurred at the end of winter). The next section will give out the dataset is used in the analysis. The large-scale synoptic pattern analysis results that caused the abnormal heat waves in 16 to 19 November 2015 and 25 to 27 Feb 2010 presents in third section. Finally, is some key findings and remarks.

2. Dataset and analysis methodology

To have sufficient scientific basis to analyze the anomalies of winter heat waves in the northern mountainous areas as well as to show the dynamic thermodynamic mechanisms that govern the abnormal activity of heat waves. In this study, we conducted two abnormal heat waves, including heat wave from 16 to 19 November 2015 (early winter) and heat wave from 25 to 27 February 2010 (late winter). In order to serve the analysis, we collected the following dataset:

- Daily maximum temperature of 21 surface meteorological observation stations in the north region of Viet Nam from 25 to 27 February 2010 and 16 to 19 November 2015. These daily maximum temperatures are checked by QC system prior to using in analysis (logic, physical and climatology checks)

- The climatological monthly average temperature in November and February that is calculated from period of 1971 - 2010 at 21 surface meteorological observation stations in the north region of Viet Nam.

- JRA55 reanalysis data of JMA (ftp://ds.data.jma.go.jp/ JRA-55/Hist/Daily) from 23 to 29 February 2010 and 14 to 21 November 2015 including presssure of mean sea level, 10 meters wind, 2 meters temperature at surface level. At upper standard pressures of 925, 850, 700 and 500hPa, the geopotential height and wind field were collected.

The abnormal factor determined according to the large different between the daily maximum temperature of these days that heat wave occurring with climatological monthly average temperature. In order to find out the synoptic patterns that drive the abnormal heat waves, the weather maps from surface up to 500hPa level derived from JRA55 reanalysis data is analyzed by synoptic resonance analysis method.

3. The large-scale weather pattern analysis that caused the abnormal heat waves in the winter in the northern areas of Viet Nam

3.1. The abnormal heat wave from 16 to 19 November 2015

From 16 to 19 November 2015, there was an abnormal heat wave spell occurring in the northern mountainous. The maximum temperature reached 31^0- 33^0C, and achieved an excess of 33^0C in some areas such as Phu Yen (Son La) 35,1^0C; Hoa Binh 35-36^0C; Van Chan (Yen Bai) 34.5^0C; Bac Me (Ha Giang) 33.7^0C; Vinh Yen (Vinh Phuc) 34.4^0C; Tp. Cao Bang 33.0^0C; Hiep Hoa (Bac Giang) 34.2^0C; …. The above obsserved maximum temperatures is larger about 2 to 2.5 times than climatological standard deviation of monthly average temperature in November (climatological monthly average temperature of northern region of Viet Nam is 21.5^0C in November). The daily maximum temperature distribution at 00UTC from 16 -19 November 2015 was shown in the Fig. 1. Different from the abnormal heat wave spell in February 2010, the maximum temperature in this spell tended to deflect towards the east and concentrated on the Viet Bac and Dong Bac mountainous areas. The heat wave focused on the period from 16 to 18, and then significantly decreased in 19 November 2015.

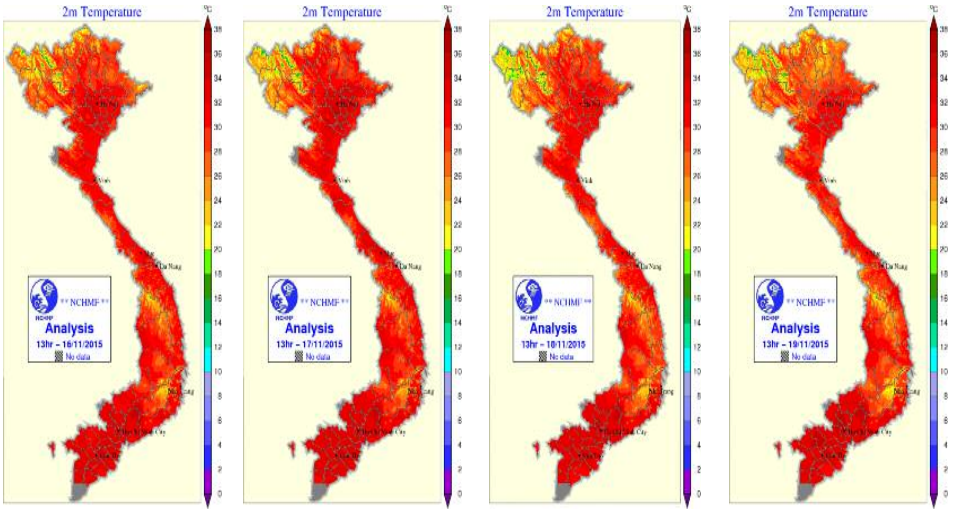

Fig. 1. The maximum temperature distribution at 00UTC from 16-19 November 2015 (from left to right)

In Fig. 2, the reanalysis map illustrates 10m wind and sea level pressure on 16 November (onset) and 17 November (date of occurence). The left figure shows an unfully-developed low pressure in the north of North Viet Nam along the longitude of 103 -112^{0}E, a high pressure in the north of India and a developing low-pressure in northeast China. The prevailing winds in the north Viet Nam was changing from east winds to southeast winds with average speed of 3 - 5m/s. On 17 November 2015, this high pressure moved eastwards quickly and located in north Bangladesh, while the low pressure in the northeast China disappeared completely and was replaced by a high continent pressure. Also, the low pressure in the north of Northern Viet Nam moved towards the south and located in the north border regions. The winds in Tonkin Gulf remained south winds and reached 7-10m/s.

The distribution of pressure of mean sea level at 00UTC in 18 and 19 November 2015 respectively shown in Fig. 3. The Fig. 3a shows the clear cold surge in the northeast region of China which was extending to the northeast border region of Viet Nam. The mentioned low-pressure was forced westward gradually with incomplete shape. The wind speed of the prevailing southwinds over the north of Viet Nam was decreased. In 18 November 2015 (the Fig. 3b) the low-pressure area was squeezed by the continental high from China. In the west of Northern Viet Nam, the wind direction changed to north-east and the temperature was decreased for ending this unusual heat wave.

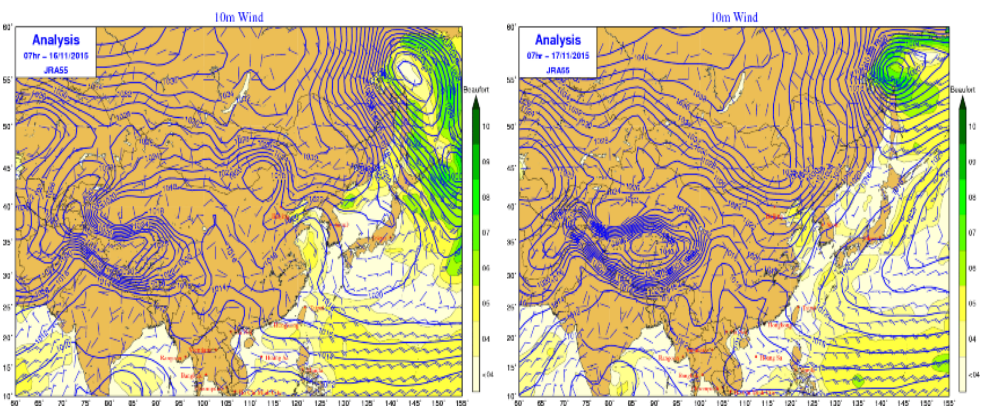

(a) (b)

Fig. 2. The 10 meters wind and pressure distribution at 00UTC 16 (a) and 17 (b) November 2015

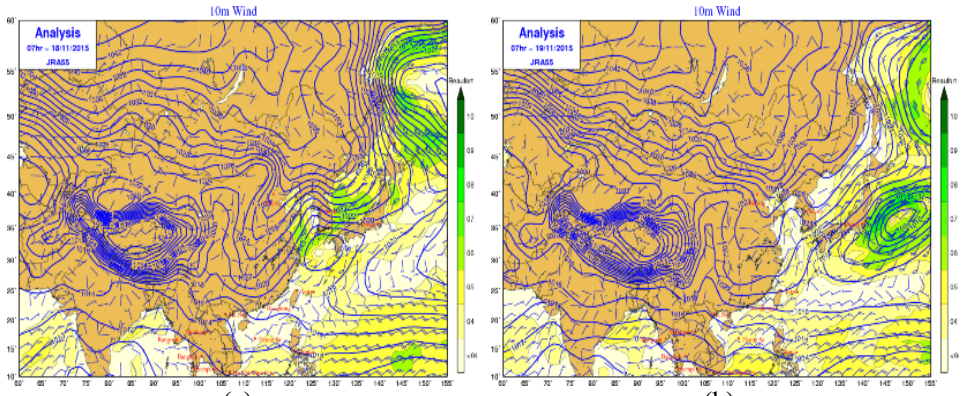

(a) (b)

Fig. 3. The 10 meters wind and pressure distribution at 00UTC 18 (a) and 19 (b) November 2015

The Fig. 4 shows the strong continental high area with center at the north of Indian and two high pressure areas in China (cleared close isobaric line). These two high areas over China have maximum pressure values about 1014hPa and 1016hPa. A low pressure area in the Bay of Bengal is forecasted to enhance and move to north-east and then a trough will be formed over Northern Viet Nam. In 17 November, the continental high pressure was strengthened and the isobaric line 1020hPa was extended to the north of China. After that, the low pressure area moved southward and covered the north of Viet Nam. The Fig. 5a shows the continental high (in the northeast China) was extending to south-west and close to the boundary of Northern Viet Nam and then we cannot observe the low pressure area over the North Viet Nam anymore. The Fig. 5b shows the continental high over China and the isobaric 1020hPa was closed to the boundary of the east of Northern Viet Nam. The temperature was more decreased after 19 November 2015 (Fig. 1).

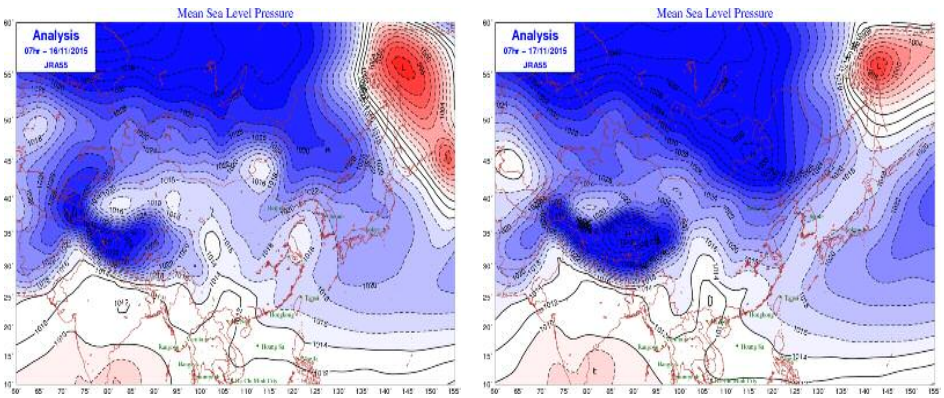

(a) (b)

Fig. 4. Mean sea pressure level at 00UTC on 16 (a) and 17 (b) November 2015

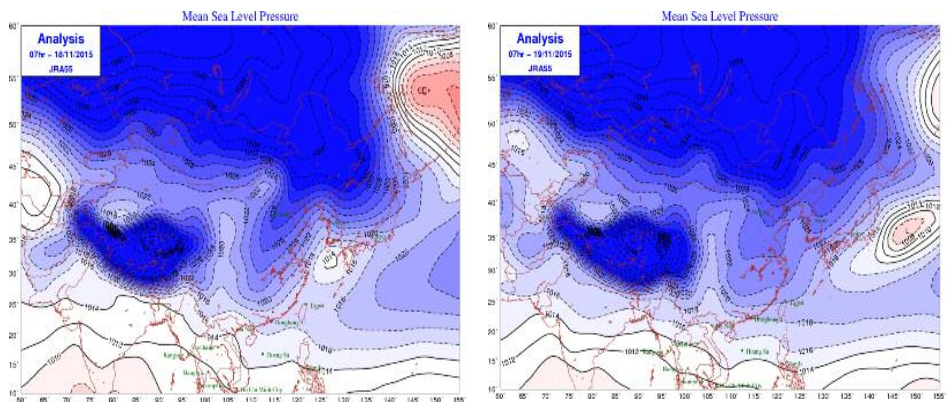

(a) (b)

Fig. 5. Mean sea pressure level at 00UTC on 18 (a) and 19 November 2015 (b)

The Fig. 6a shows the subtropical high (at level 500hPa) with axis 17^0N-18^0N, over Central Viet Nam. Over this subtropical high, there was a high pressure (in the northwest Thailand). In upper level, dry north-west wind from the subtropical high which is also located over the mountainous area in Northern Viet Nam has speed about 20 - 25m/s and 15m/s in the north of Bangladesh and the north of Northern Viet Nam respectively. In 17th November 2015, the subtropical high moved northward and the high-pressure area in the northwest Thailand was disappeared. Therefore, the winds in the north of Northern Viet Nam changed to southwest winds with speed about 10 -15m/s. This is clear that before the heat wave, there was a weak divergence in 500hPa pressure level and after that there was no divergence anymore

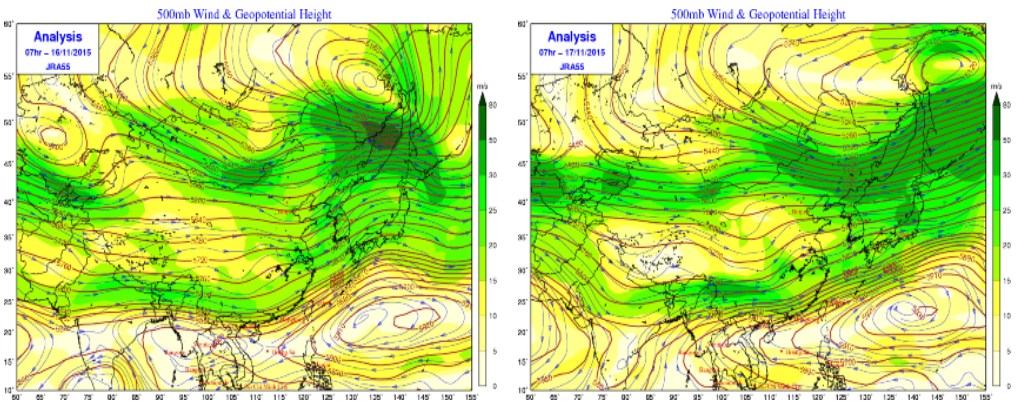

(a) (b)

Fig. 6. Wind and pressure in 500hPa at 00UTC on 16 (a) and 17 (b) November 2015

Fig. 7a shows the north Pacific high is moving eastward and the southwest winds over Northern Viet Nam with speed around 10 - 15m/s. In the north of the Bay of Bengal, a westerly disturbance moves eastward. Fig. 7b shows the wind stronger convergence in the north of Northern Viet Nam, wind speed increased by 15 - 20m/s, some wind speed about 25m/s. In the afternoon, it was raining in the north of Northern Viet Nam, this is a sign ending the heat wave.

In summary, the reason for the unusually heat wave from 16 -19 November 2015 was the effect of the heat low pressure area in the north of Northern Viet Nam. The enhanced continental high from China and convergence wind over 500hPa level caused the ending of the heat wave.

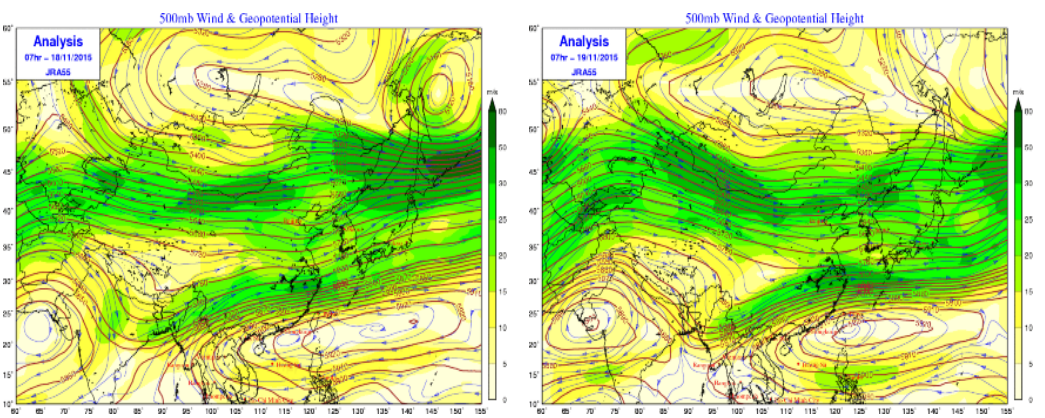

(a) (b)

Fig. 7. Wind and pressure in 500hPa at 00UTC on 18 (a) and 19 (b) November 2015

3.2. The abnormal heat wave from 25 to 27 February 2010

From 25 to 27 Feb 2010 in the mountainous provinces of North Viet Nam, there was an unusually heat wave. The highest temperature of the day has rosen around 33 - 35^{o}C. Daily max-

imum temperatures have passed the heat wave threshold (≥ 35^{0}C): Muong La, Quynh Nhai (Son La) 36.5^{0}C; Hoa Binh 36- 37^{0}C; Lao Cai 36.6^{0}C; Dinh Hoa (Thai Nguyen) 36.6^{0}C; Minh Dai (Phu Tho) 36.4^{0}C; Cao Bang 35.4^{0}C; That Khe (Lang Son) 35.6^{0}C; ... The above obsserved maximum temperatures is larger about 2.5 to 3 times than climatological standard deviation of monthly average temperature in February. The climatological monthly average temperature of northern region of Viet Nam in February is 17-18^{0}C.

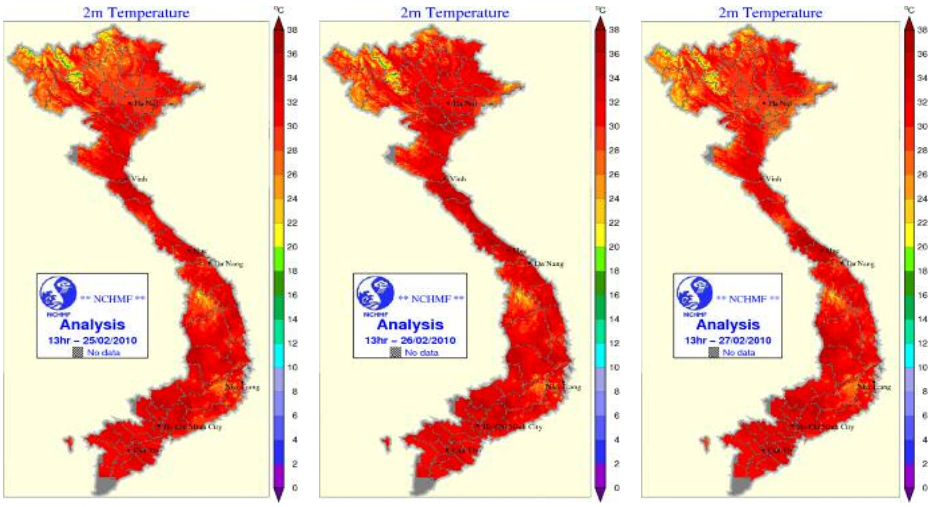

Fig. 8. The temperature at 00UTC on the 25, 26 and 27 February 2010 (in order from left to right)

Fig. 8 shows the highest temperature distribution at 00UTC on 25, 26 and 27 Feb 2017 in the northern mountainous provinces. Unlike the unusually heat wave in the northern mountainous area as above analyzed, the highest temperature distribution in this heat wave is quite similar to the North West, Viet Bac and Northeast areas. The hottest area is still in the northern midland provinces and it is very clear in the February 26th temperature distribution. The highest temperature distribution in the Northeast mountainous provinces was the same for all three days of 25, 26 and 27 February. It means that the intensity of given heat wave is more prolonged in comparison with the normal in February.

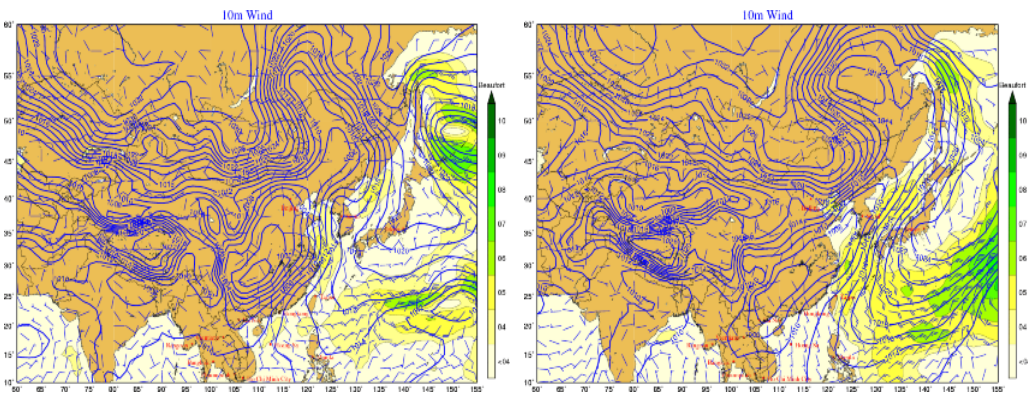

(a) (b)

Fig. 9. The 10 meters wind and pressure of mean sea level fields at 00UTC on 24 (a) and 25 (b) February 2010

Fig. 9 illustrates 10m - wind and surface pressure reanalysis on 24 February 2010 (before the onset of unusually heat wave) and February 25, 2010 (the onset of unusually heat wave). Fig. 9a shows a low-pressure area below 1000hPa. This low-pressure circulation covers a large area of

mainland China. The prevailing wind direction throughout the northern mountainous provinces is the southwest. Wind intensity is not strong and located in the impact zone at the southwestern edge of the low pressure zone. On Feb 25, the low-pressure shape changed to the compressed elliptical form and expanded over the Southwest. The whole of the North for this moment was covered by the southwestern part of the low-pressure area.

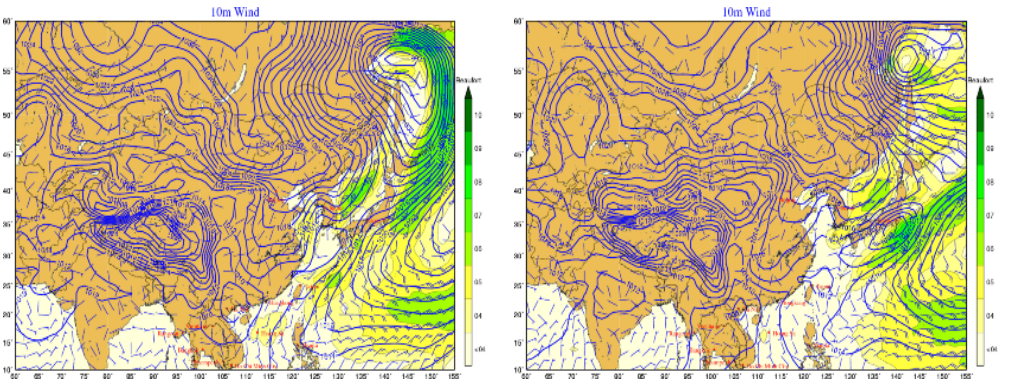

(a) (b)

Fig. 10. The 10 meters wind and pressure of mean sea level fields at 00UTC on 26 (a) and 27 (b) February 2010

On February 26 (Fig. 10a), the low-pressure center moved south and covered the Northern provinces. The low-pressure center is located in the Northeast region. In the northern part of China, there was a high-pressure ridge that was stretching southward. This is the reason why a large low-pressure area two days before was narrowed rapidly. In the northern mountainous area, the wind direction was changed towards the lower center of the low area. The next day (Fig. 10b), the low-pressure area became smaller and covered a relatively narrow area in the northern coastal provinces (the low-pressure center also located on this area). The continental high-pressure ridge also expanded to the northeastern border of Viet Nam.

Fig. 11 represents the pressure mean sea level reanalysis map at 00UTC on February 24 and 25, 2010 (before and after beginning of the unusually heat wave). Fig. 11a indicates a low-pressure region with relatively low atmospheric pressure at the center (red colored region). At this time, the low-pressure center located at about 30^{o}N - 110^{o}E. It has small impact on the northern mountainous provinces. The 1008hPa line run through the northern mountainous area has proven itself. On 25 February 2010, the low-pressure region in northeastern China moved closer to the northeastern mountainous provinces. The intensity of the low-pressure has weakened considerably while the central pressure has increased (shown in light pink shaded color). The low-pressure circulation now covers the whole of the northwestern and northeastern parts of Viet Nam which provided the evidence that there is an impact of the above-mentioned low-pressure region.

In Fig.12, the reanalysis map illustrates pressure distribution which was calculated to sea level pressure at 00UTC of 26 and 27 February in 2010 when abnormal heat wave occurred. In these sea level pressure reanalysis maps (Fig.12a), it is clear that the low-pressure area moved towards the northeast mountainous areas of Viet Nam and its center located over the Northeast Viet Nam. The circulation of this low pressure covered the northern part. However, the center pressure is significantly high at 1006hPa. Turning to 27 February, while the maximum temperature decreased in the north mountainous part, this low-pressure center was pushed back to the Northern Plain and intensified to 1008hPa. This could be a signal for the cessation of this anomal heat wave.

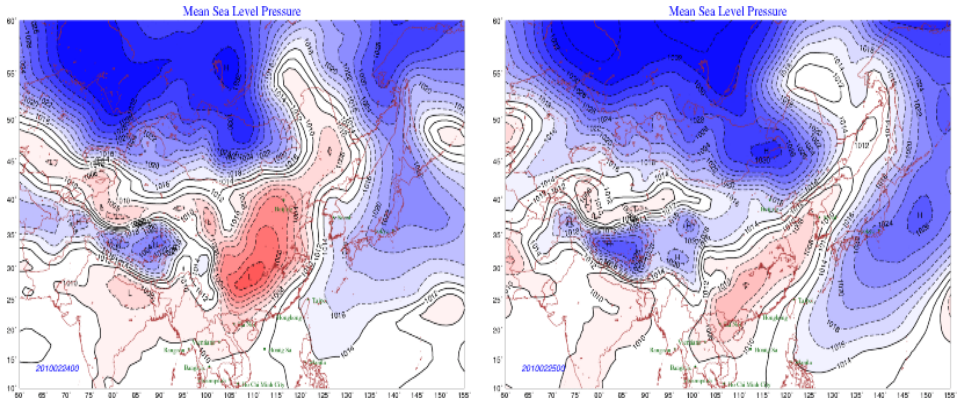

(a) (b)

Fig. 11. The pressure of mean sea level at 00UTC on 24 (a) and 25 (b) February 2010

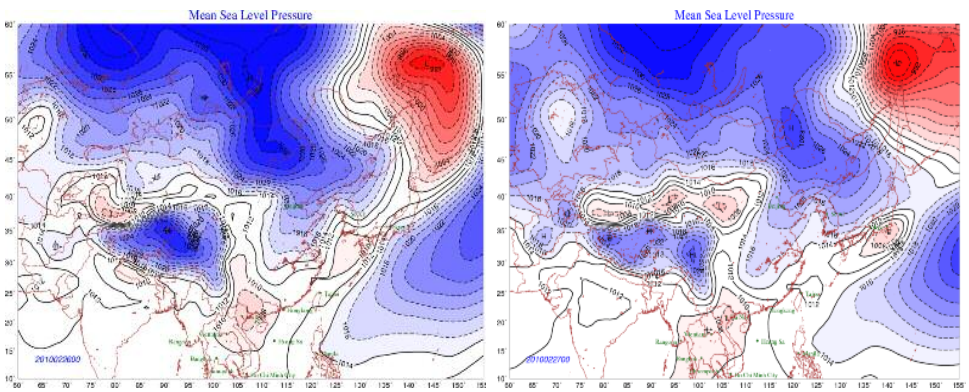

(a) (b)

Fig. 12. The pressure of mean sea level at 00UTC on 26 (a) and 27 (b) February 2010

Considering Fig. 13 showing the reanalysis map of 500hPa wind and geopotential height before and after the period of anomal heat wave, the left map illustrates the subtropical high pressure located in low-latitude ran along the latitude of 100N though Southern Viet Nam. At the same time, Northern Viet Nam in general and mountainous areas in specific experienced high-velocity southwest winds with an average of 25 to 30 m/s and 30 to 40 m/s in some mountainous area in the north. Turning to 25 Feb 2010, the axis of this subtropical high was move to the north, whereas the north mountainous part still suffered from southwest wind, however, with slightly decreased wind velocity at an average of 20 to 30 m/s. This could explain that there was no effect of divergence field to the weather of north mountainous area both before and after the occurrence of abnormal heat wave.

Fig. 14 shows the reanalysis map of 500hPa wind and geographical height in 26 and 27 February 2010 before and after the period of anomal heat wave. In the Fig. 14a, there was northeast to southwest subtropical high forming a high pressure in South China sea - East sea of Viet Nam. Meanwhile, the north part was covered by the southwest winds prevailing in the area from Belgan Bay through northern Viet Nam to South China. The southwest wind was at 20-25m/s. In 27 February, while there was a sharp decrease in the temperature in Northern Viet Nam, the north mountainous area still suffered from Southwest to West winds with a decrease in its intensity to 15 to 20 m/s.

We can see that with reanalysis maps for the abnormal heat wave in northern Viet Nam and north mountainous area during the period from 25 to 27 February 2010, the key element had caused this phenomenon was the direct effect of heat low pressure located in China since it was pushed back to the northern Viet Nam. The southward movement of cold surge in the north facilitated for ending this abnormal heat wave

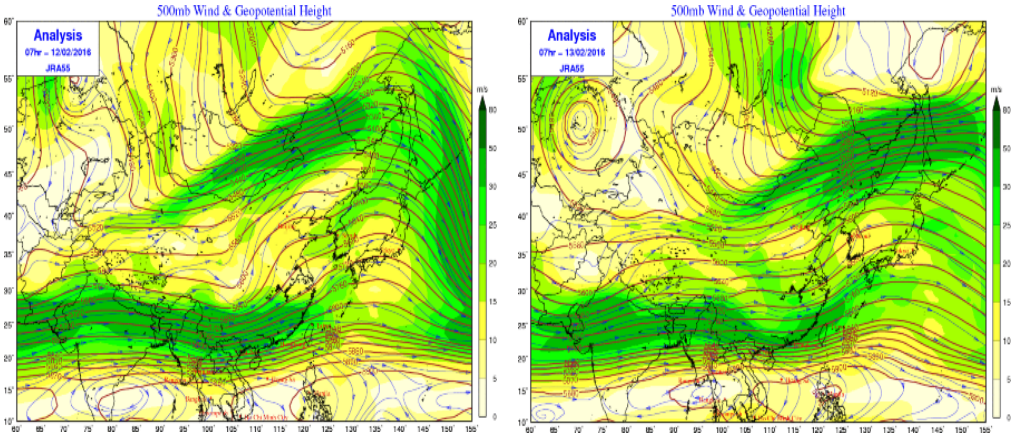

(a) (b)

Fig 13. The wind and geopotential height field of 500hPa pressure level at 00UTC of 24 (a) and 25 (b) February 2010

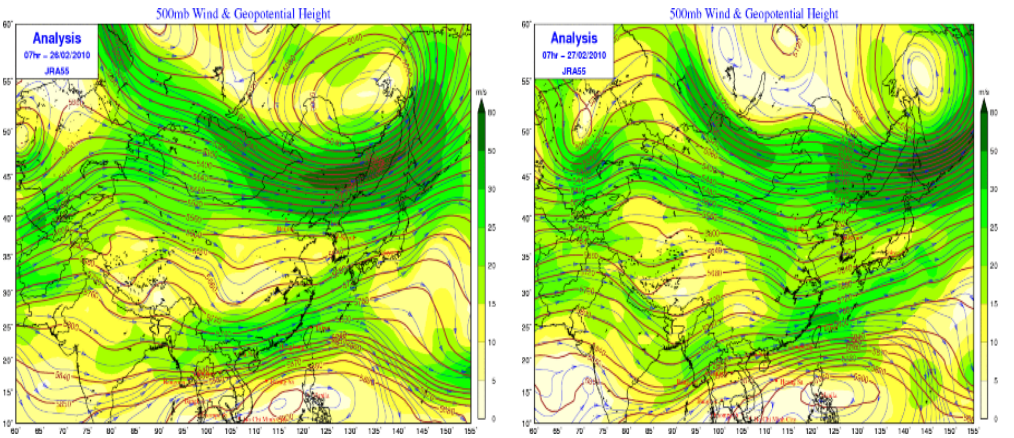

(a) (b)

Fig. 14. The wind and geopotential height field of 500hPa pressure level at 00UTC of 26 (a) and 27 (b) February 2010

4. Conclusion

Under the climate change, the abnormal extreme weather phenomena had been increasing in both of occurring frequency and intensity, specially the abnormal heat waves in the winter. The paper shows out the results of thermodynamic analysis that caused two abnormal heat waves in the winter in northern areas of Viet Nam (one case occurred in the early winter, the other occurred at the end of winter) based on the dataset of obsserved daily maximum temperature, the climatological monthly average temperature in November and February that is calculated from period of 1971 - 2010 and JRA55 reanalysis data of JMA from 25 to 27 February 2010 and 16 to 19 November 2015. The abnornal factor determined according to the large different between the daily maximum temperature of these days that heat wave occurring with climatological monthly average temperature. In order to find out the synoptic patterns that drive the abnormal heat waves, the weather maps from surface up to 500hPa level derived from JRA55 reanalysis data is analyzed by synoptic resonance analysis method. We found out the main cause of the unusual activities of the heat wave in winter is that the heat low pressure area in the north of Northern Viet Nam had been moving southward by the continental high pressure from China and in combining with the effect of the wind divergent at levels 3000 - 5000 meters over Northern Viet Nam. In addition, unusual activies of westhern Pacific subtropical high pressure, southwest moonsoon in combination with “foehn” effect caused by Hoang Lien Son high rock moutain

chain is also significantly considered. In some cases, the combination between strong cold surge that desending from the south China and western hot low-pressure is also caused an abnormal heat wave in the winter. Finally, the effect of urban heating is significantly contributed to abnormal heat wave in northern urban areas, speacially is in early winter period.

Acknowledgments: *This work was supported by the Ministry of Natural Resources and Environment through the national Project "The impact of climate change on abnormal cold surge and heat wave in the winter at the Viet Nam northern mountain areas to serve for socio-economic development" (code: BDKH.25/16-20)*

References

1. Bin, W., Renguang, Wu., Lau, K.M, 2001. Interannual Variability of the Asian Summer Monsoon: Contrasts between the Indian and the Western North Pacific-East Asian Monsoons. *Journal of Climate*. 14, 4073 - 4090.

2. Bingyi W., Jia W., 2002. Winter Arctic Oscillation, Siberian high and East Asian Winter Monsoon. *Geo. Res. Letters*. 29 (9): 1-3.

3. Hansen, J., Ruedy, R., Glascoe, J., Sato, M., 1999: GISS analysis of surface temperature change. *J. Geophysi. Res.* 104: 30997-31022

4. Sirapong Sooktawee, Usa Humphries, Atsamon Limsakul, Prungchan Wongwises, 2014. Spatio-Temporal Variability of Winter Monsoon over the Indochina Peninsula. *Atmosphere.* 5:101-121.

5. Wallace, Gutzle, 1981: Teleconnections in the geopotential height field during the northern hemisphere winter. *Mon. Wea. Rev.* 109: 784 - 812.

6. Yi Zhang, Kenneth R. Sperber, James S. Boyle, 1997. Climatology and Interannual Variation of the East Asian Winter Monsoon: Results from the 1979 - 1995 NCEP/NCAR Reanalysis. *Mon. Wea. Rev*. 125: 2605-2619.

Vietnam Journal of Hydrometeorology, ISSN 2525 - 2208, Volume 01: 54 - 63

Research Paper

ARTIFICAL NEURON NETWORK FOR FLOOD FORECASTING AS INFLOW OF PLEIKRONG RESERVOIR IN POKO RIVER

Truong Van Anh[1], Duong Tien Dat[1]

ARTICLE HISTORY

Received: April 12, 2018; Accepted: May 08, 2018

Publish on: December 25, 2018

ABSTRACT

In Vietnam, modern and small hydropower reservoirs play an important role in socio-economic development. However, the effective operation of such reservoirs based on the argument of the release function and expected future inflow is one of the most important variables that the operators will reply on to control such release. In other words, to attenuate floods, the operators have to release water in advance, so to create an empty volume (flood volume) in the reservoir, into which the excess in flow can be accommodated during the flood events. Therefore, the predicted periods should be as long as possible to create a sufficient large flood volume in the reservoir, while releasing a flow that is not so high to mitigate the impacts on downstream. Nevertheless, predicting the future inflow is still a big challenge for the local hydrologists due to the lack of information and technology. This paper proposes a method to predict the inflow of Pleikrong hydropower reservoir which located in downstream of Poko river, a second tributary of SeSan River and the observation data is insufficient and incorrect. This method uses MIKE NAM to construct the inflow then the Artificial Neuron Network to predict the inflow based on the availability of data. The result is surprising when R^2 for 6 hourly forecasted inflow is about 0.97 and for 12 hourly forecasted is about 0.79 which correspond to the catchment concentration time of 9 hours. The results of this study will hopefully be an example to apply on many case studies in Viet Nam and other ungauged stations system.

Keywords: *Reservoir management, flood forecast, MIKE NAM, ANN, PleiKrong.*

1. Introduction

Flood forecasting is an important and integral part of a multi-purpose reservoir management, and can help to provide early warning for efficiency operation (Guo, 2009). Various flood forecasting models, including data driven flood forecasting such as regression model, and more sophisticated real time catchment-wide integrated hydrological and hydrodynamic models such as using MIKE 11 module of DHI software may be adopted (Jain et al., 2012). These models provide forecasted flow and water level at the controling locations known as Forecast Points. The Forecast Points are usually located along major rivers or known as the inflow of reservoir and they will be operated for flood mitigation during a flood event (Socini, 2007). However, current reservoir operation does not fully realize and appreciate the benefits that accrue from the enhanced level of forecasting accuracy and the current innovative techniques (Castelletti, 2012). Forecasts about the discharge are calculated in real-time, by using the model to transform the input functions into a corresponding discharge function time.

The physical based models describe the hydrological processes occurring in a basin which

TRUONG VAN ANH
tvanh@hunre.edu.vn

[1]Department of Hydrology and Meteorology, Hanoi University of Natural Resources and Environment

are expected to have significant advantages over purely empirical models. The main advantages of these models are their accuracy and the potential for performing comprehensive sensitivity analyses. The parameters of these models have direct physical interpretation, and their values might be established through field or laboratory investigations (Sulafa HagElsafi et al., 2014). On the contrary, the data driven models as the black box showing the relationship between inputs and outputs are developed then using this function latter to simulate or forecast interest variables. Therefore, it requires less data and detailed information.

The stream flow modeling is a key tool in water resources management, early warning for flood hazards, and related impacts. Many advanced types of models exist, but they have been developed for a diverse range of climatic regions. The physical based models like hydrology and hydrodynamic models for this purpose have the capability of simulating a wide range of flow situations. However, these models require accurate river geometric and hydrological data, which may not be available at many locations. For forecasting purpose, the types of model use forecasted climate data for prediction which may cause more errors in the result. On the other hand, the data driven models for stream flow forecasting can be applied in the case study where there is not much data available. Among these models, Artificial Neural Network (ANN) provides a quick and flexible approach for data integration and model development. Therefore, this research used ANN models to forecast floodis to PleiKrong reservoir. It is anticipated that this work will provide baseline information toward the establishment of a flood warning system for the case study and other similar regions in the Central part of Viet Nam.

2. Study area

The Poko river is located in the Western part of Kon Tum province. It is the secondary tributary of SeSan river with the area of 3,210 km^2 and has 152 km long. The river originates from the high mountain of Chu Prong in Dak Glei district, flowing in the north-south direction. Frequent floods have caused serious damage in recent years. According to statistics, in the last 35 years, the basin has been suffered to severe flood events. In 1994, flood damage was 18 billion VND while it reached 2.6 billion VND in 1996, 7.5 billion VND in 2009 and 30 billion VND in 2009 (Song Tra ECCL, 2015). However, meteo-hydrologica stations are not sufficient for water related studies. There are only three rain stations including Dak Mot, Dak To and Dak Glei of which Dak Glei is not continuous to operate. For hydrological purpose, there is only one discharge station at Dak Mot and one water level station at Dak To (Fig. 1).

In 2003, PleiKrong reservoir was built in 14 km downstream of DakMot station for hydropower purpose and it went to operate in 2006 after two years of construction. In 2014, Thuy Loi University conducted a survey of longitude profiles and cross sections along Poko river and DakBsi river to simulate and analyze the inundation maps of the system. However as seen above, there is no controling points to calibrate and validate this system by using the hydrodynamic models. Therefore, it is necessary to find out a method to predict the inflow of the reservoir (PleiKrong inflow from now on) that cannot based on physical based models (hydrological model in combination with hydraulic model) using forecasted rainfall events if the data of the river cross sections is available. Other potential way is using only hydrological models with forecasted rainfall but there is a big gap in predicted future meteorological variables in Viet Nam due to the uncertainty of climate in the study case. the Artificial Neuron Network (ANN) is used for flood forecasting purpose.

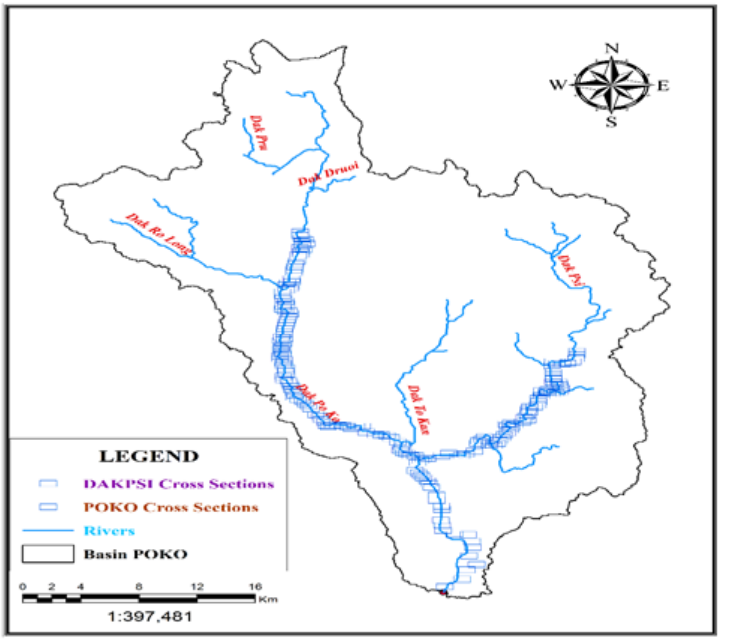

Fig. 1. PleiKrong reservoir catchment in Poko river

3. Methodology

Based on the available data, the proposed method here is using MIKE NAM to simulate the past inflow events in Pleikrong. This model is validated with the discharge time series observed at Dak Mot hydrological station then its parameter set will be transferred to PleiKrong catchment as a similar watershed (step 1 to step 3 in Fig. 2). In fact, Dak Mot catchment accounts for two-third area of PleiKrong and they are located in the similar climate region. That is why the set of parameters from the Dak Mot model was slightly modified on concentration time related parameters and applied in Pleikrong catchment). Then these estimated inflows will be used as the output of system while inputs can be any available information at previous time step for training an ANN network (Fig. 2). The main advantage of this method is the information used to predict the inflow is deterministic which should be known at predicted time by observation. The errors can be reduced by not using predicted information for flood forecasting. This method worked well in the case study and hopefully it will be useful when applying in other similar problems.

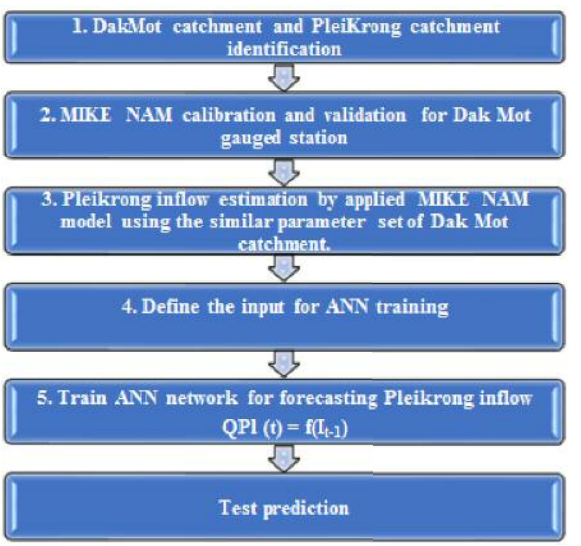

Fig. 2. The flood forecasting procedure of Pleikrong inflow QPl $_{(t)}$ where I_{t-1} can be any well known information at previous time step.

3.1 MIKE NAM model

MIKE NAM is a rainfall-runoff model contained in MIKE package that developed by DHI. This conceptual model simulates some hydrological processes that happened within the catchment including overland flow, interflow, base flow and recharge from groundwater. This is one of the most common hydrological models which were used in Viet Nam since 2000. The structure of the model is described in Fig.3.

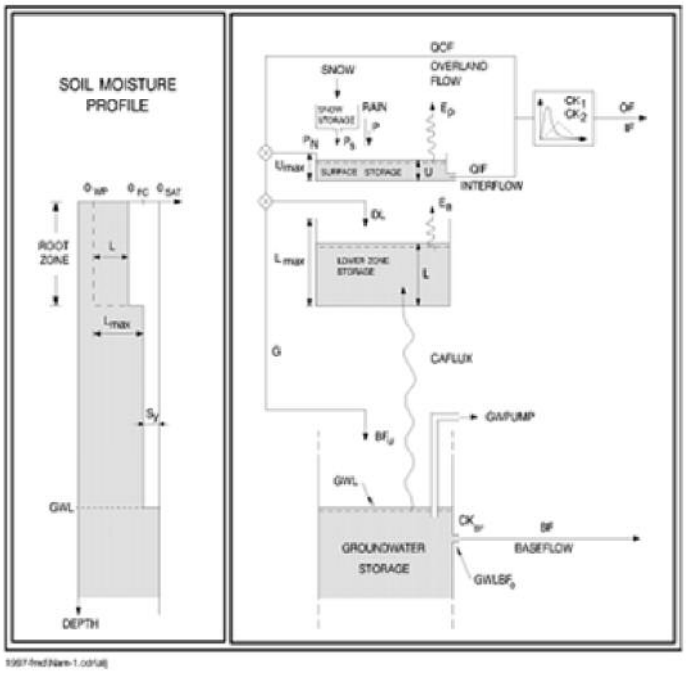

Fig. 3. Structure of MIKE NAM [5]

This structure is an imitation of the of the hydrological cycle in the continent. NAM simulates the rainfall-runoff process and the water content is divided into four different and mutually interrelated storages that represent different physical elements of the catchment including:

- Snow storage
- Surface storage
- Lower or root zone storage
- Groundwater storage

Based on the input data, NAM produces catchment runoff as well as information about other elements of the of the hydrological cycle, such as the temporal variation of the evapo-transpiration, soil moisture content, groundwater recharge, and groundwater levels. The catchment runoff is split conceptually into overland flow, interflow and base flow components (DHI, 2017).

3.2 ANN model

The ANN is a computer program that is designed to intimate the human brain and its ability to learn tasks. This program, acts as an expert system and is trained to recognize and generalize the relationship between a set of variable inputs and outputs (Sulafa HagElsafi et.al, 2014). There are two characteristics of the brain as primary features which are used in ANN: the ability to (1) "learn" and (2) generalize from limited information. The knowledge stored as the strength of the interconnecting weights (a numeric parameter) in ANNs is modified through a process called learning, using a learning algorithm. The more important information is the more weighted value is. Then the algorithmic function which based on back-propagation is used to modify the weights in the network. ANN network is "taught" to give an acceptable answer to a particular problem when the input and output values are sent to the ANN for "learning", initial weights to the connections in the architecture of the ANN are assigned, and the ANN repeatedly adjusts these interconnecting weights until it successfully produces output values that match the original values. The ANN maps the relationship between the inputs and outputs, and then modifies its internal functions to determine the best relationship that is represented by the ANN. The inner work and process of an ANN are often thought of as a "black box" with inputs and outputs. One useful analogy that helps to understand the mechanism occurring inside the black box is

to consider the neural network as a super-form of multiple regression. Like linear regression resulting from the relationship that {y} = f{x}, the neural network finds some functions f{x} when trained. The most common type of artificial neural network consists of three groups, or layers, of units: (1) a layer of "input" units is connected to (2) a layer of "hidden" units, which is connected to (3) a layer of "output" units (Fig. 4).

In this study, ANN network was identified and trained with past flood events in the PoKo river from 2011 to 2013 and known as the inflow to PleiKrong. Later, this network is used to forecast the Pleikrong inflow as describe in step 5 of flood forecasting procedure in Fig. 3.

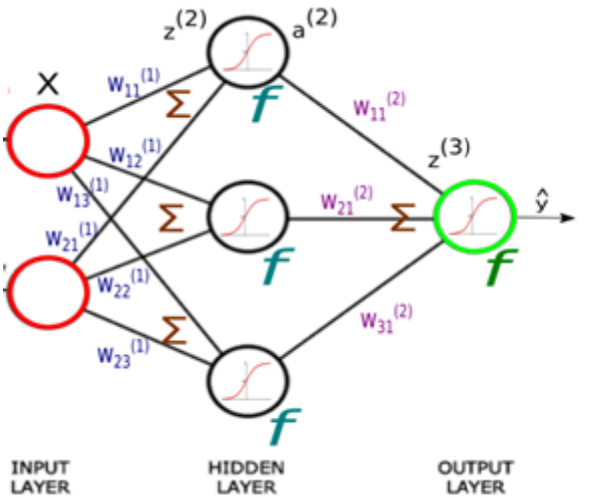

Fig. 4. An Example of a simple feed forward network, in which aj equals to the activation value of unit j, $w_{j,i}$ equals to the weight on the link from unit j to unit i, ini equals to the weighted sum of inputs to unit i, ai equals to the activation value of unit i (also known as the output value), and g equals to the activation function.

4. Results and discussion

In this study, it is necessary to clarify 2 subcatchments: Dak Mot catchment that is Poko basin up to Dakmot station and Pleikrong catchment that is Poko basin up to the Pleikrong reservoir. MIKE NAM model was calibrated and validated used the hourly recorded discharge time series. The weights of the rainfall at the gauging stations was estimated by Thiessen polygon method using data of Dak Mot and Dak To stations as presented in Fig. 5 and Table 1.

Table 1. Catchment area and its weighted values.

Period	Calibration	Validation	
Year	2003	2009	2011
NASH	0.89	0.91	0.93

Fig. 5. Subcatchment and rain gauges in the Poko river basin

4.1 MIKE NAM Calibration and Validation for Dak Mot gauged station

In this research, MIKE NAM simulated very well the discharge at Dak Mot station. The values of evaluated criteria NASH for calibration and validation are acceptable as shown in Table 2 and the observed and estimated water discharge matched very well for calibration and validation (Fig. 6).

Table 2. NASH coefficients of calibrated and validated Dak Mot models

Period	Calibration	Validation	
Year	2003	2009	2011
NASH	0.89	0.91	0.93

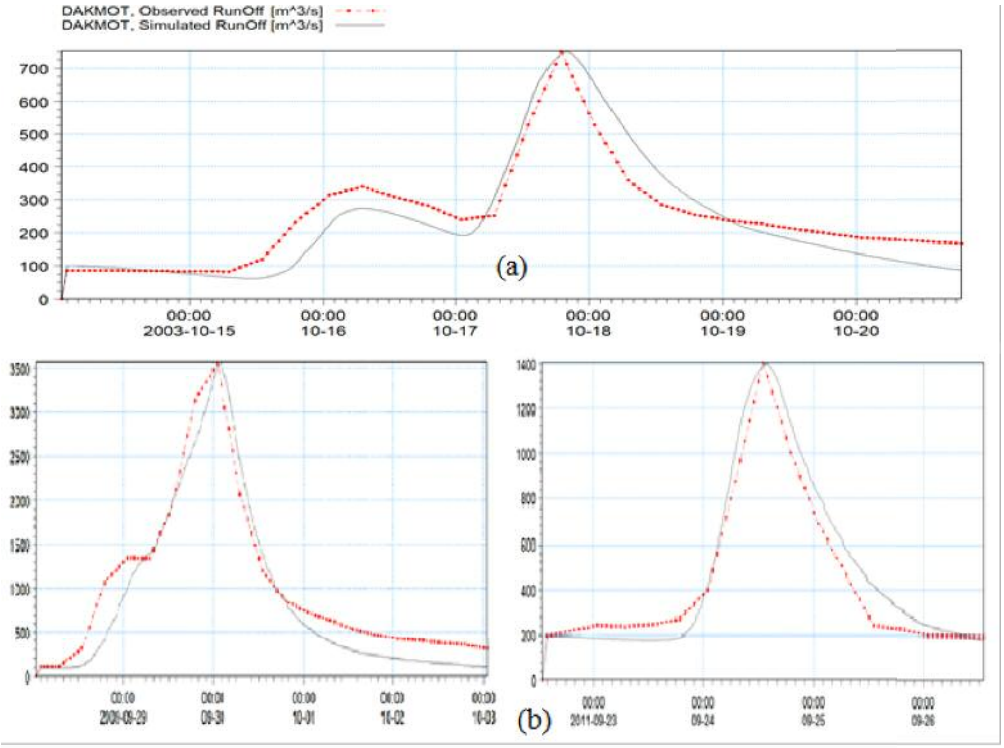

Fig. 6. Calibration and Validation of water discharge at Dak Mot

Therefore, it can be concluded that MIKE NAM model can be effectively used to simulate the water discharge in the Poko river with the set of validated parameters in Table 3.

Table 3. Validated parameters of MIKE NAM model for Dak Mot catchment

Parameter	Values
Lmax (mm)	100
Umax (mm)	10.2
CQOF	0.77
TOF	0.0296
TIF	0.0703
TG	0.953
CKIF (hours)	335.3
CK12 (hours)	25
CKBF	1585

4.2 Estimation of the outflow of Pleikrong catchment

The study made the comparison on the characteristics of Dak Mot and PleiKrong catchments. Because Dak Mot is a two-third part of PleiKrong, two catchments have similar characteristics. The concentration time of each catchment is the only parameter to be modified and the concentration time of Pleikrong should be higher than that of Dak Mot. Therefore, we keep the same value for all parameters except the concentration time. The set of parameters will be used to simulate the past flood events in 2011 - 2013 for PleiKrong when the data is available. These estimated discharges will be used to train ANN and test the model prediction.

4.3 Development of ANN network for PleiKrong inflow forecasting

a. Data set

The concentration time of PLeiKrong catchment is about 9 hours. Then the hydrological principle taught that PleiKrong inflow can be affected by 6 to 12 hourly rain in the system. In addition, it can be effective by the outflow of Dak Mot and PleiKrong catchments at the previous time steps. However, for more accurate estimation, Pleikrong inflow did not consider in the argument of prediction. In conclusion, there are 9 variables were considered as presented in Table 4.

Table 4. Variables for simulation of inflow at Pleikrong

No.	Variables	Time steps	Available period	Note
1	tnat	06 hour	02/06/2011 – 31/12/2013	Interval values from 1 to 365 days
2	$X_{ĐM\_6h}$	06 hour	02/06/2011 – 31/12/2013	6 hourly rain at Dak Mot station
3	$X_{ĐM\_12h}$	06 hour	02/06/2011 – 31/12/2013	12 hourly rain at Dak Mot station
4	$X_{ĐT\_6h}$	06 hour	02/06/2011 – 31/12/2013	6 hourly rain at Dak To station
5	$X_{ĐT\_12h}$	06 hour	02/06/2011 – 31/12/2013	12 hourly rain at Dak To station
6	$Q(ĐM)_{t-3}$	06 hour	02/06/2011 – 31/12/2013	Dak Mot discharge
7	$Q(ĐM)_{t-2}$	06 hour	02/06/2011 – 31/12/2013	Dak Mot discharge
8	$Q(ĐM)_{t-1}$	06 hour	02/06/2011 – 31/12/2013	Dak Mot discharge
9	$Q(ĐM)_t$	06 hour	02/06/2011 – 31/12/2013	Dak Mot discharge

b. ANN Inputs selection

To select the most effective inputs for ANN network, IIS (Galelli and Castelletti, 2013) was used and selected from three inputs. The Pleikrong inflow later is estimated as the function of $X(DM)_{6h}$; $X(DT)_{6h}$; $Q(DM)_{t-1}$ as shown in Equation 1.

$$Q(PL)_t = f[X(DM)_{6h}; X(DT)_{6h}; Q(DM)_{t-1}] \quad (1)$$

c. Set up ANN network

The network was described by 10 neurons as the total neurons should not be lower then the number of variables used for inputs and outputs and must not be very large for saving computation time. Two third of time series will be used for training and the remaining of one third will be used for validation and testing.

d. Training ANN network

The relevant data from 1/6/2011 - 30/11/2012 was used to train the ANN network. The predictands are advanced 6, 12, 18 and 24 hourly Pleikrong inflows and the predictors are the presented 6 hourly rain at Dak Mot, Dak To and the presented discharge at Dak Mot station. The result is presented in Fig. 7 to Fig. 10.

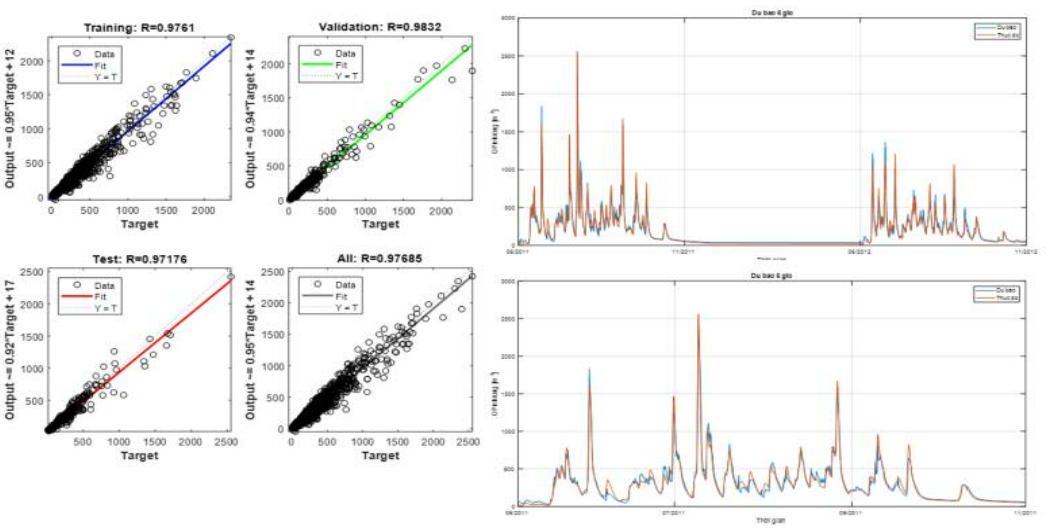

Fig. 7. Advanced 6 hourly predicted Pleikrong inflow: result and evaluation.

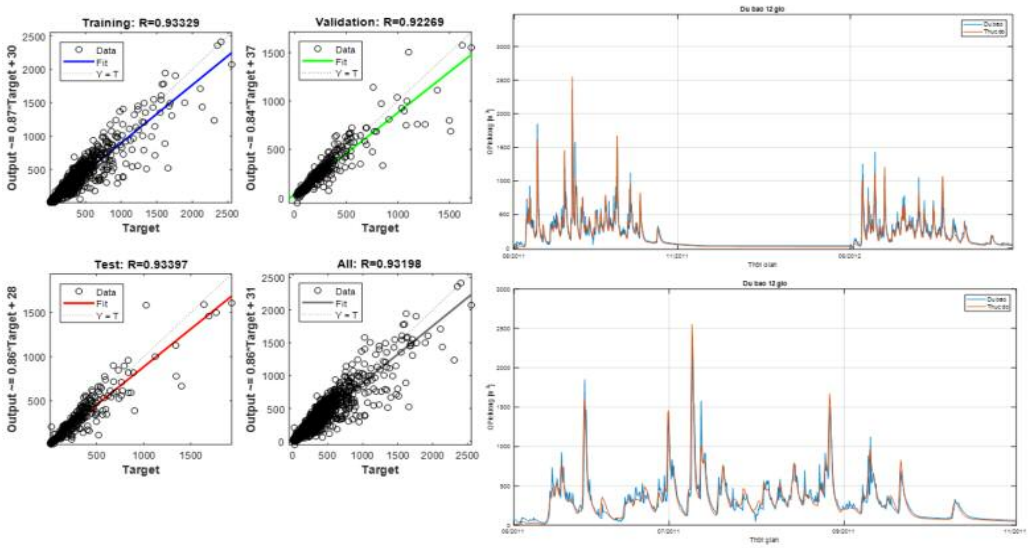

Fig. 8. Advanced 12 hourly predicted Pleikrong inflow: result and evaluation.

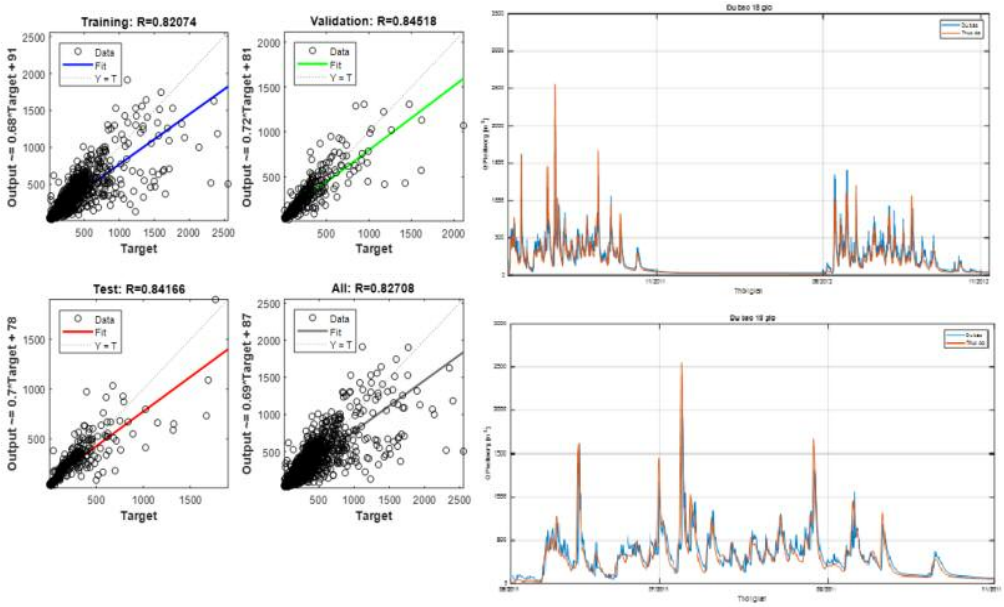

Fig. 9. Advanced 12 hourly predicted Pleikrong inflow: result and evaluation.

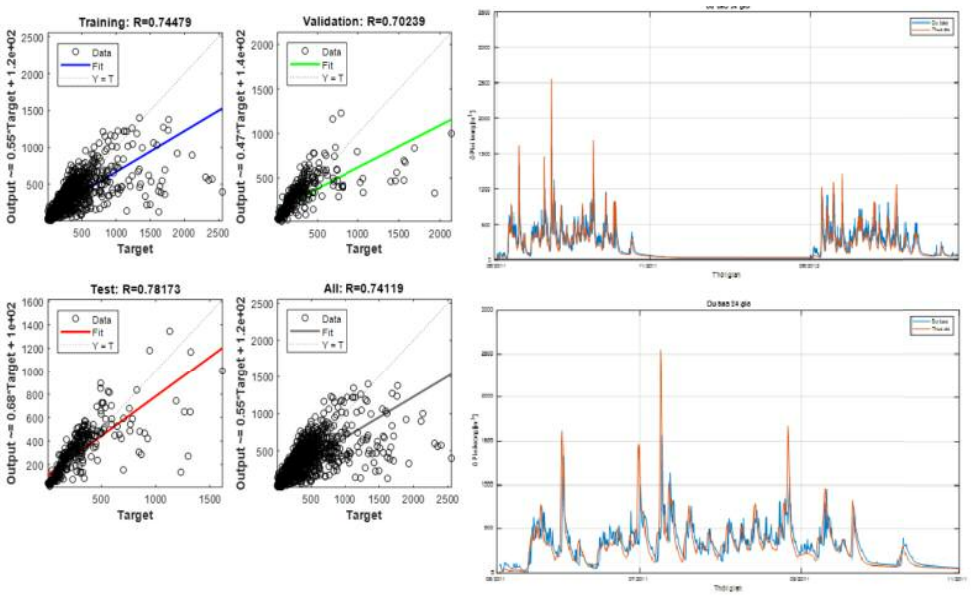

Fig. 10. Advanced 18 hourly predicted Pleikrong inflow: result and evaluation

Table 5. Evaluation of ANN training for flood forecasting to Pleikrong reservoir

Criteria	6hr	12hr	18hr	24hr
R^2	0.98	0.93	0.86	0.74

The results show the good prediction of Pleikrong inflows with NASH coefficients larger than 0.7 for 6 hours, 12 hours, even for 18 hours and 24 hours predicted time as shown in Table 5. Then the network was accepted for predicted test using past event in September to November, 2013.

e. Predicted test for the period from September to November, 2013

Using the validated ANN network to test the predicted inflow in the period from September to November, 2013. The visualized result is presented in Fig. 11.

In addition, there are three criteria which were used to evaluate the efficiency of the predicted alternatives: determination coefficient R^2, S/σ ratio in which S is the deviation of predicted error time series and σ is the deviation of predictor time series and correlation coefficient . Beside them, the time and magnitude of peaks, and the matching of observed and predicted time series were also considered as the evaluation criteria.

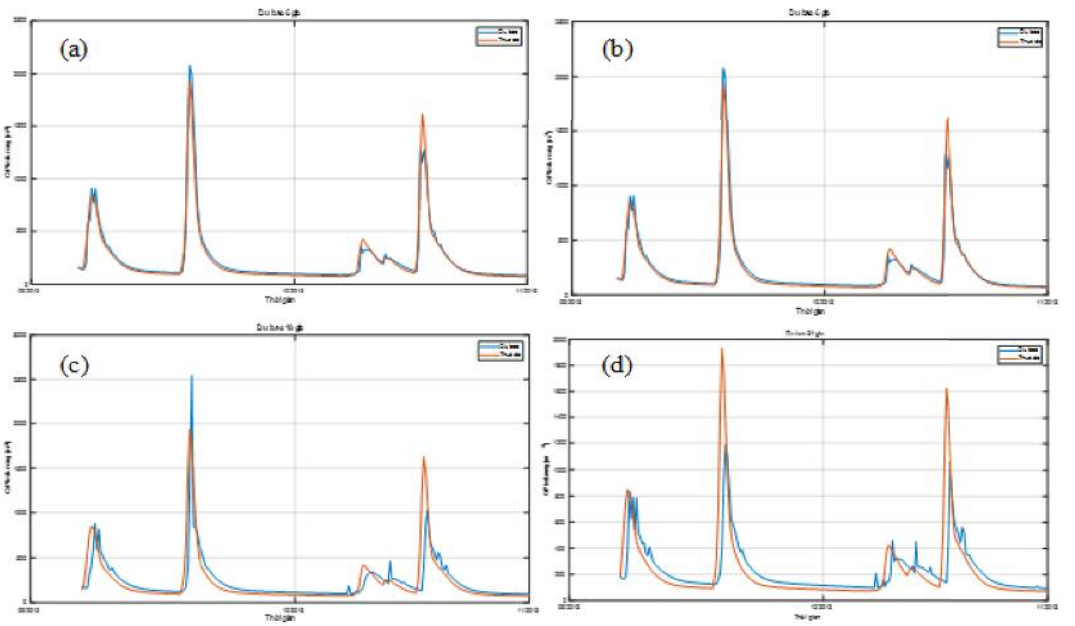

Fig. 11. Predicted (green) and observed (red) values of Pleikrong inflow in advance of 6 hourly (a), 12 hourly (b), 18 hourly (c) and 24 hourly (d)

Table 6. Evaluation of the testing results during September to November, 2013

Criterial	6hr	12hr	18hr	24hr
R^2	0.97	0.79	0.66	0.47
S/σ	0.19	0.35	0.6	0.72
η	0.90	0.81	0.65	0.62

From Fig.11 and Table 6 one can be seen that 6 hours forecasting give a very good result. The peaks' time of observed and predicted flows matches perfectly and the different between the peak values are in the acceptable limit (smaller than 10% of observed one). In addition, R^2, S/σ ratio and η get very good values. For 12 hours forecasting, the value of evaluation criteria still has good values as shown in column 2 of Tab.6 which are in their acceptable ranges. However,

for 18 hours and 24 hours forecasting, the prediction are poor with the very bad values of evaluated criteria (column 3 and 4 in Table 6 respectively). This is due to the fact that the concentration time of the basin and also the time lag to convey flood from Dak Mot to Pleikrong are smaller than these periods. Then 18 hours and 24 hours forecasts in advance using rain data are not meaningful in the real world.

In conclusion, ANN can be used for flood forecasting of Pleikrong inflow in short duration like 6 hours and 12 hours ahead to predict the flood caused by heavy rainfall events in the system. It will be an importance advantage for Pleikrong reservoir operation and a reference for other similar studies.

5. Conclusion and Recommendation

With the limitation in data and information, flood forecasting for hazard mitigation and reservoir operation has a big gap for implementing in many regions over the world and especially in Vietnam. This research proposed the method using ANN to predict the Pleikrong inflow as an example of flood forecasting for limited gauges. The results showed that ANN can work well if it is trained with past flood events.

In addition, ANN can be better than physical based model in this situation due to the fact that it used the deterministic data to predict the flood that can reduce the error during forecasting process. However, it needs a long and representative time series of variables to give a good network or it will be difficult to predict the events that never happen in the past. For this limitation, synthesis data can be generated and used as training data set.

References

1. Castelletti, A., Galelli, S., Restelli, M. and Soncini-Sessa, R., 2012. Data-driven dynamic simulation modelling for the optimal management of environmental systems. *Environmental Modelling & Software*. 34(0): 30 - 43.

2. DHI (2014). *MIKE NAM user guide*.

3. Guo, S. et at., 2000. Reservoir Comprehensi ve and Automatic Control System. *Wuhan University of Hydraulic and Electrical Engineering Press*. Wuhan (in Chinese). η

4. Jain, S.K., Mani, P., Jain, S.K., Prakash, P., Singh, V.P., Tullos, D., Sanjay Kumar, S., Agarwal, S.P. and Dimri, A.P., 2017. A Brief review of flood forecasting techniques and their applications. *International Journal of River Basin Management*, UK.

5. Le Van Nghinh, Hoang Thanh Tung, Nguyen Ngoc Hai, 2015. Research on application of neural network in forecasting flood in rivers in Binh Dinh and Quang Tri.

6. Truong Van Anh et al., 2016. Estimating the foreign flow from China to Vietnam supporting water resources planning and management in Da river basin. *Meteorolical and Hydrological Journal*

7. Rodolfo, S.S., Weber, E., Castelletti, A., 2007. Integrated and Participatory Water Resources Management. *Elsevier publisher*.

8. Sulafa, HagElsafi et al., 2014. Artificial Neural Networks (ANNs) for flood forecasting at Dongola Station in the River Nile, Sudan, *Alexandria Engineering Journal*. Elsevier publisher.

9. Song Tra Energy Consultant Company Limited, 2015. *Dak Po Ko Hydropower Project.*

10. Xiao, Y., Guo, S.L., Liu, P., Yan, B.W. and Chen, L., 2009. Design Flood Hydrograph Based on Multicharacteristic Synthesis Index Method. J*ournal of Hydrologic Engineering Press, ASCE, USA.*

Vietnam Journal of Hydrometeorology, ISSN 2525-2208, Volume 01: 64 - 69

Research Paper

ASSESSING THE IMPACTS OF THE CHANGES IN THE UPSTREAM FLOW AND SEA LEVEL RISE DUE TO CLIMATE CHANGE ON SEAWATER INTRUSION IN HO CHI MINH CITY USING THE HEC - RAS 1D MODEL

Nguyen Thi Diem Thuy[1], Nguyen Ky Phung[2], Nguyen Xuan Hoan[1], Dao Nguyen Khoi[3]

ARTICLE HISTORY

Received: April 12, 2018; Accepted: May 08, 2018
Publish on: December 25, 2018

ABSTRACT

The aim of this study was to assess the impacts of the changes in upstream flow and sea level rise due to climate change on seawater intrusion in the Sai Gon and Dong Nai Rivers in Ho Chi Minh City. The HEC-RAS model was used for simulating the salinity intrusion. The results of model calibration and validation indicated that the HEC-RAS model could simulate reasonably the streamflow and salinity concentration with NSE values exceeding 0.5 for both calibration and validation periods. Based on the results in the calibration in the HEC-RAS model, differences in salinity concentration under the separate and combined impacts of the changes in the upstream flow and sea level rise were analyzed. The results indicated that the salinity intrusion is likely to increase by 0.9 to 13% under the impact of sea level rise, by 1.6 to 4.3% under the impact of the changes in the upstream flow, and by 2.6 to 16.9% under the combined impacts of changes in the upstream flow and sea level rise. The research obtained in this study could be useful for local authorities in proposing solutions to reduce the impacts of seawater intrusion in Ho Chi Minh City.

Keywords*: HEC-RAS, Ho Chi Minh City, sea level rise, seawater intrusion, changes of river flow in the upstream.*

1. Introduction

Climate change is one of the biggest challenges to humanity in the 21st century. The Intergovernmental Panel on Climate Change - Fifth Assessment Report (IPCC-AR5) indicated that the coastal countries in Southeast Asia, including Vietnam, are highly vulnerable to climate change and sea level rise (SLR) (IPCC, 2013). One of identified major impacts of climate change and SLR in Viet Nam is salinity intrusion in the dry season. Thus, understanding the changes in salinity intrusion under these impacts will be useful for water resource management and agricultural development.

In recent years, many researcher have investigated the impact of climate change and SLR on salinity intrusion. For example, Ha et al. (2016) used the one-dimensional hydraulic model to simulate the salinity intrusion under the impact of SLR in the Mekong Delta and they showed that the salinity concentration increases by 1.2 to 10% in the future. Tri and Tuyet (2016) investigated the effect of climate change on the seawater intrusion in the Ca River Basin and they indicated that the impacts of salinity intrusion to the inland will increase in the future. However, there are very few studies on evaluating the separate and combined impacts of climate change and SLR on salinity intrusion. The objective of

NGUYEN THI DIEM THUY
Email: nguyenthidiemthuyapag@gmail.com
[1]Ho Chi Minh City University of Food Industry, Ho Chi Minh City, Vietnam
[2]Institute for Computational Science and Technology, Ho Chi Minh City, Vietnam
[3]Faculty of Environment, VNU-HCM University of Science, Ho Chi Minh City, Vietnam

this study was assessing the separate and combined impacts on saltwater intrusion under changes in the upstream flow and SLR due to climate change in the Sai Gon and Dong Nai Rivers in Ho Chi Minh City (HCMC). The model used in this study was the HEC-RAS 1D model. This model was selected because of its availability and user-friendliness in handling input data and output results. Besides that, the HEC-RAS model has been used as a powerful tool for modeling the streamflow and water quality in the rivers.

2. Study area

HCMC is one of the largest cities in Vietnam, which has the fastest economic growth in the country. HCMC is situated on the downstream of the Dong Nai River Basin. The distance of the city center to the East Sea is about 50 km (Van Leeuwen et al., 2016) (Figure 1).

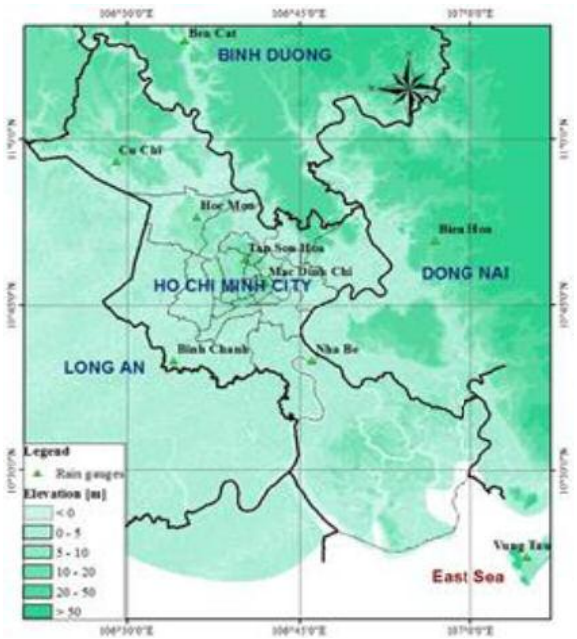

Fig. 1. Location of the study area

The city has an area of about 2061 km^2 and a population of nearly 8.45 million in 2017 (GSO, 2018). HCMC consists of 24 districts, including 19 urban districts and 5 suburban districts. These suburban districts are accounting for 79% of the total area of the city and 16% of the total urban population. HCMC is the biggest economic center in Vietnam and a transport hub of the southern region. This area is located in tropical area and has two distinct seasons: the rainy season and the dry season. The average annual rainfall is quite high, about 1800mm. The rainy season lasts from May to October and accounts for 80-85% of the total annual precipitation. In addition, HCMC is vulnerable to flooding due to land subsidence, urbanization, heavy rainfall, flow changes from the upstream, and SLR (Van Leeuwen et al., 2016).

3. Methodology

3.1 HEC-RAS model

HEC-RAS 1D model is developed by the Hydrologic Engineering Center, a division of the Institute for Water Resources, U.S Army Corps of Engineers. It is used to simulate one-dimensional unsteady flow and water quality in the rivers. In the HEC-RAS model, two modules, including hydrodynamic module and advection-dispersion module, were used for the present study.

In the hydrodynamic module, HEC-RAS solves the following 1-D equations of continuity and momentum known as the Saint-Venant equations (Brunner, 2010). These equations are written as follows:

$$\frac{\partial A}{\partial t} + \frac{\partial S}{\partial t} + \frac{\partial Q}{\partial x} - q_l = 0 \quad (1)$$

$$\frac{\partial Q}{\partial t} + \frac{\partial (VQ)}{\partial x} + gA\left(\frac{\partial z}{\partial x} + S_f\right) = 0 \quad (2)$$

Where: Q: flow discharge (m^{3}s^{-1})

A: the cross-sectional area (m^2)

X: distance along the channel (m)

S: storage from non-conveying portions of cross section (m^2)

q_l: lateral inflow per unit length (m^{2}s^{-1})

V: velocity (ms^{-1})

G: acceleration of gravity (ms^{-2})

S_f: friction slope for the entire cross section

T: the time (s).

The solution of these equations is based on an

implicit finite difference scheme.

In the advection-dispersion module, the basic equation is the mass balance equation of a conservative constituent (Brunner, 2010). This is written as follows:

$$\frac{\partial AC}{\partial t} = \frac{\partial}{\partial x}\left(AD\frac{\partial C}{\partial x}\right) - \frac{\partial QC}{\partial x} \quad (3)$$

Where: C: the salinity concentration (gL^{-1})

A: the cross-sectional area (m^2)

Q: the freshwater discharge (m^3s^{-1})

D: the longitudinal dispersion coefficient ($m^2 s^{-1}$).

3.2 HEC-RAS model set up

The HEC-RAS 1D model was applied to simulate flow and salinity intrusion in Sai Gon and Dong Nai Rivers. In the hydrodynamic module, the discharge at three upstream stations and water level at six downstream stations water-level boundaries were assigned as boundary conditions. These boundary conditions were given based on the observed data in 2009 at stream gauges, collected from Hydro-Meteorological Data Center (HMDC). The cross section of the rivers was collected from Southern Institute of Water Resources Research (SIWRR). For simulation of salinity intrusion, the salinity concentration of the upstream boundaries was zero and the salinity concentration of the downstream boundaries was given by measured data. The salinity data in 2009 also were collected from HMDC. Calibration was performed from 06/03/2009 to 15/03/2009 and the observed data from 16/03/2009 to 31/03/2009 was used for validating. The location of observed stations was shown in Figure 2.

The model performance was evaluated by using three statistical indices, including coefficient of determination (R^2), Nash-Sutcliffe efficiency (NSE), and ratio of the root mean square error to the standard deviation of measured data (RSR). According to Moriasi et al. (2007), the model simulation can be considered as satisfactory when NSE and R^2 are above 0.5 and RSR is less than 0.7.

3.3 Scenarios of the upstream flow change and sea level rise

In this study, scenarios of SLR and changes in upstream flow due to climate change in Sai Gon – Dong Nai Rivers were given based on the previous studies conducted by Katzfey et al. (2014) and Khoi et al. (2015). The RCP 8.5 scenario (high emission) was considered in this study. The RCP 8.5 scenario was selected for this study because it emphasizes the largest impacts of climate change due to the assumption of this greenhouse gas emission scenario, which is suitable to the studies on salinity intrusion. Table 1 summarizes the changes in sea level and upstream flow for the 2020s (2015-2040), 2050s (2045-2070), and 2080s (2075-2100) in the dry season under the RCP 8.5 scenario.

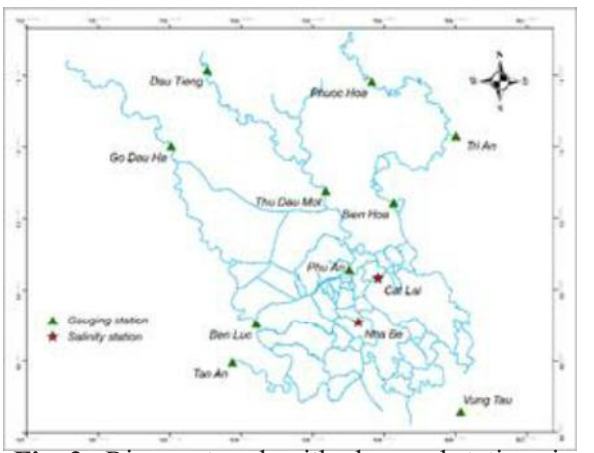

Fig. 2. River network with observed stations in study area

Table 1. Scenarios for SLR and changes of upstream flow in the dry season in the study area

Period	Sea level rise	Upstream flow change
2020s	0.04m	-30%
2050s	0.21m	-29%
2080s	0.47m	-47%

4. Results and discussion

4.1 Calibration and validation of HEC-RAS for simulating the streamflow and salt concentration

Calibration and validation were performed to improve model performance at the main gauging stations. Water level calibration was conducted first, followed by salinity calibration.

Figure 3 compares simulated and observed hourly water level for calibration and validation periods at Nha Be station. Good agreement can be seen between the simulated and observed water level during these periods. The values of NSE, R^2, and RSR for hourly calibration and validation at all stations are listed in Table 2. For both calibration and validation periods.

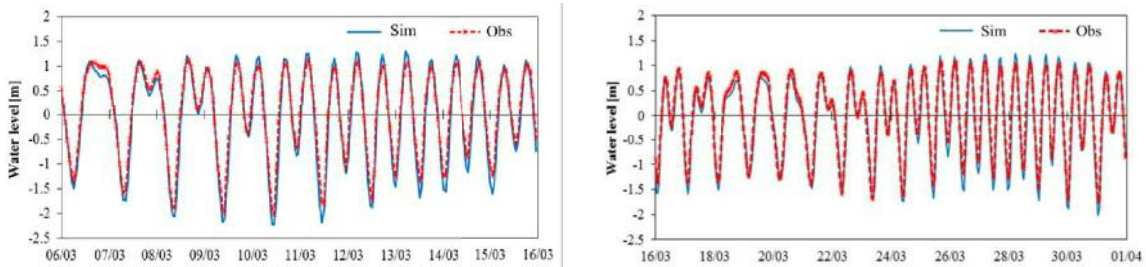

(a) Calibration period (06/03 - 15/03/2009) *(b) Validation period (16/03 - 31/03/2009)*

Fig. 3. The calibration and validation results of water level at the Nha Be station

Table 2. The performance of HEC-RAS for the flow simulation

Station	Calibration (06 - 15/03/2009)			Validation (16 - 31/03/2009)		
	NSE	***R^2***	***RSR***	***NSE***	***R^2***	***RSR***
Thu Dau Mot	0.87	0.95	0.36	0.87	0.94	0.38
Bien Hoa	0.94	0.96	0.25	0.91	0.96	0.30
Nha Be	0.92	0.96	0.29	0.92	0.96	0.28
Phu An	0.92	0.96	0.29	0.95	0.97	0.21
Ben Luc	0.90	0.94	0.32	0.85	0.94	0.39

Because of a lack of salinity data, the salinity calibration was performed for three days. The calibration and validation results of salinity concentration for at the Nha Be station was presented in Figure 4. The results of statistical evaluations at all stations (Table 3) suggest an agreement between measured and simulated salinity concentration. This is confirmed by the NSE and R^2 values above 0.52, and the RSR values below 0.6.

Considering the goodness-of-fit statistics and calibration and validation results discussed above, it is generally concluded that the HEC-RAS model can simulate satisfactorily the streamflow and salinity concentration for the Sai Gon and Dong Nai Rivers. And, the well-calibrated model was used to investigate the salinity intrusion under the separate and combined impacts of the upstream flow change and SLR.

Table 3. The performance of HEC-RAS for the simulation of salt concentration

Station	Calibration (12 - 15/03/2009)			Validation (27 - 29/03/2009)		
	NSE	***R^2***	***RSR***	***NSE***	***R^2***	***RSR***
Nha Be	0.63	0.68	0.60	0.52	0.69	0.60
Cat Lai	0.78	0.79	0.47	-	-	-

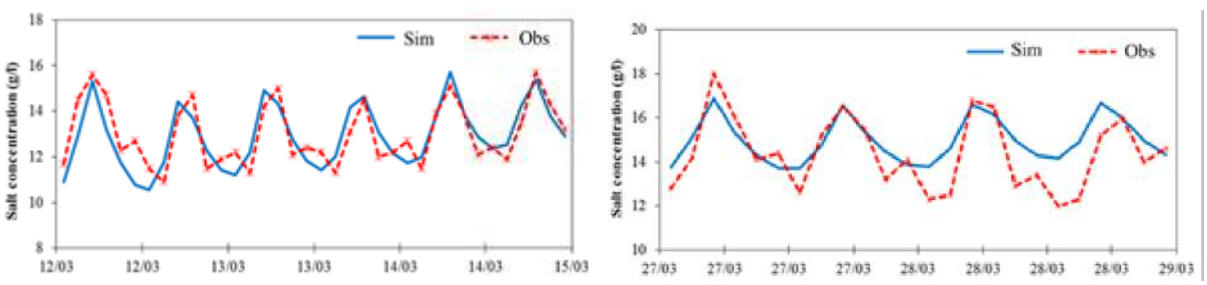

(a) Calibration period (12/03 - 15/03/2009) *(b) Validation period (27/03 - 29/03/2009)*

Fig. 4. The calibration and validation results of salt concentration at the Nha Be station

4.2 Separate and combined impacts of the changes in upstream flow and SLR on salinity intrusion

Based on the simulation results for the dry season in 2009, the map of salinity intrusion for the study area in the baseline period was estab-

lished (Figure 5). In general, the salinity with a concentration greater than 4 g/l, which affects the agricultural activities, had intruded up to 68 km into the rivers. The salinity concentration reduced when it goes up to the upstream river. And, the salinity level of 0.25 g/l had intruded up to 93 km from the Soai Rap estuary.

To investigate the separate and combined impacts of climate change and SLR on salinity intrusion, the approach which varies only one factor or variable at a time while keeping others fixed was used. The following three scenarios were investigated, including changes in SLR considered in Scenario 1, changes in the upstream flow considered in Scenario 2, and changes in SLR and upstream flow considered in Scenario 3. Table 4 illustrates the average changes in salinity concentration in the RCP 8.5 scenario under the three scenarios. Under the impact of SLR, the salinity concentration increases by 0.9 to 13%. In addition, the changes in the upstream flow will increase the salinity concentration by 1.6 to 4.3%. In case of combined impact of changes in sea level and upstream flow, the salinity concentration is predicted to increase by 2.6 to 16.9%. In general, the separate and combined impacts of SLR and the upstream flow change will increase salinity intrusion in the Sai Gon and Dong Nai Rivers in the future, and the salinity intrusion have stronger responses to SLR than the upstream flow change. These changes mean that the saltwater will move to inland in the Sai Gon and Dong Nai Rivers in the future and have significant impacts on agricultural activities as well as livelihoods for the HCMC citizens.

Table 4. Percentage changes in salinity concentration under sea level rise scenarios

Period	Nha Be			Cat Lai		
	Sce. 1	Sce. 2	Sce. 3	Sce. 1	Sce. 2	Sce. 3
2020s	0.9%	1.7%	2.6%	1.3%	2.8%	4.1%
2050s	4.6%	1.6%	6.1%	6.7%	2.7%	9.2%
2080s	8.8%	2.6%	11%	13%	4.3%	16.9%

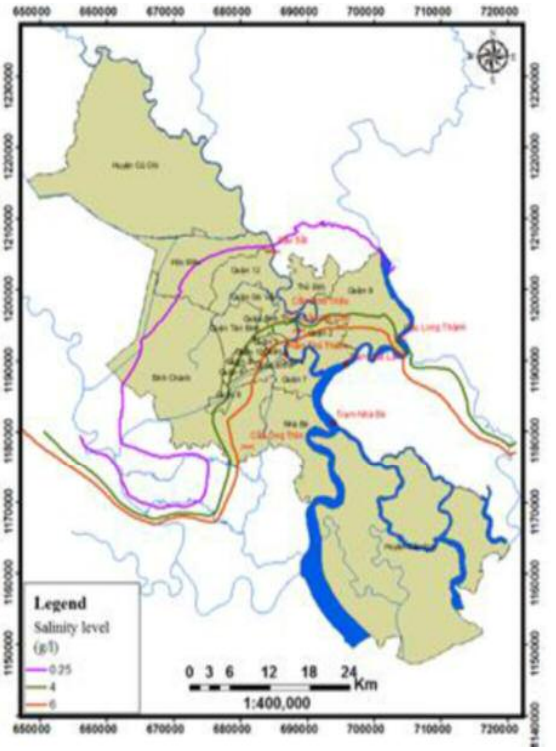

Fig. 5. Map of the salinity intrusion in the baseline period

5. Conclusion

This study investigated the separate and combined effects of SLR and the changes in the upstream flow c due to climate change on salinity intrusion in HCMC by using the HEC-RAS model. The calibration and validation results were carried out to evaluate model performance in simulation of streamflow and salinity concentration. The results indicated that the HEC-RAS is a useful tool for assessing impacts of SLR and changes in the upstream flow in HCMC. Under the separate and combined impacts of changes in sea level and upstream flow, the saltwater will move deeply into inland in the dry season. And, the SLR influences salinity intrusion in the study area more strongly than due to the changes in the upstream flow. The results obtained in this study could be useful for managing water resources in this region through enhancing the understanding of the impacts of climate change and SLR on salinity intrusion.

Acknowledgements

The study was supported by Science and Technology Incubator Youth Program, managed by Center for Science and Technology Development, Ho Chi Minh Communist Youth Union, the contract number is "20/2018/HĐ-KHCN-VU".

References

1. Brunner, G.W., 2010. HEC-RAS River Analysis System Hydraulic Reference Manual (version 4.1). US Army Corp of Engineers. Hydrologic Engineering Center (HEC), Davis California, USA.

2. GSO - General Statistics Office, 2018. *Statistical Yearbook of Vietnam in 2017.*

3. Ha, N.T.T., Trang, H.T., Vuong, N.V., and Khoi, D.N., 2016. Simulating impacts of sea level rise on salinity intrusion in the Mekong Delta, Vietnam in the period 2015-2100 using MIKE 11. *Naresuan University Engineering Journal*. 11: 21-24.

4. IPCC, 2013. The Physical Science Basis: Contributing of Working Group I to the Fifth Assessment Report of the Intergovernmental Panel on Climate Change. Cambridge University Press, Cambridge, UK.

5. Katzfey, J., McGregor, J., Ramasamy, S., 2014. High-resolution climate projections for Vietnam, Technical Report.

6. Khoi, D.N., Thom, V.T., Linh, D.Q., Quang, C.N.X., Phi, H.L., 2015. Impact of climate change on water quality in the Upper Dong Nai River Basin, Vietnam. *Proceedings of the 36th IAHR World Congress*. Netherland.

7. Moriasi, D.N., Arnold, J.G., Van, Liew M.W., Bingner, R.L., Harmel, R.D., Veith, T.L., 2007. Model evaluation guidelines for systematic quantification of accuracy in watershed simulations, *Transaction of ASABE*, 50: 885-900.

8. Tri, D.Q., Tuyet, Q.T.T., 2016. Effect of climate change on salinity intrusion: case study Ca River Basin. V*ietnam. Journal of Climate Change*, 2(1): 91-101.

9. Van, L.C.J., Dan N.P., Dieperink, C., 2016. The Challenges of Water Governance in Ho Chi Minh City. *Integrated Environmental Assessment and Management*. 12(2): 345-352.

Vietnam Journal of Hydrometeorology, ISSN: 25252208, Volume 01: 70 - 75

Research Paper

RESEARCH ON BOTTOM MORPHOLOGY AND LITHODYNAMIC PROCESSES IN THE COASTAL AREA BY USING NUMERICAL MODEL: CASE STUDIES OF CAN GIO AND CUA LAP, SOUTHERN VIETNAM

Nguyen Thi Bay[1], Dao NguyenKhoi[2], Tran Thi Kim[3], Nguyen Ky Phung[4]

ARTICLE HISTORY

Received: August 20, 2018; Accepted: October 10, 2018
Publish on: December 25, 2018

ABSTRACT

A numerical model to simulate Litho-dynamic processes and bottom morphology at the coastal area such as the flow, sediment transport and bed changes under the effects of tides, waves and winds have been suggested. The model is based on the system of Reynolds equation coupled with sediment transport and bed load continuity equation. There are three verification cases of the model: verification of the tide-induced current, the wave-induced current and the sediment transportation., The results from the model are good in accordance with the analytical solution. The model is then applied to the coastal zone of Can Gio mangrove forest and Cua Lap estuary (South East of Vietnam). As a result, the trend of sediment accretion and erosion in these two areas are qualitatively in agreement with satellite observation and practical measurement.

Keywords: *The numerical model, Litho-dynamicprocesses, Sediment transportation, Eccretion and erosion.*

1. Introduction

Hydrodynamic in estuaries coastal zone has a direct impact on the societal issues such as coastal engineering, environmental protection, and recreation. Waves, current, sediment transport, and morphology are important processes within coastal and estuaries setting, so accurate predictions of waves, currents, and sediment transport plays a key role in solving estuary and coastal problems, especially those related to bedded morphological evolution. Waves and currents mobilize and transport sediment, and gradients in the transport cause deposition or erosion, affecting the local topology. Therefore, understanding of hydrodynamic regime in the coastal zone and simulating its potential changes over the years are important information to support coastal management plan toward sustainability. A coastal morphodynamic modeling is the best way to convert scientific information to practical application and to improve communication between scientists and managers or practitioners.

The model has been developed by the authors since 2004. It is used to simulate simultaneously the flow due to wave, wind, and tide and combined with sediment transport and bed level changes in the coastal and estuary area. The model has been verified with some analytical solutions and applied for the real cases in some coastal and estuary areas such as Can Gio coastal area and Cua Lap estuary area.

BAY NGUYEN THI
Email: ntbay@hcmut.edu.vn
[1]HCMC University of Technology
[2]HCMC University of Science
[3]HCMC University of Natural Resources and Environment
[4]HCMC Department of Science and Technology

2. Material and methods

2.1 Governing equations

The adopted model is a 2D surface where Ox and Oy represent the length and the width of the study area. The model is based on the system of four governing equations as follows:

Reynolds equations

$$\frac{\partial u}{\partial t}+u\frac{\partial u}{\partial x}+v\frac{\partial u}{\partial y}-fv = -g\frac{\partial \varsigma}{\partial x}+\frac{\tau_{Sx,wind}-\tau_{Sx,w}}{\rho(h+\varsigma)} - \frac{\tau_{bx}}{\rho(h+\varsigma)}+A\nabla^2\bar{u} \quad (1)$$

$$\frac{\partial \varsigma}{\partial t}+\frac{\partial[(h+\varsigma)\bar{v}]}{\partial x}+\frac{\partial[(h+\varsigma)\bar{v}]}{\partial y}=0 \quad (2)$$

Continuity equation

$$\frac{\partial \varsigma}{\partial t}+\frac{\partial[(h+\varsigma)\overline{u}]}{\partial x}+\frac{\partial[(h+\varsigma)\bar{v}]}{\partial y}=0 \quad (3)$$

Suspended sediment transport equation

$$\frac{\partial C}{\partial t}+\gamma_V\left(u\frac{\partial C}{\partial x}+v\frac{\partial C}{\partial y}\right) = \frac{1}{H}\frac{\partial}{\partial y}(HK_x\frac{\partial C}{\partial y}\left(HK_y\frac{\partial C}{\partial y}\right)+\frac{S}{H} \quad (4)$$

Bed load continuity equation

$$\frac{\partial h}{\partial t}=\frac{1}{1-\varepsilon_p}\left[S+\frac{\partial}{\partial x}\left(HK_x\frac{\partial C}{\partial x}\right)+\frac{\partial}{\partial y}\left(HK_y\frac{\partial C}{\partial y}\right)+\frac{\partial q_{bx}}{\partial x}+\frac{\partial q_{by}}{\partial y}\right] \quad (5)$$

where A is Horizontal viscosity coefficient [m^2/s]; u,v arethe depth-averaged horizontal velocity components in x, y direction[m/s]; C is thedepth-averaged concentration of suspended load [kg/m^3]; h isthe static depth from the still water surface to the bed[m]; ς is thefluctuation of water surface [m]; S is thedeposition or degradation of grain [kg/m^2s]; H = ς + h; with H is defined by static depth h and fluctuation ς illustrated in figure 1[m].

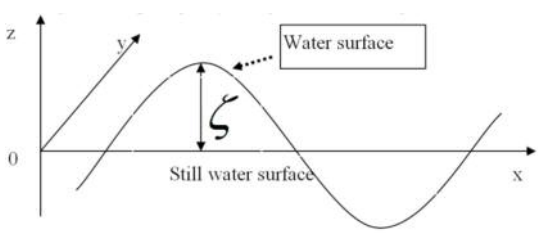

Fig. 1. Initial static level

2.2 Computational method

A numerical code based on finite difference method was built to solve the governing system of equations above with variables u, z, v, and C. In the paper, a visual basic is used to build the model. The scheme ADI (Alternating Direction Implicit) is used to solve the system of converted algebraic equations. Computational grid for the governing system of equations is shown in figure 2. The main concept of the ADI method is to split the finite difference equations into two, one with the x-derivative and the next with the y-derivative, both taken implicitly (Douglas, 1955). The system of equations involved is symmetric and tri-diagonal (banded with bandwidth 3), and is typically solved using tri-diagonal matrix algorithm. It can be shown that the method is unconditionally stable and second order in time and space (Douglas, 1955).

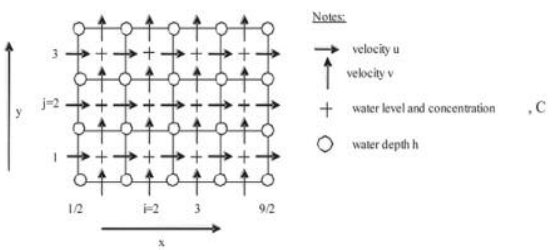

Fig. 2. Computational grid for the governing system of equations

3. Result and discussion

3.1 Verification of the model

There are three verifications: Verification of the tide-induced current, verification of the wave-induced current and verification of sediment transportation.

• Verification of the tide-induced current: Analytical solution for water level and velocity of a wave transmitted in a narrow frictionless channel to the end of the channel and reflect totally (G. Airy, 1845). Figure 3 is the result of the water level at the middle of the channel, blue line stands for the simulation results and the pink one stands for the analytical solutions. The figure shows that there is a good agreement between 2 results.

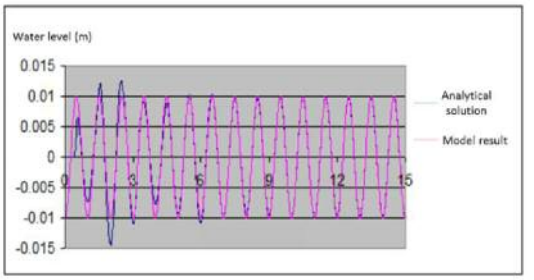

Fig. 3. Water level at the middle of the channel

•Verification of the wave-induced current: the results are presented in figure 4.a and 4.b. The calculated results from the model show that the wave-induced current occurs strongly in the surfzone. The maximal value of velocity V of 0.67 m/s and direction of current are parallel to the shoreline. Compared to the analytical solution (the maximal value of velocity V of 0.64 m/s), a good agreement is observed.

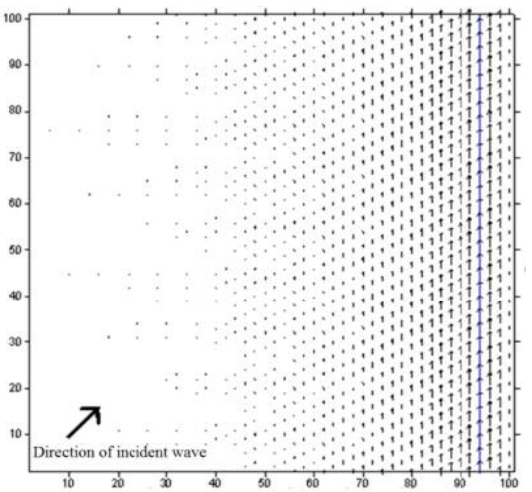

Fig. 4. (a) Alongshore current along the uniform beach computed by the model (angle of incident wave 45^0)

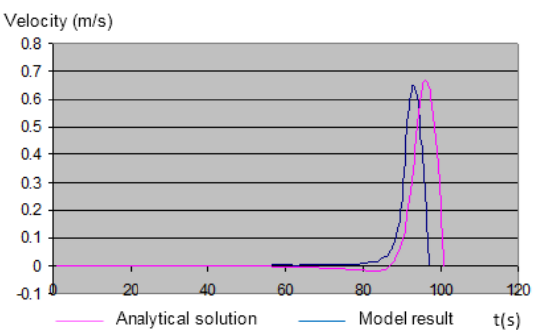

Fig. 4. (b) Velocity in x-direction across the beach.

The above figure represents the vector of the alongshore current. Meanwhile, the below figure shows the velocity values along the x-direction, the comparison between our method and analytical solution.

• Verification of sediment transportation: The simulated results are presented in the form of contour levels at times. The results from the model are good in accordance with the analytical solution. This confirms the reliability of the sediment transport model and the possibility to apply in practice.

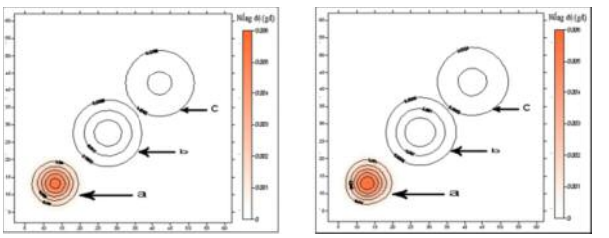

Fig. 5. Comparison of simulated result (left) and analytical solution (right) after (a) 1 hour (b) 3 hours;(c) 5 hours.

3.2 Can Gio coastal area

Can Gio coastal area is located in South of Vietnam (figure 6). The obtained data from our model are evaluated based on the satellite date presented in Vinh and Deguchi (2004).

Fig. 6. Location of Can Gio coastal zone and study area

Simulation results shown in figure 7 illustrate the bed changes of Can Gio coast after 3-month calculation. The agreement between the results by our current modeling approach and satellite data confirms the reliability of the suggested model. In other words, satellite data are served as the validation base for our mathematical model.

Moreover, while satellite data just provides the information on certain local zones at a fixed time of measurement, modeling approach can describe at different series of time, in the past, in the presence and even in the future (predicting and forecasting roles).

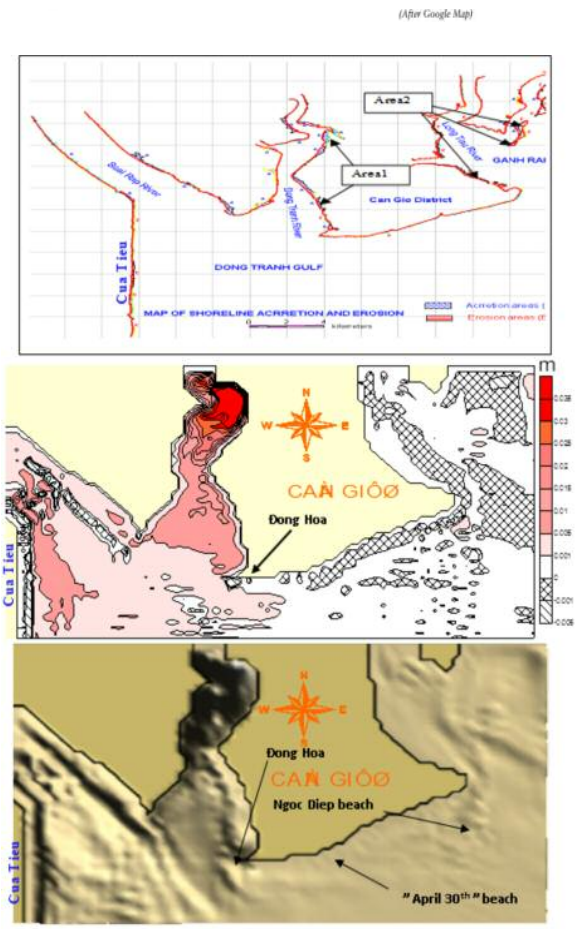

Fig. 7. The bottom topography changes at the Can Gio Coast

It's noted that satellite database (from GIS and remote sensing technology), especially multi-temporal and multi-sensing data provide useful information for coastal monitoring, while the numerical models are now the essential tool for monitoring the changes of near-shore topography, in the shoreline and riverbanks, and offer benefits over the satellite observations.

Figure 7 shows the bottom topography changes at the Can Gio Coast. Where figure 7(a) is results of accretion and erosion location by remote sensing and satellite photo, from 1992 to 2003, figure 7(b) and 7(c) is simulation results after 90 days of calculation (The hatched positions are the erosion zone and the positions which red color changes from light to dark are the accretion zone in (b) and 3D illustration in (c))

This general trend of accretion and erosion in the study area (figure 7) of Can Gio coast obtained from the model corresponds fairly well to the results from the satellite picture presented in Vinh and Deguchi (2004).

3.3 Cua Lap estuary area

Cua Lap estuary is located at the coastal strip from Vung Tau province to Binh Chau province, Vietnam. The shoreline runs from Northeast to Southwest with two cliffs: Nghinh Phong cape and Ky Van cape. This area is strongly influenced by the East Sea tidal regime.

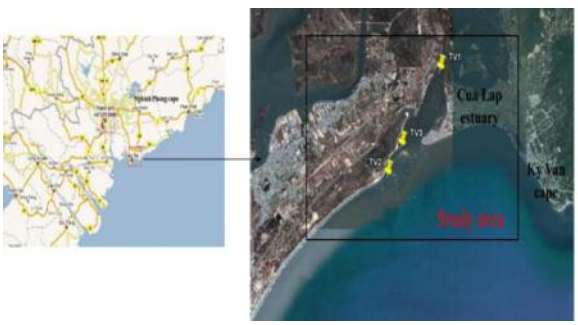

Fig. 8. Location of Cua Lap estuary and study area

The bottom topographic data was obtained from the Cua Lap storm shelter (2009) and the Vung Tau coastal both tomography map (reprinted 1993), with mesh: 340 x 220, $\Delta x = \Delta y = 50$ m.

Simulation results in Northeast monsoon: The results of bed changes are presented in figure 9. In this figure, the color scale from pale orange to dark orange is standing for increasing of erosion. In this area, the velocity is quite high so it

generates a force weathering the bottom layer, causing the erosion phenomena in the narrow passage of the river. This area is eroded 4 to 8 cm in depth.In the B area, the current in this season are mainly directed from Cua Lap to Vung Tau, so this area mainly received the sediment from Cua Lap given. Additionally, reducing the gradient of the current velocities due to the friction with the bank that makes the sediment settle in this area. Therefore, the accretion process in this area is mainly. The C area occurs alternately the processes of deposition and erosion. Overall, the level of deposition is larger than the level of erosion so the deposition occurs mainly in this area. In the D area, the calculated results show that the deposition occurs near Cua Lap estuary. The other area occurs mainly the erosion because these areas are not provided the sediment from the river to compensate the amount of sediment lost due to erosion.

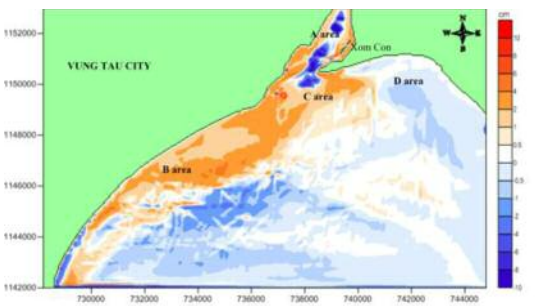

Fig. 9. Bed level change in the Northeast monsoon after 3-month simulated

Simulation results in Southwest monsoon: The deposition and erosion area in the Southwest monsoon are shown in figure 10.In the A area, there are two erosion areas. One is in the narrow passage of Cua Lap River, the other bends according to Xom Con. At the areas of both side bank, decreasing the gradient of the current velocity due to friction make the suspended sediment settling. Therefore, the deposition occurs mainly in these areas. In the B area, due to the influence of southwest wind and wave coming from Southwest, the sediment cannot move to this area. Therefore, the amounts of sediment lost that are not compensate. The erosion is dominant. In the C area, similarly in the northeast monsoon, the area takes place alternately the processes of erosion and deposition. In general, the deposition prevails. In the D area, the deposition is dominant. It is explained that the bottom friction makes reducing the gradient of the current so that the sediment settles in the Xom Con.

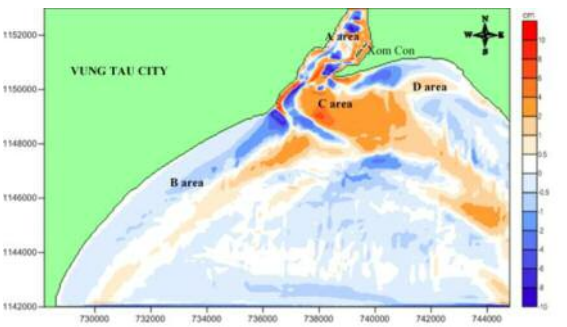

Fig. 10. Bed level changes in the Southwest monsoon after 3-month simulated

The results of bed level change in the Northeast monsoon and Southwest monsoon were compared with the previous research of Sub-Institute of Physics (2000). There are a good agreement in A and C area. In the Thuy Van – Vung Tau area (A area), it happed erosion in Southwest monsoon and deposition in Northeast monsoon. Besides that, the sand dune in front of the estuary (C area) occurred erosion in Northeast monsoon and deposition in Southwest monsoon.

4. Conclusion

The two-dimensional model simulating the current under the influence of the combination of tides, waves, and winds has been developed. The verification of the model shows that the simulated results of the wave-induced current and the tide-induced current area good accordance with the analytical solutions.

The model is applied to simulate water movement, sediment transport, accretion and erosion in Can Gio coastal area and Cua Lap estuary in the Northeast monsoon and Southwest monsoon. The model performs well in reflecting the actually occurring water movements, sediment transport, deposition, and erosion.

Acknowledgements

This research was funded by Institute for Computational Science and Technology, with the topic "Development of bank erosion numerical model basing on HPC in connection with hydraulic model and to apply for some river reaches of the Mekong River", code No.NĐT.28.KR/17.

References

1. Airy, G.B., 1845. On the laws of the tides on the coasts of Ireland, as inferred from an extensive series of observations made in connexion with the Ordnance Survey of Ireland. *Philos. Trans. R. Soc. London*. 1 - 124.

2. Adele, M., Christopher, W. R., and Alan, K.Z., 2004. Two-dimensional depth-averaged circulation model M2D: Verion 2.0, Report 1, Technical documentation and User's guide. U. S. Army Corps of Engineers Washington.

3. Bay, N.T., 1997. Modeling of Hydrological and Morphological dynamic processes in tidal basin. *Doctoral dissertation in Oceanography*, Saint-Petersburg University.

4. Bay, N.T., Toan, T.T., Phung, N.K., and Tri N.Q., 2011. Numerical investigation on the sediment transport trend of Can Gio coastal area (Southern Vietnam), *J. of Marine Env*.

5. Bay, N.T., 2009. Apply the mathematical model for investigating the current, sediment transport and bed level change in Bac Lieu coastal area. *Journal of Meteorology and Hydrology.* 588 (12): 35-41

6. Douglas, J., 1995. On the numerical integration of uxx + uyy = utt by implicit methods. *Journal of the Society of Industrial and Applied Mathematics.* 3: 42–65.

7. Fischer, H.B., List, J., Koh, C., Imberger J., Brooks, N., 1979. Mixing in inland and coastal waters. *Elservier, New York, Academic Press*, 302 pages.

8. Vinh and Deguchi, I., 2004. The potential application of Remote Sensing & GIS and numerical models to investigate coastal process in Can Gio region (Saigon river mouth - South Vietnam). *Proceedings of International Symposium on Advanced Science and Engineering, the 2nd Asian Pacific International Conference*.